

12-2012

The role of endogenous Bcl-xL in regulation of apoptotic signaling pathways.

Colins Ogwandi Eno 1982-
University of Louisville

Follow this and additional works at: <https://ir.library.louisville.edu/etd>

Recommended Citation

Eno, Colins Ogwandi 1982-, "The role of endogenous Bcl-xL in regulation of apoptotic signaling pathways." (2012). *Electronic Theses and Dissertations*. Paper 408.
<https://doi.org/10.18297/etd/408>

This Doctoral Dissertation is brought to you for free and open access by ThinkIR: The University of Louisville's Institutional Repository. It has been accepted for inclusion in Electronic Theses and Dissertations by an authorized administrator of ThinkIR: The University of Louisville's Institutional Repository. This title appears here courtesy of the author, who has retained all other copyrights. For more information, please contact thinkir@louisville.edu.

THE ROLE OF ENDOGENOUS Bcl-x_L IN REGULATION OF APOPTOTIC
SIGNALING PATHWAYS

By

Colins Ogwandi Eno

B.S., University of Buea, Cameroon, 2004
M.S., North Dakota State University, 2008
M.S., University of Louisville, 2010

A Dissertation

Submitted to the Graduate Faculty of the
University of Louisville School of Medicine
in Partial Fulfillment of the Requirements
for the Degree of

Doctor of Philosophy

Department of Pharmacology and Toxicology
University of Louisville
Louisville, Kentucky

December, 2012

Copyright 2012 by Colins Ogwandi Eno

All Rights Reserved

THE ROLE OF ENDOGENOUS BCL-x_L IN REGULATION OF APOPTOTIC
SIGNALING PATHWAYS

By

Colins Ogwandi Eno

B.S., University of Buea, Cameroon, 2004
M.S., North Dakota State University, 2008
M.S., University of Louisville, 2010

A Dissertation Approved on

September 27, 2012

by the following Dissertation Committee:

Chi Li, Ph.D.

John W. Eaton, Ph.D.

Thomas Mitchell, Ph.D.

Brian Wattenberg, Ph.D.

J. Christopher States, Ph.D.

DEDICATION

This dissertation is dedicated to my dear brother, Dr. Robert Wundeh Eno, for his unconditional love, encouragement, and financial and moral supports throughout my studies. Growing up, although I knew I had the will power and determination to pursue my education to the highest level, I knew my parents could not afford the big dreams I had for myself. Brother Robert selflessly sacrifices everything he had to ensure that I pursue and realize my dreams. He is the most altruistic person I know and I will eternally be grateful to him. He is like the “father” I never had, and each day I pray God gives him long life and blesses him abundantly.

ACKNOWLEDGEMENTS

First, I would like to thank the almighty God for giving me the strength, patience, knowledge, determination, courage, confidence, good health and wisdom to pursue and finish my dissertation. Although I am responsible for conceiving this thesis research, this work would not have been completed without the support of many individuals I met throughout the years. This dissertation would not be complete without the support of my mentor, Dr. Chi Li. I am very thankful for his support, trust and guidance, and for always pushing me to reach my full potential almost to my breaking point. I am truly privileged to have worked with Dr. Li as my mentor and will always be grateful to him for all of his encouragement and for believing in me. My thanks are extended to my graduate committee members, Drs. John W. Eaton, Thomas Mitchell, Brian Wattenberg and J. Christopher States, for their critical and insightful comments and suggestions. I would also like to extend my thanks to the past and present members of Chi Li's Laboratory including Kristen Olberding, Drs. Yanglong Zhu, Xiaoli Wang, and Guoping Zhao for their support, suggestions and constructive criticisms.

I am grateful to Dr. Onno Kranenberg at the University Medical Center Utrecht, Netherlands for providing shNoxa HCT116 cell lines, Dr. Joseph Opferman at St. Jude Children's Research Hospital, Memphis, TN, for providing Mcl-1-KO MEFs, Professor Andreas Strasser at the Walter and Eliza Hall Institute of Medical

Research, Parkville, VIC, Australia for providing Noxa-KO MEFs, Sabine Waigel, Yinlu Chen and Vennila Arumugam at the University of Louisville Microarray facility for microarray experiments, Christopher Worth at the University of Louisville Brown Cancer Center Flow Cytometry Laboratory for cell sorting, and Dr. Carl White at the Rosalind Franklin University of Medicine and Science, North Chicago for providing Ca^{2+} data. This work was supported by NIH grants CA106599, RR018733 and funding from Brown Cancer Center (CL). I am also very thankful to the Integrated Programs in Biomedical Sciences (IPIBS) for providing funding for my first two years of graduate studies, the department of Pharmacology and Toxicology for their intense training, and the School of Interdisciplinary and Graduate Studies (SIGS) for providing me with a one year dissertation completion award. I am thankful to the American Society of Pharmacology and Experimental Therapeutics (ASPET), the University of Louisville (UofL) School of Medicine (SOM), UofL Graduate Student Council (GSC), and the National Institutes of Health (NIH) National Graduate Student Research Conference for providing me with travel awards to present my work at national conferences.

I want to thank my wife, Traicy Awaing Eno nee Itambi, for her endurance, moral support, patience, encouragement and understanding especially for all the long hours I spent in the laboratory. I am equally thankful to my entire family for their moral, spiritual and financial support. I am especially thankful to my siblings, Dr. Robert Eno, Julius Eno, Alice Eno, Cyprain Eno, Divina Eno and Binda

Gilbert, and my mom, Mrs. Elizabeth Enow, for their unconditional love. Special thanks to all of my nieces and nephews (Wundeh, Abanda, Brandon, Rhema, Prince, Blesse, Awaiwing Eliza, Tetris, Elmira, Awaiwing Ambumban, Wilma, Janelle and Tiana) for their adorable smiles. I can never thank them enough. I am also indebted to other family members whom made it possible in one way or another for me to achieve my goals including Dr. and Mrs. Pascal Binda, Mrs. Ngwi Eno, Akwi Lilian, Godlove Binda, Glory Ambang Abah, Vallerie Kabba, Simon Abah, Itambi Jessy and Drs. Itambi Cletus and Maxwell Asoh Itambi. I also recognize the moral support of my very good friends including TAO, Efangafa, Bolima, Fortty, Franco, Sahidu, Itambi Collins, Waponcho, Drs. Mongoh and Enoru, and the Cameroonian students here at the University of Louisville health science center both past and present for their input.

Last but not least, I want to thank Prof. and Mrs. Tafah Edokat and Mr. and Mrs. Itambi Zachariah, for all of their moral, spiritual and financial support.

ABSTRACT

THE ROLE OF ENDOGENOUS BCL-x_L IN REGULATION OF APOPTOTIC SIGNALING PATHWAYS

Colins Ogwandi Eno

September 27, 2012

Bcl-2 proteins are major regulators of cellular responses to various apoptotic stimuli. Among them, overexpression of the anti-apoptotic Bcl-2 protein Bcl-x_L modulates organelle-specific apoptotic pathways. To understand the mechanisms by which endogenous Bcl-x_L regulates apoptosis, mouse embryonic fibroblasts (MEFs) deficient in Bcl-x_L expression (Bcl-x-KO) was generated. Studies of Bcl-x_L exclusively targeted to an organelle in Bcl-x-KO MEFs indicate that the mitochondria- and ER-localized Bcl-x_L play distinct roles in apoptosis resistance and Ca²⁺ homeostasis. Specifically, mitochondrial Bcl-x_L can regulate apoptosis independently of ER Bcl-x_L, and when localized exclusively at the ER, Bcl-x_L impinges on Ca²⁺ homeostasis but does not affect apoptosis unless Bcl-x_L is present in additional cellular compartments. Furthermore, I investigated how Bcl-2 proteins, especially Bcl-x_L, might regulate oxidative stress-induced apoptosis. My studies reveal a signaling pathway, in which the oxidative stress inducer hydrogen peroxide (H₂O₂) activates Noxa, leading to a decrease in Mcl-1

expression levels and subsequent increase in apoptosis in the absence of Bcl-x_L expression. Finally, I studied the exact roles of lysosomal membrane permeabilization in apoptosis cascade triggered by oxidative stress and how LMP is regulated by the complex Bcl-2 protein network. My studies elucidate a novel molecular mechanism that couples lysosomal membrane permeabilization with mitochondrial membrane permeabilization and ultimate cell death during oxidative stress-induced apoptosis.

TABLE OF CONTENTS

	PAGE
DEDICATION	iii
ACKNOWLEDGEMENTS	iv
ABSTRACT	vii
LIST OF FIGURES	xi
LIST OF TABLE	xiv
CHAPTER I: GENERAL INTRODUCTION	1
Programmed cell death (Apoptosis).....	1
Biological significance of apoptosis.....	5
Pathways of apoptosis	10
Regulation of apoptosis.....	17
Hypothesis and significance of the projects	30
CHAPTER II: DISTINCT ROLES OF MITOCHONDRIA- AND ER-LOCALIZED BCL-x _L IN REGULATION OF APOPTOSIS AND Ca ²⁺ HOMEOSTASIS	33
Introduction	33
Materials and Methods.....	36
Results	47

Discussion	74
CHAPTER III: ENDOGENOUS BCL-x _L MODULATES CELLULAR RESPONSE TO OXIDATIVE STRESS-INDUCED APOPTOSIS	78
Introduction	78
Materials and Methods	80
Results	87
Discussion	112
CHAPTER IV: THE IMPORTANT ROLE OF LYSOSOMAL MEMBRANE PERMEABILIZATION DURING OXIDATIVE STRESS- INDUCED APOPTOSIS	118
Introduction	118
Materials and Methods	121
Results	128
Discussion	152
CHAPTER V: CONCLUSION AND FUTURE DIRECTIONS	157
REFERENCES	161
APPENDIX: List of abbreviations	175
CURRICULUM VITAE	178

LIST OF FIGURES

	PAGE
1.1 Morphological differences between cells during apoptosis and necrosis.....	4
1.2 Apoptosis is important for proper development	7
1.3 The intrinsic (mitochondria) pathway of apoptosis.....	11
1.4 The extrinsic (death receptor) pathway of apoptosis	13
1.5 The mixed pathway of apoptosis	15
1.6 Activation of outer mitochondrial membrane permeabilization by Bcl-2 protein family	28
2.1 Generation of wild type and Bcl-x-KO MEFs	39
2.2 <i>bcl-x</i> deficiency does not cause compensatory changes in expression of other Bcl-2 proteins.....	51
2.3 Endogenous Bcl-x _L modulates cellular response to different apoptotic stimuli	53
2.4 Reexpression of Bcl-x _L in Bcl-x-KO MEFs restores its resistance to apoptotic stimuli in a Bcl-x _L dose-dependent manner	56
2.5 Generation of mitochondrial- and ER-targeted Bcl-x _L mutants	60
2.6 Mitochondrially targeted Bcl-x _L inhibits apoptosis more efficiently than Bcl-x _L targeted to the ER	63
2.7 ER-localized Bcl-x _L but not mitochondrially targeted Bcl-x _L modulates ER Ca ²⁺ homeostasis	68

2.8	Anti-apoptotic activities of ER-targeted Bcl-x _L depends on endogenous Bcl-x _L	71-72
3.1	Endogenous Bcl-x _L inhibits H ₂ O ₂ -induced apoptosis in a dose dependent manner.....	89
3.2	Expression levels of pro-apoptotic BH3-only Bcl-2 proteins in MEFs	92
3.3	Endogenous Bcl-x _L most effectively inhibits Noxa-induced apoptosis	94
3.4	Expression of Bcl-x _L in Bcl-x-KO MEFs restores their ability to prevent BH3-only Bcl-2 proteins-induced apoptosis	95
3.5	H ₂ O ₂ induces Noxa expression.....	98
3.6	H ₂ O ₂ -induced apoptosis is mediated by Noxa	101
3.7	Mcl-1 expression reduction in response to H ₂ O ₂ depends on Noxa but not Bcl-x _L	103
3.8	Mcl-1 overexpression inhibits H ₂ O ₂ -induced apoptosis	106
3.9	Reduction in Bcl-x _L and Mcl-1 expression simultaneously induces spontaneous apoptosis.....	110
3.10	Bcl-2 proteins coordinately regulate H ₂ O ₂ -induced apoptosis	117
4.1	H ₂ O ₂ induced Noxa-independent LMP.....	130
4.2	Mitochondria membrane permeabilization is dependent on Noxa expression	134
4.3	Stabilizing lysosomal membrane by DFO inhibits Noxa-dependent apoptosis induced by H ₂ O ₂	138
4.4	DFO fails to prevent apoptosis induced by other apoptotic stimuli	142-143
4.5	DFO does not prevent apoptosis induced by ectopic Noxa expression	146
4.6	H ₂ O ₂ -induced increase in Noxa expression is specifically mediated by lysosomal membrane permeabilization.....	148

4.7	Exogenous iron specifically increases Noxa expression	151
4.8	Oxidative stress-induced LMP promotes Noxa-dependent apoptosis	156

LIST OF TABLE

	PAGE
2.1 Changes in mRNA expression of Bcl-2 genes induced by <i>bcl-x</i> deficiency were determined by microarray analysis	43

CHAPTER I

GENERAL INTRODUCTION

1.1. Programmed cell death (Apoptosis)

The word apoptosis is coined from Greek origin meaning “dropping off or falling off,” and it is taken from the process by which leaves fall from trees or petals from flowers. Apoptosis is a biological process by which all multicellular organisms selectively eliminate damaged, infected, unwanted, or potentially neoplastic cells from the body [1-3]. It involves a programmed sequence of events ultimately resulting in the elimination of cells and/or cell debris. Apoptosis is one of the most common mechanisms by which the body eliminates damaged cells without local inflammation from leakage of cellular contents. Cell contents are eliminated from the body by phagocytic macrophages [4]. Apoptosis plays critical role in normal development, disease progression, and maintenance of tissue homeostasis, and serves as a defense strategy against the emergence of cancer [5]. Apoptosis is usually under stringent genetic control and can be activated by stimuli from multiple sources.

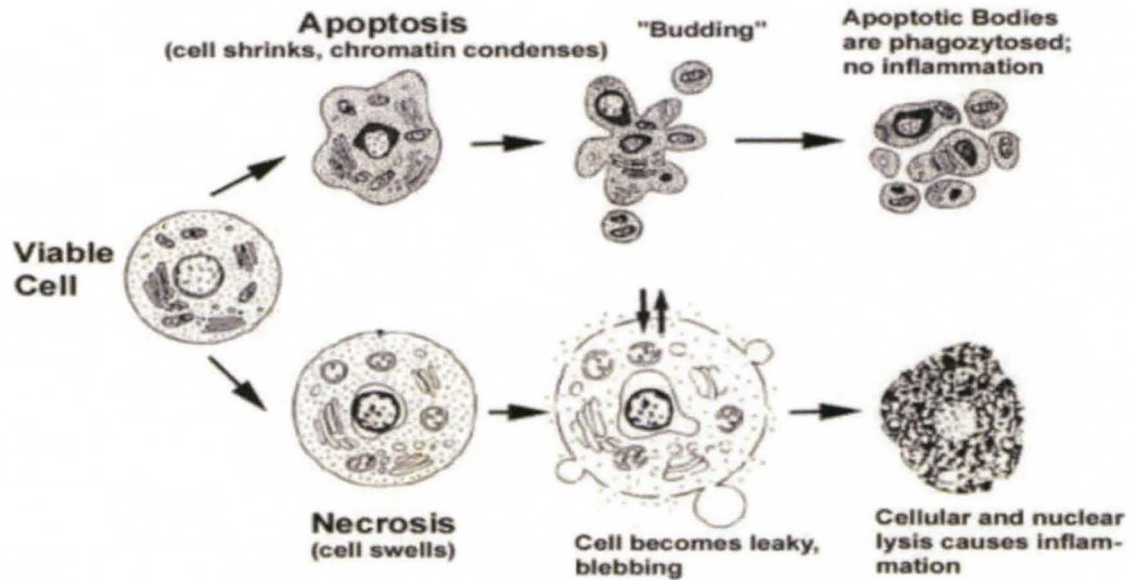
Apoptosis occurs through a series of biochemical events which cause a large number of morphological changes in the cells including shrinking of the cells, blebbing of membrane, condensation and fragmentation of the nuclear material,

and formation of apoptotic bodies. In apoptotic cells, the membrane phospholipid phosphatidyl serine (PS), which is normally localized on the cytosolic side of cell membrane, becomes exposed on the extracellular side of the cell. The mitochondrial membrane breaks open with the release of apoptogenic proteins including cytochrome c and Diablo/Smac from the inter-membrane space (IMS) of the mitochondria to the cytosol ultimately leading to cell death [4, 6, 7]. Apoptosis is initiated in response to certain developmental signals or in the presence of various stimuli including deprivation of essential growth factors, binding of ligand receptors such as tumor necrosis factor receptors (TNFR) on cell surfaces, DNA damage, loss of cellular attachment, decrease in local concentration of tissue morphogens, or major changes in homeostatic state of the cell [3, 8].

Another form of cell death is known as necrosis. Cell death by necrosis differs from cell death by apoptosis, and it can be the result of injury, excessive stress or extreme exposure to intolerable physiological conditions including heat, toxins, hypothermia, mechanical trauma or hypoxia [9-11]. Morphological changes in cells undergoing necrosis include cell swelling, cell rupture, chromatin digestion, and disruption of organelle membranes such as the mitochondrial membrane (Figure 1.1) [11]. As a result, cell contents are released into surrounding tissues where they cause cellular and nuclear lysis, leading to an inflammatory response [11, 12]. Inflammatory response is not present in apoptotic cell death because cell debris and apoptotic bodies are removed by phagocytic macrophages.

Necrosis is almost always detrimental and can be fatal to the organism, whereas apoptosis is a natural cellular process that can either be detrimental or provide some beneficial effects to the organism.

Dysregulation of apoptosis is implicated in the development of many disease states such as cancers and neurodegenerative diseases including Alzheimer's, Huntington's and Parkinson's diseases [13-15]. Excess or limited apoptosis can disrupt tissue homeostasis of multicellular organisms. If apoptosis occurs more than cell proliferation, neurodegenerative diseases will be exacerbated. Insufficient apoptosis on the other hand can accelerate cancer development [7, 15]. Therefore, maintaining a balance between apoptosis and cell proliferation is critical for the well-being of all multicellular organisms.



Van Cruchten, S. and Van Deb Broeck. Anatomia, Histologia, Embryologia, 2002. 31(4): p. 214-223

Figure 1.1. Morphological changes in cells during apoptosis and necrosis

[11].

1.2. Biological significance of apoptosis

1.2.1. Proper development

Since the 1930s, apoptosis has been recognized as an important process in development. The involvement of apoptosis in development has been well studied in three organisms: nematodes (*Caenorhabditis elegans*), fruit flies (*Drosophila melanogaster*) and mouse (*Mus musculus*). In *C. elegans*, during embryogenesis and soon after cell division, development of the hermaphrodite involves cell death of approximately 131 of the 1090 somatic cells through apoptosis [16]. In *D. melanogaster*, apoptosis is critical for the completion of development, and studies have shown that developmental disorders and/or death may occur once apoptosis is inhibited [5, 17].

During the early stages of development in the mammalian nervous system, about 50% of neurons undergo apoptosis [18]. The formation of synapses between neurons in brain and spinal cord also requires the elimination of excess cells by apoptosis. During nerve cell development and attachment to their target cells and organs, more nerve cells are generated than their target cells. Excess nerve cells are eliminated by apoptosis to adjust the number of nerve cells to the size of target organ(s), thereby matching the number of developing nerve cells to the number of target cells and organs. During embryonic development, apoptosis helps to remodel tissues, sculpture the body, shape the organs, and carve out the fingers and toes. For instance, formation of proper fingers and toes in the

fetus requires removal of tissues between them by apoptosis. In this process, massive apoptosis occurs between the digits (fingers and toes), resulting in the separation of the digits (Figure 1.2A). Without sufficient apoptosis, the digits remain joined by soft tissues as seen in the duck hind limbs (Figure 1.2B) [19].

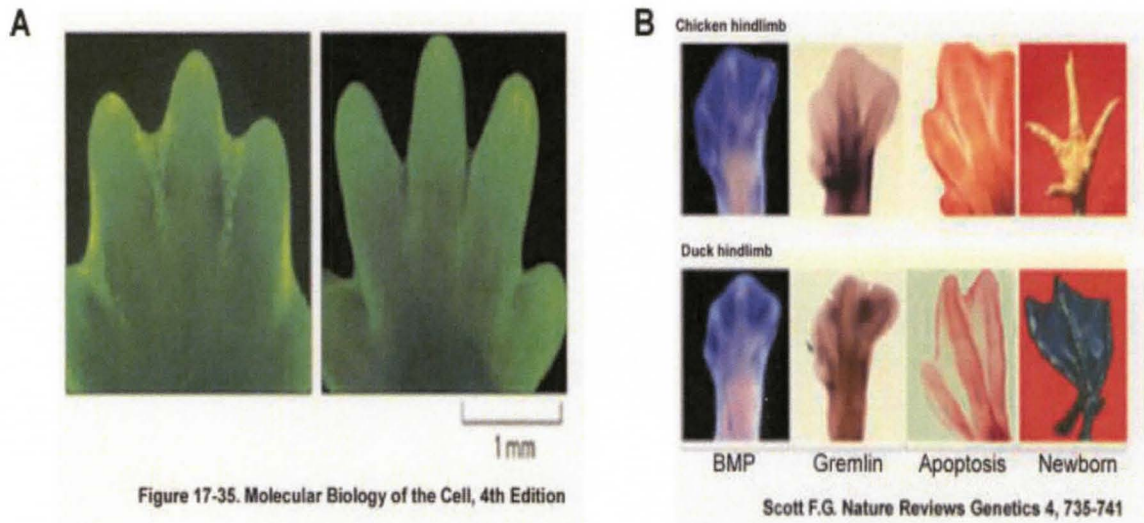


Figure 1.2. Apoptosis is important for proper development. (A) Cells between the digits undergo apoptosis to generate proper fingers and toes. **(B)** Insufficient apoptosis cause the cells in digits to remain joined by soft tissues as seen in the duck hind limbs [19].

1.2.2. Maintenance of tissue homeostasis

In an average human adult, billions of cells die every day due to apoptosis. Dead cells are constantly replaced with new cells originating from the body's stem cell populations [20]. Normal tissue homeostasis or constant internal environment is regulated by apoptosis. In a healthy organism, the rate of cell proliferation is approximately the same as the rate of apoptosis. This balance in apoptotic state is critical for the well-being of all multicellular organisms. If cells die more than they are being replaced, disease conditions such as neurodegeneration will be accelerated. On the other hand, insufficient apoptosis can result in cancer development [21]. Millions of B and T cells are generated daily in the immune system. The majority of these cells (> 95 %) die during maturation by apoptosis. Deletion of expanded effector T cells during immune responses, preservation of T cell memory and general homeostasis of immune cells are caused by apoptosis.

1.2.3. Elimination of unwanted cells

Abnormal cells, cells with unrepaired damaged DNA, and/or potentially neoplastic cells are eliminated from the body by apoptosis. Cells respond to DNA damage in one of three ways: (i) damaged DNA is either repaired by the cell's DNA repair machinery and cells resume their normal activity; (ii) damaged DNA can guide dividing cells into cell cycle arrest. Cell division stops until the damaged DNA is either repaired or destroyed. Cells resume normal cell cycle only when the damaged DNA is repaired; (iii) finally, if the damage to the DNA is

too severe to be repaired, cells are forced to undergo apoptosis. DNA damage in cells can disrupt proper embryonic development that induces severe teratogenic and mutagenic effects leading to development of many cancers [22, 23]. Cells therefore have developed protective defensive machinery to detect and repair damaged DNA or trigger apoptosis. In response to DNA damage, cells activate the genomic guardian protein p53 [24-26]. As a potent inducer of apoptosis, p53 triggers apoptosis to eliminate the cells with irreparable DNA damage from the body. Most cancer cells often have defective p53 proteins which allow them to evade apoptosis and proliferate uncontrollably.

Apoptosis also plays an important role in elimination of cells that pose threats to the organism. For example, self-reactive cells of the immune system and virally infected cytotoxic T cells are eliminated from the body by apoptosis [27].

1.3. Pathways of apoptosis

Apoptosis generally occurs through one of three signaling pathways, including the mitochondrial (intrinsic), the death receptor (extrinsic), and the mixed pathways.

1.3.1. Intrinsic (mitochondrial) pathway of apoptosis

Death stimuli generated from within the cell activate the intrinsic pathway of apoptosis. In the presence of death stimuli, signals are translocated to the mitochondria where they activate the pro-apoptotic Bcl-2 proteins, resulting in formation of permeation channels on the outer mitochondrial membrane (OMM) through which apoptogenic proteins including cytochrome c and Diablo/Smac leave the mitochondrial inter membrane space (IMS) and enter the cytosol. While in the cytosol, cytochrome c and Diablo/Smac activate a cascade of caspase reactions ultimately leading to apoptosis [28, 29]. Cytochrome c activates the apoptotic protease activating factor 1 (apaf-1), which in turn promotes the transition of the inactive forms of caspases (zymogen, pro-caspases) to their active counterparts (caspases), while Diablo/Smac directly interacts with inhibitors of apoptosis proteins (IAPs) and disrupts their ability to inactivate caspases, thereby promoting apoptosis (Figure 1.3) [30, 31].

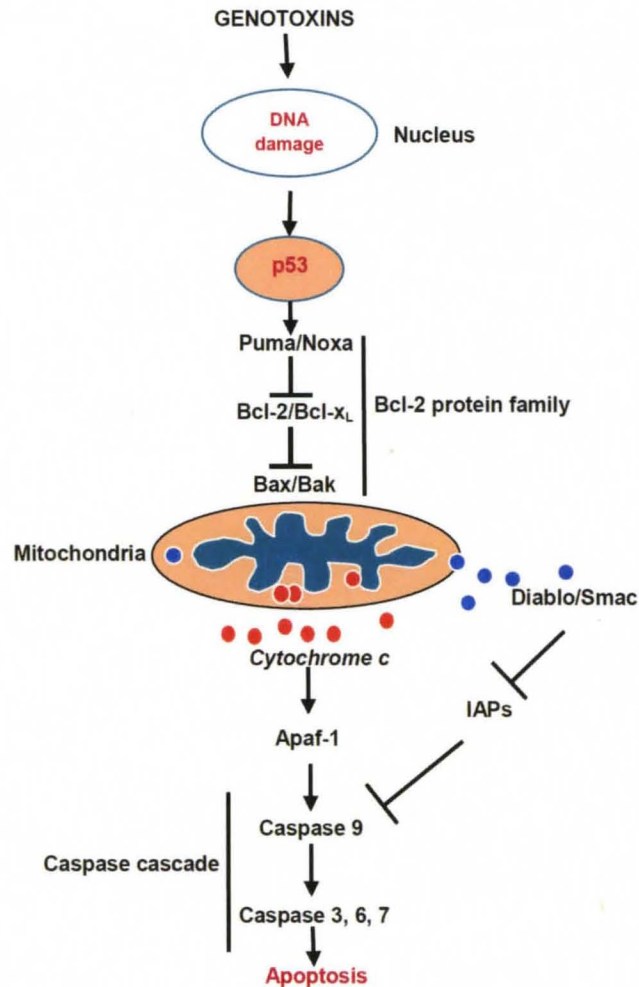


Figure 1.3. The intrinsic (mitochondrial) pathway of apoptosis. In the presence of apoptotic stimuli such as DNA damage, p53 is activated. Activated p53 then activates pro-apoptotic Bcl-2 protein members which interact on the OMM to form permeation channels which allow cytochrome C and Diablo/Smac to leave the mitochondria and enter the cytosol. In the cytosol, cytochrome c then initiates a caspase cascade ultimately leading to apoptosis, while Diablo/Smac interacts with IAPs and disrupts their ability to inhibit caspases thereby also leading to apoptosis.

1.3.2. Extrinsic (death receptor) pathway of apoptosis

Unlike the intrinsic pathway of apoptosis where death signals are initiated from within the cell, death signals for extrinsic pathways of apoptosis are initiated from outside the cell. Activation of extrinsic pathways of apoptosis does not involve the mitochondria, interactions of the Bcl-2 proteins or release of cytochrome c from the mitochondrial IMS to the cytosol. Here, specific death ligands such as tumor necrosis factor (TNF), Fas Ligand (FasL) or TNF-related apoptosis-inducing ligand (TRAIL) bind to their respective specific transmembrane death receptors including Fas, tumor necrosis factor receptor 1(TNFR1), p75, DR4 [32].

Binding of death ligands to their respective death receptor promotes the clustering and recruitment of the adaptor protein Fas-associated death domain (FADD) and the inactive forms of the initiator caspases 8 and 10 (pro-caspases 8 or 10), thereby forming the death-inducing signaling complex (DISC). Therefore, the DISC is made up of the FADD, caspase 8 and caspase 10. The DISC brings the pro-caspase molecules in close proximity, ensuring access for their autocatalysis and release into the cytosol [33-37]. Caspase 8 or 10 then activates the effector caspases 3/6/7 in a caspase cascade reaction leading to apoptosis (Figure 1.4).

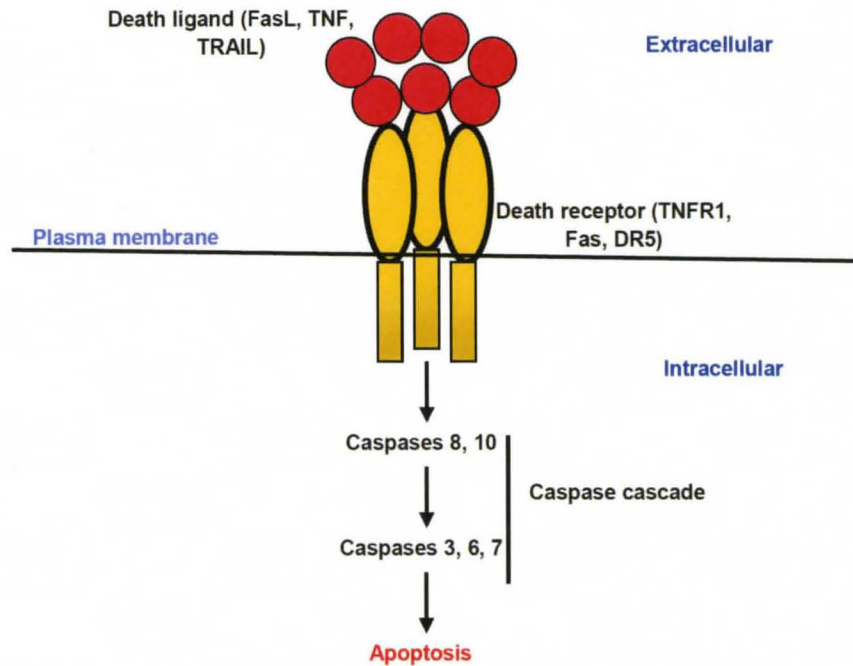


Figure 1.4. The extrinsic (death receptor) pathway of apoptosis. Extrinsic apoptotic signaling pathway is generated from outside the cell. Initiation of apoptosis results in binding of death ligands to specific transmembrane death receptors, which causes clustering and recruitment of the adaptor molecule FADD, procaspase 8, 10 to form the DISC, subsequently activating-caspase 8, 10. Caspase 8, 10 then activates caspase 3/6/7 ultimately leading to apoptosis.

1.3.3. The mixed pathway of apoptosis

While activation of apoptosis in most cells can be initiated either from within the cell (intrinsic) or outside the cell (extrinsic), there are certain instances where induction of apoptotic signaling pathways from external sources can also lead to activation of both intrinsic and extrinsic apoptotic pathways (mixed pathway). In this paradigm, death stimuli generated from outside the cell cause activation of pro caspase 8, pro caspase 10, and formation of the DISC in a similar fashion as observed with the extrinsic pathways. The formation of the DISC will ultimately lead to autocatalysis and activation of caspase 8 and 10 [33-37].

Activated caspase 8 can enter one of two routes: (i) it can activate the effector caspases 3, 6 and 7, leading to apoptosis as in the extrinsic pathway or (ii) it can enter the intrinsic pathway of apoptosis by interacting with the Bcl-2 family of proteins. In this case, caspase 8 cleaves the inactive pro-apoptotic BH3-only protein Bid into its truncated (activated) form (tBid). The tBid then activates the Bcl-2 proteins Bax and Bak at the OMM. Bak and Bax undergo conformational changes and oligomerize resulting in formation of permeation pores on the OMM. Cytochrome c and Diablo/Smac then are released from the mitochondrial IMS into the cytosol where they exert their pro-apoptotic effects in the same fashion as they do in the intrinsic apoptotic signaling pathways [28, 29] as shown in Figure 1.5.

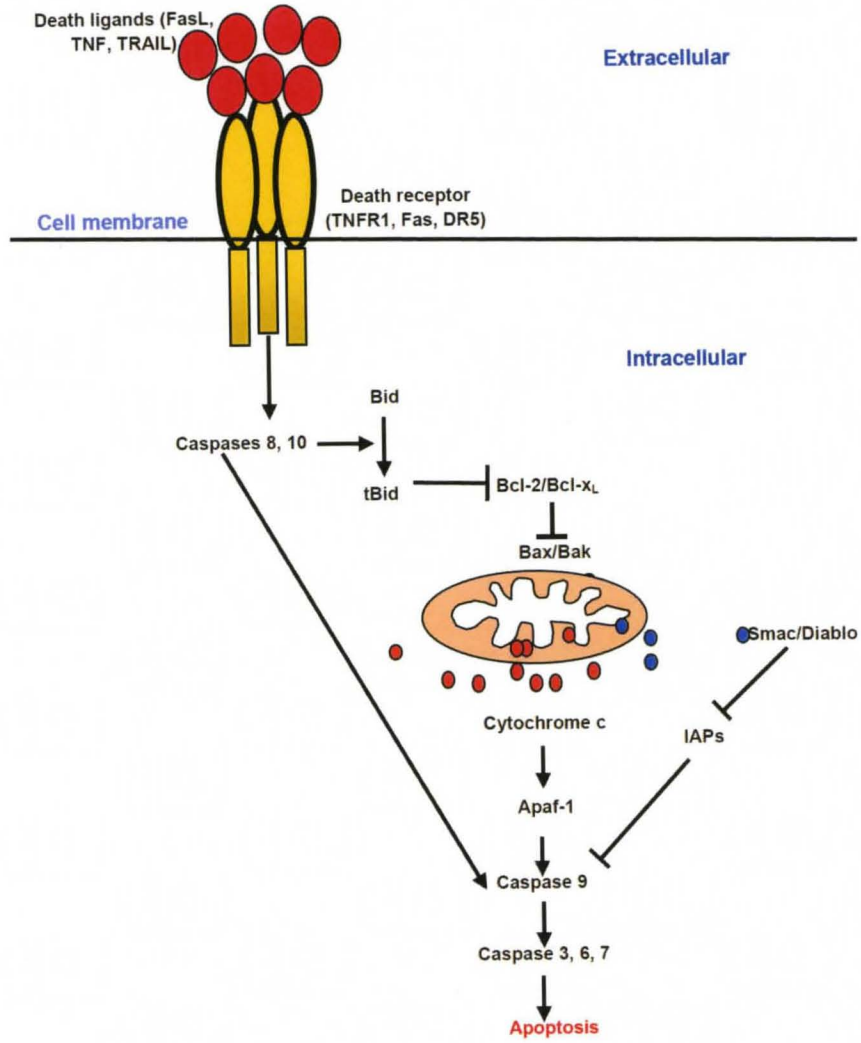


Figure 1.5. The mixed pathway of apoptosis. Stimuli from extracellular sources lead to DISC formation and activation of caspases 8 and 10. Activated caspase 8 and 10 can either cleave effector caspases to cause cell death (as with the extrinsic pathway) or can enter the intrinsic pathway by interacting with the Bcl-2 family of proteins. Caspase 8 converts full-length Bid into tBid which then interacts with Bax/Bak inducing their oligomerization and formation of permeation pores on the OMM, allowing apoptogenic proteins such as cytochrome c and Diablo/ Smac from the mitochondria into the cytosol where they exert their effects.

1.4. Regulation of apoptosis

Apoptosis is primarily regulated by the caspases and the Bcl-2 family of proteins.

1.4.1. Caspases

Caspases are a group of cysteine proteases which cleave proteins at sites proximal to aspartic acid residues [38]. Caspase activation usually is considered the molecular hallmark of apoptosis [39]. Caspases exist in their inactive forms (pro-caspase), and are activated during apoptosis by pro-apoptotic proteins [40]. To date about 12 caspases have been identified, but not all caspases are involved in regulation of apoptosis. For instance, caspase 1 is critical for the regulation of the biological processes irrelevant to cell death including maturation of red blood cells and skeletal muscle myoblasts, while caspase 14 is essential in skin cell development [41].

Two classes of caspases involved in apoptosis are the initiator (apical) and the effector (executioner) caspases. Initiator caspases, including caspases 2, 8, 9 and 10, are activated in response to upstream apoptotic stimuli. Initiator caspases cleave and process the effector caspases 3, 6 and 7. Once activated, effector caspases are responsible for triggering cell death by degrading key structural proteins within cells.

1.4.2. The Bcl-2 proteins

The Bcl-2 family of proteins is one of the major regulators of the intrinsic pathway of apoptosis. They derived their name from *B-cell lymphoma/leukemia 2*, as the second member of a range of proteins initially discovered during chromosomal translocations involving chromosomes 14 and 18 in human follicular lymphomas [42]. Bcl-2 is the founding members of the Bcl-2 family of proteins and is encoded by Bcl-2 gene [43]. To date, approximately 20 different members of the Bcl-2 protein family have been identified. Members of the Bcl-2 family of proteins all share one to four homologous Bcl-2 homology (BH) domains important for homo- and hetero-dimeric interactions among different family members. Bcl-2 proteins can be pro-apoptotic or anti-apoptotic [3, 44, 45] based on the number of BH domains and their ability to regulate apoptosis [46].

1.4.2.1. The pro-apoptotic Bcl-2 proteins

The pro-apoptotic Bcl-2 proteins are critical for the initiation and or activation of the intrinsic pathway of apoptosis. They are divided into two structurally and functionally distinct categories: multidomain and BH3-only Bcl-2 proteins [47].

1.4.2.1.1. The multidomain pro-apoptotic Bcl-2 proteins

The multidomain pro-apoptotic Bcl-2 proteins Bax, Bak and Bok share three BH domains (BH1-BH3). They are responsible for forming permeation channels on the OMM, which in turn disrupt mitochondrial membrane integrity during

apoptosis thus allowing the release of apoptogenic proteins from the mitochondria to the cytosol. While Bax and Bak are ubiquitously present in all tissues, Bok is expressed only in reproductive cells [48]. In healthy cells, Bax and Bak are localized in different subcellular compartments. Bak is constitutively integrated in the OMM, while Bax is localized in the cytosol. The carboxyl-terminal membrane-anchoring region of Bax is normally sequestered into its hydrophobic pocket keeping Bax constitutively inactive in the cytosol [49]. But in the presence of death stimuli, Bax undergoes conformational changes at both the amino- and carboxyl- termini, leading to its translocation to the OMM and eventual formation of large oligomeric complexes [50, 51]. Since Bak resides solely in the mitochondria, in the presence of apoptotic stimuli Bak changes conformation and forms oligomeric complexes as well [52]. Oligomeric Bax and Bak form permeation channels on OMM to facilitate the release of cytochrome c and Smac/Diablo from mitochondrial IMS to the cytosol where they carry out their pro-apoptotic functions.

Bax can also be activated in ER during apoptosis [53]. Studies have shown that most mice deficient in both Bax and Bak (double knockout, DKO) die during embryonic stages, but the few that survive to adulthood have an accumulation of excessive cells in various tissues [54]. Cells from Bax and Bak DKO mice are highly resistant to apoptosis induced by all stimuli triggering the mitochondrial signaling apoptotic pathway [54]. Activation of Bax and Bak proteins are therefore critical for the initiation of apoptosis in mammalian cells.

1.4.2.1.2. The pro-apoptotic BH3-only Bcl-2 proteins

The pro-apoptotic BH3-only Bcl-2 proteins, including Noxa, tBid, Puma, Bim, Bmf, Bik, Nix, Bnip3, Bad, and Hrk, all have only a single BH3 domain in common [6]. The BH3 domain is an interactive domain that is necessary and sufficient for the killing action of BH3-only Bcl-2 proteins. They are activated by many diverse apoptotic stimuli, including deprivation of essential growth factor, cell-cell or cell-matrix interactions, ER stress, exposure to physical or chemical DNA damaging agents, viruses, bacteria, or TNF-like cytokines via transcriptional upregulation, changes in subcellular localization, altered protein stability or post-translational modifications. Not all BH3-only Bcl-2 proteins are activated by a single apoptotic stimulus. They are always under stringent control at the transcriptional and post-translational levels [6].

1.4.2.1.2.1. Transcriptional and post-translational regulation of BH3-only Bcl-2 proteins

As mentioned earlier, the BH3-only Bcl-2 proteins are under strict transcriptional and/or post-translational control. Different BH3-only Bcl-2 proteins are activated by various stimuli through different mechanisms, depending on the cell type and the type of stimuli present. The BH3-only Bcl-2 proteins Puma, Noxa, Bim and Hrk are subject to stringent transcriptional control, whereas the rest of the other BH3-only Bcl-2 proteins are mostly activated by post-translational modification. Both Noxa and Puma are activated by the tumor suppressor protein p53 usually

in the presence of apoptotic stimuli that generate stress to the cell such as DNA damage [55, 56]. DNA damage causes p53 activation subsequently increasing Noxa and Puma mRNA and protein expression in thymocytes and fibroblasts [55, 56]. Transcriptional control of Bim is much more complex and different from that of Puma and Noxa. Withdrawal of essential growth factors cause increased expression of Bim in both neuronal [57] and hematopoietic cells [58]. Bim expression is also induced transcriptionally by ER stress through the transcription factor CHOP [59]. In apoptotic cells Bim is stabilized by JNK, and in healthy cells it is destabilized by Erk1/2 [60, 61]. Hrk is induced during embryogenesis in neuronal tissues containing relatively large number of apoptotic cells including the trigeminal and dorsal root ganglia, and the anterior horn of the spinal cord [62]. In murine myeloid and lymphoid progenitor cells, withdrawal of essential growth factor induces Hrk expression sufficient to trigger apoptosis [63]. Hrk is also activated transcriptionally by stress activated/c-jun N-terminal kinase (SAPK/JNK) [64, 65].

Other BH3-only Bcl-2 proteins, including Bad, Bik, Bid, Bim and Bmf, are regulated by post-translational modification, which makes them active and available to interact with other proteins. Bad is activated by dephosphorylation and deactivated by phosphorylation. Bad is deactivated by phosphorylation at several serine residues (S-112, S-136 and S-155) by kinases including AKT, protein kinase A (PKA), and Raf-1[66-68]. In cells undergoing apoptosis, Bad is dephosphorylated by the phosphatases protein phosphatase 2A (PP2A) or

calcineurin [69]. Like Bad, Bik is also modified post-translationally by phosphorylation. However, phosphorylation of Bik by casein kinase II or related enzymes activates Bik protein [70]. In contrast to Bad and Bik, Bid is activated by a different post-translational modification mechanism. In healthy cells, inactive full-length Bid is localized in the cytosol. In the presence of apoptotic insults, Bid is processed by caspase 8 into its truncated fragment, tBid [71]. The tBid is then translocated to the mitochondria where it interacts with pro-apoptotic multidomain Bcl-2 proteins including Bax and Bak to exert its pro-apoptotic activities.

In addition to transcriptional activation, Bim is also activated post-translationally. Bim and Bmf are two BH3-only Bcl-2 proteins regulated by sequestration of cytoskeleton structure inside cells [72]. In healthy cells, Bim is sequestered to the microtubule dynein motor complex through its interaction with Dynein Light Chain 1 (DLC1/LC8) [72]. Bmf is sequestered to the actin cytoskeleton-based myosin V motor complex through its interaction with dynein light chain. In response to stress stimuli such as detachment of cells from the substratum (anoikis) or drugs that depolymerize actin, Bmf is released to trigger apoptotic signaling.

The different pro-apoptotic BH3-only Bcl-2 proteins are activated based on the type of stress to the cell. The BH3-only Bcl-2 proteins interact with either anti-apoptotic members (Bcl-x_L, Bcl-2, and Mcl-1) or pro-apoptotic multidomain members (Bax and Bak) at the mitochondria level to exert their pro-apoptotic

effects. Recent studies suggest that the interaction between BH3-only Bcl-2 proteins with anti-apoptotic or pro-apoptotic multidomain Bcl-2 proteins also take place on the ER membrane thereby making the ER an important organelle for initiation and activation of apoptosis [73].

1.4.2.2. The anti-apoptotic Bcl-2 proteins

To date, five anti-apoptotic Bcl-2 proteins have been identified in mammals, including Bcl-x_L, Bcl-2, Mcl-1, Bcl-w, and A1. The anti-apoptotic Bcl-2 proteins share up to four conserved BH domains (BH1-BH4) and the membrane-targeting hydrophobic carboxy terminal regions. The anti-apoptotic Bcl-2 proteins delay or prevent apoptosis [15]. They are mostly localized on membrane surfaces including the OMM, the nuclear membrane, and the ER membrane [74]. The anti-apoptotic Bcl-2 proteins maintain the OMM integrity and protect cells against a wide range of apoptotic stimuli, therefore they are essential for cell survival [46, 74, 75]. The activities of the anti-apoptotic Bcl-2 proteins have been well examined both by overexpression and gene targeting knock-out studies. Overexpression of all anti-apoptotic Bcl-2 proteins has shown protection of cells from apoptosis initiated by various apoptotic stimuli [3]. A more defined function of each of the five anti-apoptotic Bcl-2 proteins has been established using the gene targeting studies in diverse cell types and tissues [3, 76, 77].

The founding member Bcl-2 is required for the survival of mature lymphocytes, melanocyte stem cells and cells of developing kidneys [78, 79]. Bcl-x_L and Mcl-1 are important for embryonic development, and embryos deficient in either Bcl-x_L or Mcl-1 do not survive. Embryos lacking Bcl-x_L expression die in utero, with extensive apoptosis throughout their developing nervous and hematopoietic systems [80]. In addition, Bcl-x_L is also required for the survival of mature erythrocytes [81, 82]. Mcl-1 deficiency caused failed implantation. By studying conditional knockout mice, Mcl-1 is shown to be essential for survival of the hematopoietic progenitors, mature B- and T- lymphocytes [83]. Bcl-w is required for sertoli cell survival in the testis [84] and A1 is critical for neutrophil survival [85]. The exact molecular and biochemical mechanisms by which anti-apoptotic Bcl-2 proteins keep cells alive is controversial and has not yet been universally accepted. Depending on the nature of stress to the cells, the anti-apoptotic Bcl-2 proteins specifically suppress the activities of the pro-apoptotic Bcl-2 proteins to maintain cell viability.

1.4.2.2.1. The *bcl-x* gene

One of the mammalian genes identified as a suppressor of apoptosis is the *bcl-x* gene [86]. Boise et al (1993) first discovered the *bcl-x* gene in chicken, and identified two distinct Bcl-x cDNAs in human: BCL-x_L and BCL-x_S, generated from alternative splicing of the Bcl-x [12]. BCL-x_L and BCL-x_S have similar structure except that an internal deletion of 63 amino acids of Bcl-x_L due to alternative

splicing generates Bcl-x_S. Whereas Bcl-x_L contains all the four BH domains [BH(1-4)], Bcl-x_S has only two of the four BH domains [BH(3-4)]. Bcl-x_L has remarkable amino acid and structural homology to the founding member of the Bcl-2 family proteins, Bcl-2. Bcl-x_L was shown to prevent apoptosis in interleukin-3 (IL-3)-dependent cells following deprivation of essential growth factor, but this was not the case with Bcl-x_S. Instead, Bcl-x_S promoted apoptosis by inhibiting the death suppressor activities of Bcl-2. Therefore, Bcl-x_L and Bcl-x_S display opposite activities in apoptotic regulation [12]. Later studies have shown that Bcl-x_L inhibits apoptosis by forming hetero-dimeric complexes with pro-apoptotic Bcl-2 proteins making them inactive [87]. The role of Bcl-x_S in apoptosis is poorly understood, but is mostly considered pro-apoptotic [81]. Some studies suggest that Bcl-x_S antagonizes the anti-apoptotic functions of Bcl-x_L [88, 89], but it is unclear whether Bcl-x_S functions simply as an inhibitor of anti-apoptotic Bcl-2 proteins or if it can directly induce apoptosis. Bcl-x_L and Bcl-x_S are expressed in variety of tissues and their expression is differentially regulated [12]. In cells, Bcl-x_L is localized on the mitochondria, the ER and the perinuclear envelope. Bcl-x_L is the dominant form of the Bcl-x mRNA expressed in murine tissues during embryogenesis and postnatal development.

Like other anti-apoptotic Bcl-2 proteins, Bcl-x_L is overexpressed in many cancer cells including breast cancer cells, neuroblastomas, myelomas, lymphomas and hepatomas [74, 75]. Extremely high levels of Bcl-x_L in cancer cells make them resistant to chemotherapeutic agents leading to limited apoptosis and poor

clinical outcome [74]. Therefore, new drugs designed to reduce Bcl-x_L expression levels in these cancer cells will complement current cancer therapies.

1.4.2.3. Regulation of OMM permeabilization by the Bcl-2 proteins

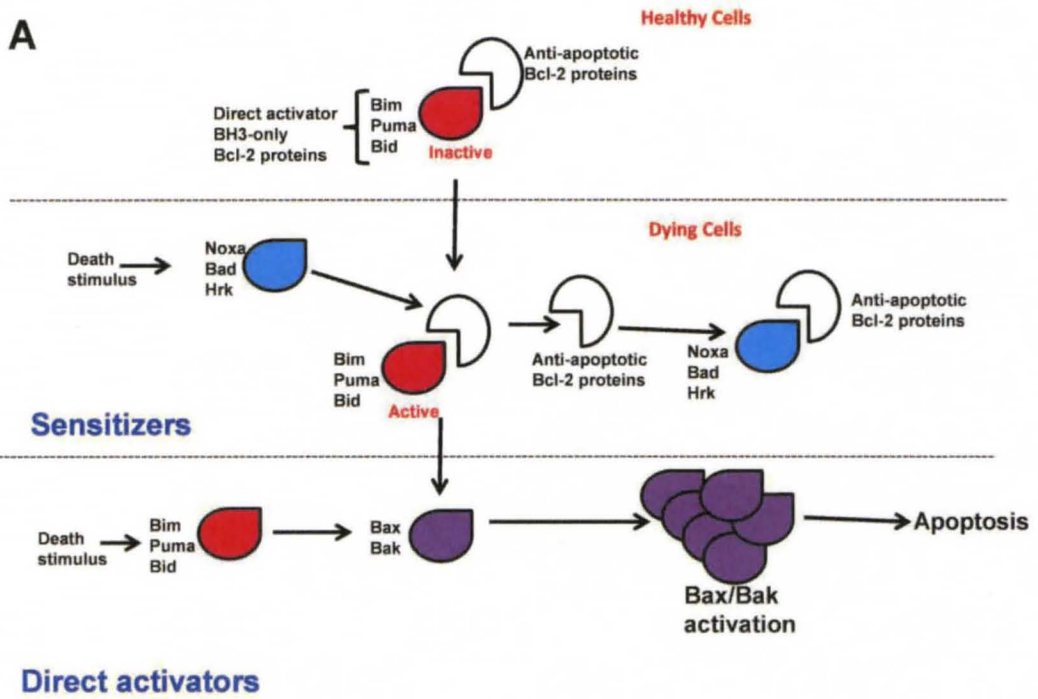
How the Bcl-2 proteins interact at mitochondrial and ER membrane levels to regulate apoptosis is still controversial and unclear. Genetic and biochemical studies showed that Bax and Bak are required for apoptosis and outer mitochondrial membrane permeabilization (OMMP) [90]. The pro-apoptotic BH3-only Bcl-2 proteins are categorized into two groups based on their ability to interact with Bax and Bak, or the anti-apoptotic Bcl-2 proteins. Two models for Bax and Bak activation have been proposed including the direct activation and the displacement models [74].

In the direct activation model, the BH3-only Bcl-2 proteins are again classified into two groups known as the direct activators, including Bim, tBid, and Puma, and the sensitizers (de-repressor), including the rest of the BH3-only Bcl-2 proteins [91]. For the direct activator BH3-only Bcl-2 proteins, direct activators directly interact with Bax and Bak. Here, in healthy cells, the direct activators are constitutively active and are kept inactive by forming hetero-dimeric complexes with anti-apoptotic Bcl-2 proteins. But in dying cells, the direct activators are dissociated from their anti-apoptotic binding partners by various mechanisms,

and interact directly with Bax and Bak leading to their activation. The interaction between Bax and Bak and the direct activators BH3-only Bcl-2 proteins is the main event necessary for engagement of OMM. In contrast, activation of Bax and Bak by the sensitizers BH3-only Bcl-2 proteins is much different. Unable to directly interact with Bak and Bax, the sensitizer BH3-only Bcl-2 proteins cannot induce Bax and Bak activation directly [74]. Instead, the sensitizers bind to the anti-apoptotic Bcl-2 proteins with high affinity freeing them from their complexes with the direct activator BH3-only Bcl-2 proteins. The released direct activators in turn initiate Bax- and Bak-mediated OMM permeabilization and subsequent apoptosis cascade [92].

Another proposed model for activation of Bax and Bak is the displacement model. In this model, Bax and Bak with constitutive activity are kept inactive by forming complexes with the anti-apoptotic Bcl-2 proteins. But in cells undergoing apoptosis, BH3-only Bcl-2 proteins bind to these anti-apoptotic Bcl-2 proteins with higher affinity and displace them from their complexes with Bax and Bak. Freed Bax and Bak are now activated and are able to induce OMM permeabilization and subsequent apoptosis.

A



B

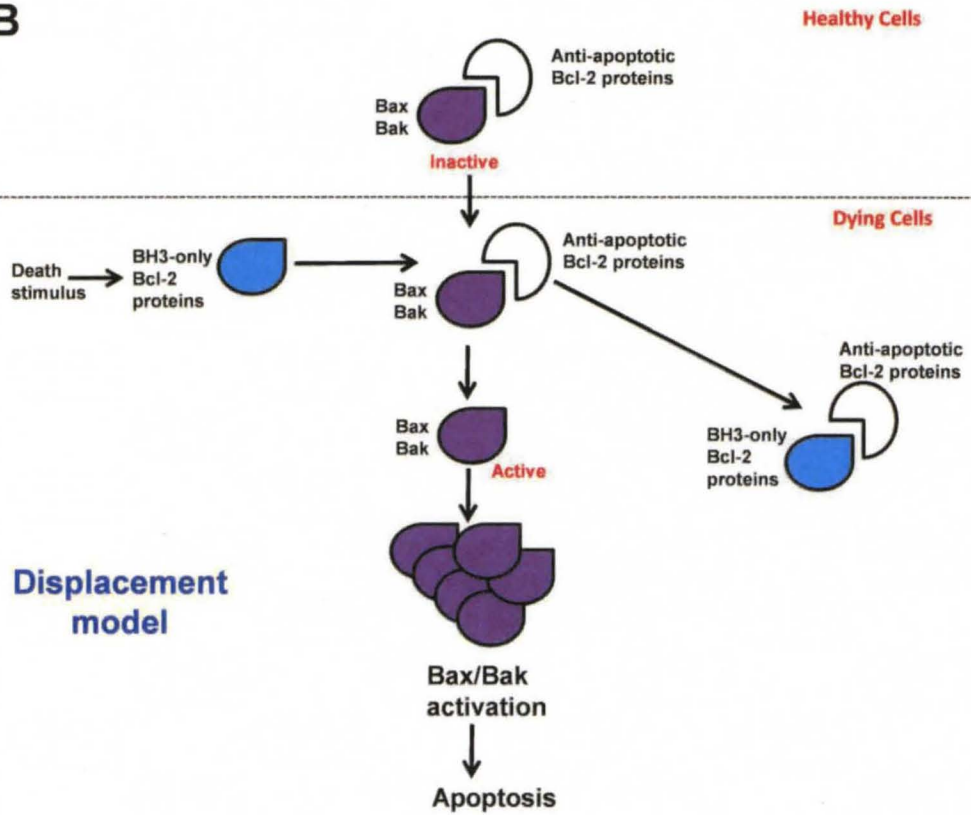


Figure 1.6. Activation of outer mitochondrial membrane permeabilization by

Bcl-2 protein family. (A) Direct activation model. Here, the BH3-only Bcl-2 proteins are classified into two groups known as the direct activators, including Bim, and the sensitizers including Noxa. The direct activator BH3-only Bcl-2 proteins Bim, tBid and Puma interact directly with Bax and Bak leading to their activation and subsequent apoptosis. The sensitizer BH3-only Bcl-2 proteins Noxa and Bad do not interact with Bax and Bak directly. Instead, the sensitizers bind to the anti-apoptotic Bcl-2 proteins with high affinity freeing them from their complexes with the direct activator BH3-only Bcl-2 proteins. The released direct activators in turn initiate Bax- and Bak-mediated OMM permeabilization and subsequent apoptosis. **(B) Displacement model.** In this model, Bax and Bak with constitutive activity are kept inactive by forming complexes with the anti-apoptotic Bcl-2 proteins. But in cells undergoing apoptosis, BH3-only Bcl-2 proteins bind to these anti-apoptotic Bcl-2 proteins with higher affinity and displace them from their complexes with Bax and Bak. Freed Bax and Bak are now activated and are able to induce OMMP and subsequent apoptosis.

1.5. Hypothesis and significant of the project

1.5.1. Hypothesis and specific aims

In this thesis, we specifically addressed the molecular, and biochemical mechanisms through which endogenous Bcl-x_L regulate apoptotic signaling pathways. As mentioned earlier, the Bcl-x_L protein is generated from alternative splicing of Bcl-x. Previous studies have shown that mouse embryos deficient die Bcl-x around day 13 of embryogenesis [80]. Bcl-x is therefore indispensable for embryonic development. Regulation of both the expression and splicing of Bcl-x during development is important in the determination of susceptibility of cells to apoptosis [80].

In this thesis, we first developed mouse embryonic fibroblasts (MEFs) either deficient in Bcl-x (knock out, Bcl-x-KO) or expressing Bcl-x (wild type, Bcl-x-WT). MEFs were then used to study the molecular mechanisms by which endogenous Bcl-x_L regulates apoptotic signaling pathways. Our overall hypothesis is that **intracellular localization of endogenous Bcl-x_L is critical for its anti-apoptotic activities and that endogenous Bcl-x_L coordinates with other members of the Bcl-2 protein family to regulate apoptosis.** Previous studies have shown that overexpression of Bcl-x_L in cells renders them resistant to apoptosis insults. The exact mechanism of how endogenous Bcl-x_L prevents apoptosis is still unclear and controversial. One possible explanation is that previous research focused on cells overexpressing Bcl-x_L many fold higher than

its physiological functional level. As Bcl-x_L likely functions by modulating OMM integrity, enforced overexpression of Bcl-x_L could relocate Bcl-x_L protein to non-physiological locations inside cells, leading to unexpected biological consequences. Therefore, studying the activities of Bcl-x_L at the endogenous levels will fill critical gaps in our understanding of the molecular and biochemical mechanisms of Bcl-x_L, and might provide potential targets for cancer therapy. We proposed the following specific aims to examine this hypothesis:

Specific aim 1: Investigate how mitochondria- and ER-localized Bcl-x_L regulate apoptosis and Ca²⁺ homeostasis. Previous studies have shown that anti-apoptotic Bcl-2 proteins regulate apoptosis initiated from different intracellular organelles. As endogenous Bcl-x_L is localized in the mitochondria, the ER, and the cytosol, we investigated the effects of Bcl-x_L targeted to these organelles on apoptosis regulation and Ca²⁺ homeostasis. The carboxyl-terminal transmembrane domain of Bcl-x_L which specifically targets Bcl-x_L to the cytosol was deleted, and replaced with either the mitochondrial targeting sequence of listerial (ActA) or the ER targeting sequence of cytochrome b5 (Cb5) which targets Bcl-x_L to the mitochondria or the ER respectively. These mutant Bcl-x_L proteins were re-expressed in Bcl-x-KO MEFs at levels comparable to that of endogenous Bcl-x_L. Bcl-x-KO MEFs re-expressing different Bcl-x_L mutants were used to investigate the effects of Bcl-x_L proteins localized on different organelles in the regulation of apoptotic stimuli and Ca²⁺ homeostasis.

Specific Aim 2: Study how endogenous Bcl-x_L regulates oxidative stress-induced apoptosis. Oxidative stress inducers, including hydrogen peroxide (H₂O₂), cause necrosis and apoptosis. Mild to moderate oxidative stress triggers apoptosis while severe oxidative stress causes necrosis [93]. The exact mechanism through which oxidative stress inducers promote apoptosis is unclear but recent evidence suggests the involvement of the Bcl-2 proteins. Here, we systematically explored the role of Bcl-2 proteins, particularly Bcl-x_L, in the regulation of H₂O₂-induced apoptosis.

Specific Aim 3: Examine the important role of LMP during oxidative stress-induced apoptosis. Lysosomal membrane permeabilization (LMP) is important in H₂O₂-induced apoptosis. However, the exact role of LMP in H₂O₂-induced apoptosis or how it is regulated by the complex Bcl-2 network is unclear. Here, we investigated the role of LMP in regulating oxidative stress-induced apoptosis by examining the temporal relation between LMP and OMM permeabilization.

1.5.2. Significance of the Project

Results from this project elucidate the detailed mechanisms through which endogenous Bcl-x_L regulates apoptosis. The data provide information for new chemotherapeutic drug targets. Since Bcl-x_L is highly expressed in many cancer cells to enable them evade apoptosis, drugs designed to inhibit Bcl-x_L activities can complement already existing drugs thereby reducing or preventing drug resistance.

CHAPTER II

DISTINCT ROLES OF MITOCHONDRIAL- AND ER-LOCALIZED BCL-x_L IN APOPTOSIS REGULATION AND Ca²⁺ HOMEOSTASIS

2.1. Introduction

The Bcl-2 family of proteins is major regulator of cellular response to apoptotic signaling [45]. Since the founding family member Bcl-2 was shown to protect cells from apoptotic insults [94], more than 20 Bcl-2-related proteins have been identified possessing either anti- or pro-apoptotic functions [45]. Among anti-apoptotic members, Bcl-x_L retains the prototypical structural organization of four BH domains [BH(1-4)] and a membrane-targeting hydrophobic carboxyl terminal region [12, 95]. One important characteristic of Bcl-2 proteins is that they display differential interactions with each other and with other regulatory proteins in the apoptotic cascade, thus profoundly influencing apoptosis [75, 96, 97].

Recent genetic and biochemical studies have revealed a conserved cascade that leads to the disruption of OMM integrity and the release of apoptosis-inducing factors into the cytosol, subsequently resulting in destruction of cells [12, 98, 99]. While anti-apoptotic Bcl-2 proteins are generally believed to promote cell survival by preventing OMM disintegration, pro-apoptotic Bcl-2 family members facilitate

OMM permeabilization during apoptosis [74, 100]. Although most studies have focused on how Bcl-2 proteins modulate OMM integrity during apoptosis, there is a large body of evidence indicating that Bcl-2 proteins are also localized and function on the ER membrane [101, 102]. It has been proposed that ER-resident pro-apoptotic Bcl-2 proteins sense insults to the ER, resulting in death-signals being communicated from the ER to the mitochondria, or apoptosis being directly initiated at the ER level [103-105].

The involvement of ER in anti-apoptotic signaling has been linked to its role as intracellular Ca^{2+} store [104]. Protection of apoptosis induced by overexpression of anti-apoptotic Bcl-2 proteins including Bcl-2, Bcl-x_L or Mcl-1 can be attributed partially to their ability to modulate ER Ca^{2+} signals through interactions with the inositol 1,4,5-trisphosphate receptor (InsP₃R) Ca^{2+} release channel [106-110]. While these studies have been highly informative, they rely largely on overexpression systems to study anti-apoptotic Bcl-2 proteins, which might not reveal the activities of endogenous proteins. More importantly, there have been no studies designed to examine the specific functions of Bcl-x_L at distinct organelles in non-overexpression systems.

To address this, we generated Bcl-x-deficient (Bcl-x-KO) MEFs to study the effect of organelle-specific Bcl-x_L reexpression on apoptosis and ER Ca^{2+} homeostasis. Bcl-x-KO MEFs displayed increased sensitivity to apoptosis and disrupted ER Ca^{2+} homeostasis. Expressing mitochondrially targeted Bcl-x_L in

these MEFs increased apoptotic protection to the levels comparable to wild-type MEFs. In contrast, expression of ER-localized Bcl-x_L completely restored ER Ca²⁺ homeostasis but had no effect on apoptotic protection. When expressed in the wild-type Bcl-x_L background, however, ER-targeted Bcl-x_L did increase apoptotic protection. These data show that mitochondrial localization alone is sufficient to provide protection, but also that it is an absolute requirement for ER-localized Bcl-x_L to be anti-apoptotic.

2.2. Materials and Methods

2.2.1. Reagents

Etoposide, doxorubicin, H₂O₂ and actinomycin D were all purchased from Sigma (St. Louis, MO), while staurosporine was purchased from Enzo (Farmingdale, NY). All reagents were dissolved in dimethyl sulfoxide (DMSO). Lipofectamine 2000 was purchased from Invitrogen (Carlsbad, CA). Unless otherwise stated, all other reagents were purchased from Sigma. Antibodies used for western blot and immunofluorescence analyses were anti-Bcl-x_{S/L} S-18 pAb (Santa Cruz, CA, Cat. # sc-634), anti-β-actin mAb (Sigma), anti-Bak pAb (Upstate; Lake Placid, NY, Cat. # 06-536 NT), anti-Bax N20 pAb (Santa Cruz, Cat. # sc-493), anti-Mcl-1 pAb (Epitomics; Burlingame, CA, Cat. # 1239-1), anti-Bcl-2 mAb (Santa Cruz, sc-7382), anti-Bcl-w mAb (Cell Signaling Technology, Cat. # 31H4), anti-calreticulin pAb (Stressgen, Cat. # SPA-600), anti-Tom20 pAb (a gift from Dr. Brian Wattenberg), peroxidase-conjugated goat anti-rabbit IgG (Thermo; Waltham, MA, Cat. # 31460), peroxidase-conjugated goat anti-mouse IgG (Thermo, Waltham, MA, Cat. # 31430), and Alexafluor 594 goat anti-rabbit IgG (Molecular Probes; Eugene, OR).

2.2.2. Bcl-x_L expression vector construction

The human Bcl-x_L cDNA was cloned into the mammalian expression vector pEF6/myc-His A (Invitrogen) to generate the plasmid pEF6-Bcl-x_L. A stop codon was introduced after amino acid 210 by polymerase chain reaction (PCR) to

generate pEF6-Bcl-x_L-ΔC. The carboxyl-terminal transmembrane region of Bcl-x_L was replaced by the cytochrome b5 (cb5) membrane targeting sequence which directs Bcl-x_L specifically to the ER membrane, or the membrane targeting sequence of the listeria protein ActA, which specifically targets Bcl-x_L to the mitochondria generating pEF6-Bcl-x_L-cb5 and pEF6-Bcl-x_L-ActA respectively. The constructs used for intracellular localization experiments were generated by subcloning appropriate cDNA fragments from pEF6 into pEGFP-C1 (Clontech; Madison, WI). The respective Bcl-x_L mutant plasmids were expressed into the Bcl-x-KO MEFs and single clones selected using the limited dilution method. Clones whose Bcl-x_L expression levels were comparable to wild type levels determined by western blot analysis were selected for further studies.

2.2.3. Generation of cell lines

Embryos from an eleven day pregnant *Bcl-x* heterozygous mouse were isolated. Primary embryonic cells were dissociated and plated on gelatin-coated dishes. Seven days later, adherent embryonic cells were immortalized by transfecting with the pCDNA3 plasmid expressing SV40 large T antigen. The limiting dilution method was used to isolate single clones from each of the 10 original embryos. After stable cell lines were established, the expression of Bcl-x_L was examined by western blot (Figure 2.1A). While expression of Bcl-x_L in the established MEFs was readily detected by western blot analysis, expression of Bcl-x_S was undetectable, indicating that Bcl-x_L is the predominant splicing product in MEFs

(Figure 2.1B). Among ten MEFs developed (from ten different embryos), cell lines 1, 3, 5 and 6 had higher Bcl-x_L expression and were considered to express Bcl-x_L from both alleles (*bcl-x*^{+/+}, designated wild-type, Bcl-x-WT). In contrast, Bcl-x_L was not detected in cell lines 2, 4 and 9, designated as Bcl-x-KO MEFs (*bcl-x*^{-/-}, knock-out, Bcl-x-KO). In cell lines 7, 8, and 10, lower Bcl-x_L expression were detected, which could be attributed to heterozygous deletion of the *bcl-x* gene (*bcl-x*^{+/-}).

To re-express Bcl-x_L in Bcl-x-KO MEFs, pEF6 plasmids encoding wild-type or mutant Bcl-x_L cDNAs were transfected into wild-type or Bcl-x-KO MEFs using lipofectamine 2000 reagent (Invitrogen). MEFs stably expressing Bcl-x_L proteins were obtained by growing transfected cells in the medium containing 1.5 µg/ml blasticidin antibiotics (Invitrogen) and subcloned by a limited dilution approach. Western blot analysis then was used to determine the expression level of different Bcl-x_L proteins in Bcl-x-KO MEFs. All MEFs were cultured in DMEM (Mediatech; Manassas, VA) supplemented with 10% FBS (Gemini; West Sacramento, CA), 100 U/ml penicillin (Mediatech), and 100 µg/ml streptomycin (Mediatech) in an incubator with 95% humidity and 5% CO₂ at 37 °C.

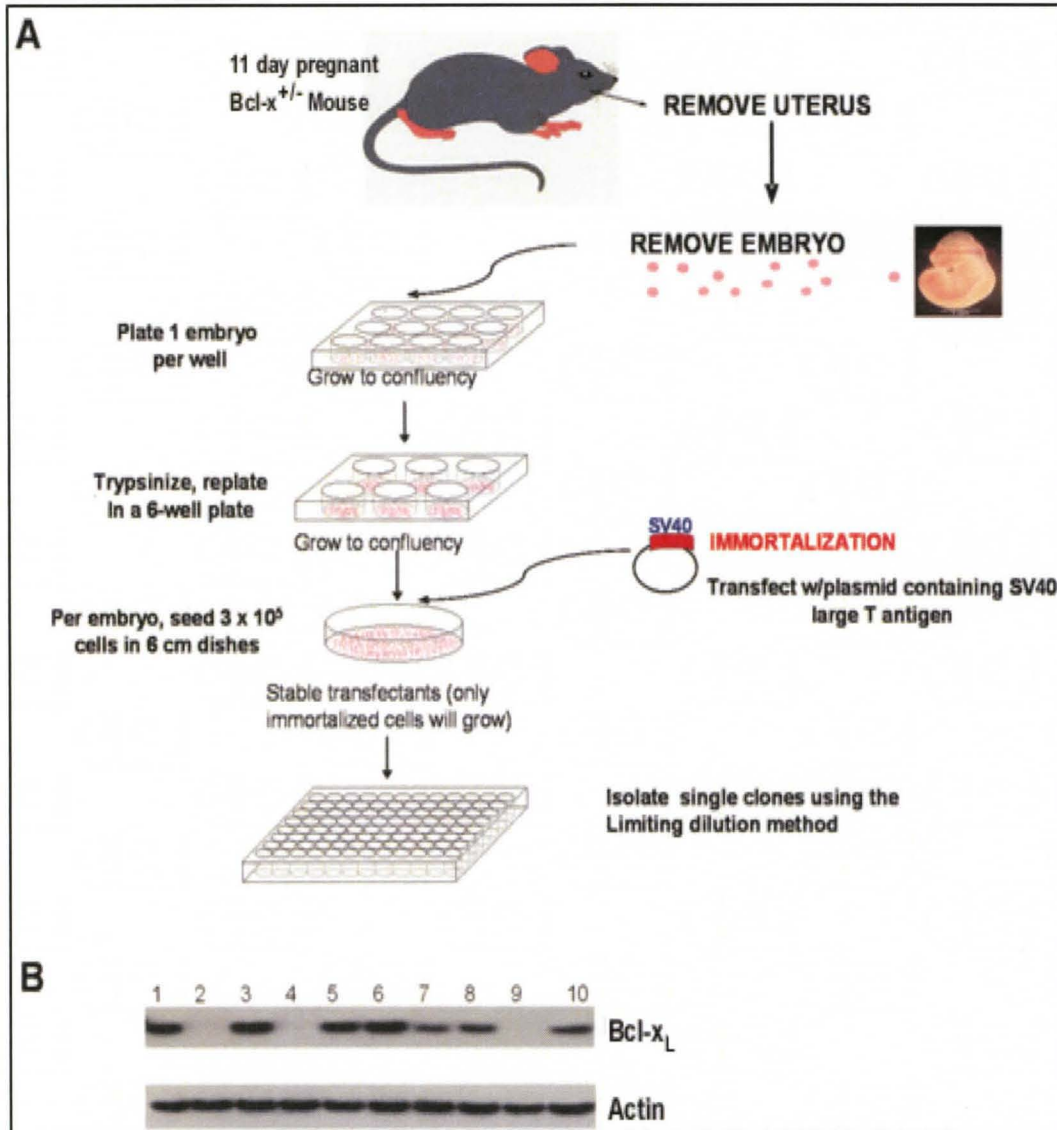


Figure 2.1. Generation of wild-type and Bcl-x-KO MEFs. (A) Embryos were isolated from an 11-day pregnant mouse heterozygous for the *bcl-x* gene. Embryonic cells were dissociated and plated in gelatin-coated 12-well plates. MEFs were transfected with a plasmid encoding SV40 large T antigen to be immortalized. The limiting dilution method was used to isolate single clones from each of 10 original embryos. (B) Bcl-x_L expression in established MEFs was detected by western blot. MEFs from embryos 2, 4 and 9 were used as Bcl-x knockout, while MEFs from embryos 1, 3, 5 and 6 appear to be wild-type and used as controls. The expression levels of the other splice variant Bcl-x_S was undetected.

2.2.4. Gene expression analysis

Total RNA from two wild-type and two Bcl-x-KO MEF cell lines was isolated using a RNeasy kit (Qiagen, Germantown, MD). The quality of total RNA was confirmed using a 2100 Bioanalyzer (Agilent; Santa Clara, CA). The cRNA was generated using a WT Expression Kit (Ambion; Austin, TX) and labeled using a GeneChip WT Terminal Labeling Kit (Affymetrix; Santa Clara, CA). Hybridization to GeneChip Mouse Gene 1.0 ST Array (Affymetrix) was carried out according to the manufacturer's protocol. After array processing and scanning, the resulting raw data were summarized and normalized using RMA in Partek Genomics Suite 6.5 (Partek Inc., St. Louis, MO) by the University of Louisville Microarray Facility. Exon level signals were summarized to gene expression levels using mean values. The significance of the changes was determined using ANOVA and applying FDR as multiple test correction.

2.2.5. Cell viability assay

The propidium iodide (PI) exclusion method was used to determine cell viability. MEFs were plated in 48 well tissue culture plates with a cell density of approximately 1×10^4 cells per well 24 hours before treatment with the respective apoptotic stimuli. At the indicated time, MEFs were trypsinized and resuspended in growth medium containing 1.0 $\mu\text{g/ml}$ PI (Invitrogen). Cell viability was measured by PI exclusion method using flow cytometry (FACScalibur, Beckon Dickinson; San Jose, CA). The experiments were performed in triplicates. Cell

viability of treated cells was presented as percentage of those of untreated control cells.

2.2.6. Caspase 3/7 assay

The Sensolyte[®] Homogeneous R110 Caspase 3/7 Assay Kit (AnaSpec; San Jose, CA) was used to directly measure caspase 3/7 activity in MEFs. Twenty-four hours before the treatment, cells were plated in white-walled 96-well plates. At the indicated time points, measurement was performed according to the manufacturer's protocols. The fluorescence signal (Ex/Em: 496nm/520nm) was measured kinetically over 2 hours at an interval of 1 minute by a Gemini EM microplate spectrofluorometer (Molecular Devices; Sunnyvale, CA). Data were presented as relative fluorescent units versus time (RFU/min). The slope was calculated and normalized to those of untreated cells.

2.2.7. Western blot analyses

Cell pellets of MEFs were collected and resuspended in RIPA lysis buffer (150 mM sodium chloride, 1.0% (v/v) Triton X-100, 0.5% sodium deoxycholate, 0.1% sodium dodecyl sulphate, and 50 mM Tris, pH 8.0) containing protease inhibitors (Complete, Roche; Indianapolis, IN). To remove debris and nuclear materials, cells were first sonicated for 30 seconds at 10% amplitude (Sonic Dismembrator, Model 500, Fischer Scientific; Hampton, NH) before centrifugation at 13,200 x

rpm at 4°C for 10 minutes, and supernatant collected. The protein concentration was determined using bicinchoninic acid (BCA) assay (Pierce; Rockford, IL). Twenty micrograms of protein sample were loaded on a 4-12% Bis-Tris gel (BioRad; Hercules, CA) and transferred to PVDF (Millipore; Billerica, MA). The membrane filters were incubated in buffer containing 1X PBS, 0.2% (v/v) Tween 20, and 10% (w/v) nonfat dry milk (BioRad) with appropriate primary antibodies at 4°C overnight or at 25°C for about three hours. After three 10 minute washes with 1x PBS/0.2% Tween solution, the membrane filters were then incubated with the appropriate peroxidase-coupled secondary antibodies at 4°C overnight or at 25°C for about three hours. Proteins were detected using the enhanced chemiluminescent (ECL) detection system (Pierce, Rockford, IL).

2.2.8. Immunofluorescence

Bcl-x-KO MEFs were plated on 18 mm coverslips in a 6-well tissue culture plate and allowed to grow overnight. Cells were then transiently transfected with the pEGFP-C1 plasmids expressing the cDNAs of various Bcl-x_L mutants using the jetPRIME® transfection reagent (Polyplus-transfection SA; Illkirch, France) following the manufacturer's instructions. Forty eight hours post transfection; coverslips were transferred into a 12-well cell culture plate and washed twice with 1.0 ml 1X HBSS (Hanks balanced salt solution). Following 15 minute fixation with 0.4 ml 0.4 % paraformaldehyde, cells were washed three times with 1.0 ml 1X HBSS, and then permeabilized with 0.4 ml 0.2 % TritonX-100 for 15 minutes.

After three washes with 1.0 ml incubation solution (0.02 % TritonX-100 and 1.5 % FBS in 1X HSSB), cells were incubated with primary antibodies in incubation solution for 1 hour at room temperature. Following three 10 minute washes with incubation solution, cells were incubated with secondary antibodies for 1 hour at room temperature, and again washed three times with incubation solution. The coverslips were then immersed in mounting medium (Dako, Carpinteria, CA), put on slides, and sealed with nail polish. The fluorescence images were visualized and acquired using a PlanApo 60x, 1.40 NA oil immersion objectives on a Nikon Eclipse Ti (Melville, NY) confocal microscope according to the manufacturer's protocol.

2.2.9. Measurement of cytoplasmic and ER Ca²⁺ concentrations

Cytoplasmic and ER Ca²⁺ concentrations measurement data were collected by the Carl White laboratory from the Rosalind Franklin University of Medicine and Science, North Chicago. For cytoplasmic [Ca²⁺], MEFs cultured on glass coverslips were loaded with 2 μ M fura-2AM (Invitrogen) and incubation at room temperature for 45 minutes and mounted in a recording chamber positioned on the stage of an inverted microscope (IX71; Olympus). Fura-2 was alternately excited at 340 nm and 380 nm and the emitted fluorescence filtered at 510 nm collected and recorded using a CCD-based imaging system running SimplePCI software (Hamamatsu; Sewickley, PA). The chamber was continuously perfused

with HBSS (pH 7.4) at room temperature. A rapid solution changer was used to switch the composition of the solution bathing the cells under study.

To measure ER $[Ca^{2+}]$, MEFs were loaded with mag-fura-2AM (5 μ M) for 60 minutes at room temperature and perfused with intracellular-like medium (ICM) containing: 125 mM KCl, 19 mM NaCl, 10 mM HEPES, 1 mM EGTA (pH 7.3 with KOH) and permeabilized by a 20-30 minute exposure to ICM containing 20 μ M digitonin. After 20-30 minute incubation in ICM, stores were Ca^{2+} -loaded by switching to ICM solution with free $[Ca^{2+}]$ adjusted to 200 nM and 1.5 mM MgATP. To induce Ca^{2+} release, $InsP_3$ was applied in the same Ca^{2+} -containing ICM solution but without MgATP to prevent reuptake. Data were acquired as described for fura-2 and ratiometric data (R) and were normalized to basal store-depleted levels (R_0). For experiments using flash photolysis of caged- $InsP_3$, cells were loaded with the membrane-permeable caged $InsP_3$ compound ci- $InsP_3$ /PM (D-2,3-O-isopropylidene-6-O-(2-nitro-4,5-dimethoxy)benzyl-myo-inositol 1,4,5-trisphosphate-hexakis(propionoxymethyl) ester; SiChem, Bremen, Germany) by incubation with 1 μ M for 60 minutes at room temperature. $InsP_3$ was photo-released by brief pulses (250 ms) of UV light (350-400 nm) delivered uniformly throughout the image field. The application of UV pulses precluded the use of fura-2 as a $[Ca^{2+}]$ indicator, therefore, cells were co-loaded with the longer wavelength dye fluo-2AM (5 μ M; TEFLabs, Inc., Austin, TX) and fluorescence data (F) normalized to basal levels (F_0).

2.2.10. Statistical analysis

All experiments were performed in triplicates and each experiment was carried out at least three times. Statistical analysis was performed using the student t-test and the two way analysis of variance (ANOVA). A *P* value < 0.05 was considered significant.

2.3. Results

2.3.1. Bcl-x knock-out does not cause compensatory changes in expression levels of other Bcl-2 proteins.

As mentioned earlier, Bcl-x_L is generated from alternative splicing of the Bcl-x [12]. Massive cell death has been found in a variety of tissues in the Bcl-x-deficient mouse, which dies at embryonic day 13, therefore reflecting its important role in development [80]. To investigate the function of endogenous Bcl-x_L protein in apoptosis regulation, we established MEFs deficient in Bcl-x_L expression (Bcl-x-KO) as described earlier (Figure 2.1). As reduced expression of the anti-apoptotic Bcl-2 has been shown to affect the expression of other apoptotic regulators [111], we determined whether *bcl-x* gene knock out will cause changes in expression levels of other genes, particularly those of the Bcl-2 protein family. To this purpose, microarray analysis was carried out in two Bcl-x-KO (lines 4 and 9) and two wild-type (lines 3 and 6) MEFs. Gene expression levels were determined and the fold change between Bcl-x-KO and wild type MEFs were determined (Table 2.1). In this assay (GeneChip® Mouse Gene 1.0 ST Array), analysis of multiple probes on different exons was summarized into an expression value representing all transcripts from the same gene.

A

Gene Description	fold of changes (KO/WT)	p value
Bcl2-like 1 (Bcl-X)	-3.69	1.69e-10
B-cell leukemia/lymphoma 2 (Bcl-2)	-1.01	0.79691
myeloid cell leukemia sequence 1 (Mcl-1)	1.09	0.007846
Bcl-W (Bcl-2L2)	1.06	0.333466
A1/Bfl-1(Bcl-2A1)	1.05	0.253429
Bcl2-antagonist/killer 1 (Bak)	1.07	0.111168
Bcl2-associated X protein (Bax)	1.03	0.389398

B

Gene Description	Fold changes (KO/WT)	p value
Bcl-2-interacting killer (Bik)	1.29	0.001245
Harakiri, Bcl-2 interaction protein (Hrk)	1.12	0.497068
Bcl-2 modifying factor (Bmf)	1.09	0.086236
Bcl-2 binding component 3 (Puma)	1.05	0.045677
Bcl-2-like 11 (Bim)	-1.37	0.000303
Bcl-2 associated agonist of cell death (Bad)	1.02	0.610081
Bcl-2 /adenovirus E1B interacting protein 3 (Bnip3)	1.12	0.49768
Phorbol-12-myristate-13-acetate-induced protein1 (Pmaip1, Noxa)	1.43	0.071210
BH3 interacting domain death agonist (Bid)	1.33	0.011095
Bcl-2 /adenovirus E1B interacting protein 3-like (Bnip3l, Nix)	1.04	0.381809

Table 2.1. Changes in mRNA expression of Bcl-2 genes induced by Bcl-x deficiency were determined by microarray analysis. (A) Data are represented as fold-changes in mean value of mRNA levels of the anti-apoptotic Bcl-2 proteins and the multidomain pro-apoptotic Bcl-2 proteins in two wild-type and two Bcl-x-KO MEFs. **(B)** BH3-only Bcl-2 proteins did not show changes in mRNA expression levels between wild-type and Bcl-x-KO MEFs. Negative values indicate down-regulation.

As the Bcl-x-deficient mouse was generated by homologous recombination, some exons in the targeted *bcl-x* gene were still intact. By this approach, Bcl-x mRNA was still detectable in Bcl-x-deficient cells, and *bcl-x* mRNA level in Bcl-x-KO MEFs was significantly reduced compared with that in wild-type MEFs, validating the disruption of intact Bcl-x mRNA in Bcl-x-KO MEFs. Knocking out of the Bcl-x gene does not cause significant changes in mRNA expression of other Bcl-2 proteins, including anti-apoptotic Bcl-2 proteins (Table 2.1A), pro-apoptotic multi domain Bcl-2 proteins (Table 2.1A) and pro-apoptotic BH3-only Bcl-2 proteins (Table 2.1B). Western blot analysis was performed to further validate that Bcl-x-deficiency does not cause significant changes in Bcl-2 protein expression (Figure 2.2). These results indicate that alterations in cellular apoptotic signaling in response to apoptotic stimuli in Bcl-x-KO MEFs is attributed to Bcl-x_L deficiency, therefore providing an excellent cell system to study the molecular and biochemical mechanism of apoptosis regulation by endogenous Bcl-x_L.

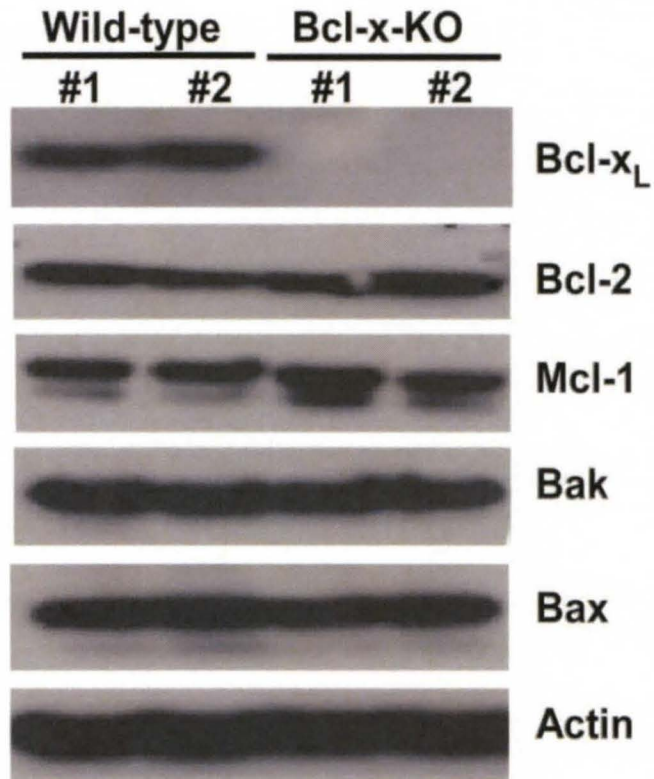


Figure 2.2. Bcl-x deficiency does not cause compensatory changes in expression of other Bcl-2 proteins. Expression of Bcl-2 proteins in the indicated MEFs was determined by western blot analysis. WT #1, cell line 3; WT #2, cell line 6; KO #1, cell line 9; KO #2, cell line

2.3.2. Endogenous Bcl-x_L modulates cellular responses to apoptosis

To investigate the functional activity of endogenous Bcl-x_L in apoptotic signaling, two wild-type (cell lines 3 and 6) and two Bcl-x-KO (cell lines 4 and 9) MEFs were exposed to death causing agents with diverse mechanisms to induce apoptosis including the topoisomerase inhibitor etoposide (5.0 μM), the transcriptional inhibitor actinomycin D (0.2 μg/ml), the DNA intercalating agent doxorubicin (1.0 μM), the protein kinase inhibitor staurosporine (5.0 nM), and the oxidative stress inducer H₂O₂ (0.4 mM). When wild-type and Bcl-x-KO MEFs were treated with all of these agents, there was significantly more cell death in Bcl-x-KO compared to wild type MEFs, except that the protection against actinomycin D in wild type cells seems to be transient (Figure 2.3A). As Bcl-x_L is the major splicing product of the Bcl-x gene in MEFs, higher sensitivity of Bcl-x-KO MEFs to apoptotic insults suggests that endogenous Bcl-x_L is able to protect cells against these apoptotic insults. To confirm further that endogenous Bcl-x_L is able to inhibit apoptosis, caspase 3/7 activity was measured in all the wild-type and Bcl-x-KO MEFs treated with apoptotic agents. As shown in Figure 2.3B, caspase 3/7 activity was enhanced in Bcl-x-KO MEFs to higher levels than that in wild-type MEFs upon treatment with all apoptotic insults. The increase in caspase 3/7 activity correlated with the increase in cell death, suggesting that endogenous Bcl-x_L protects cells against those apoptotic stimuli (Figure 2.3B).

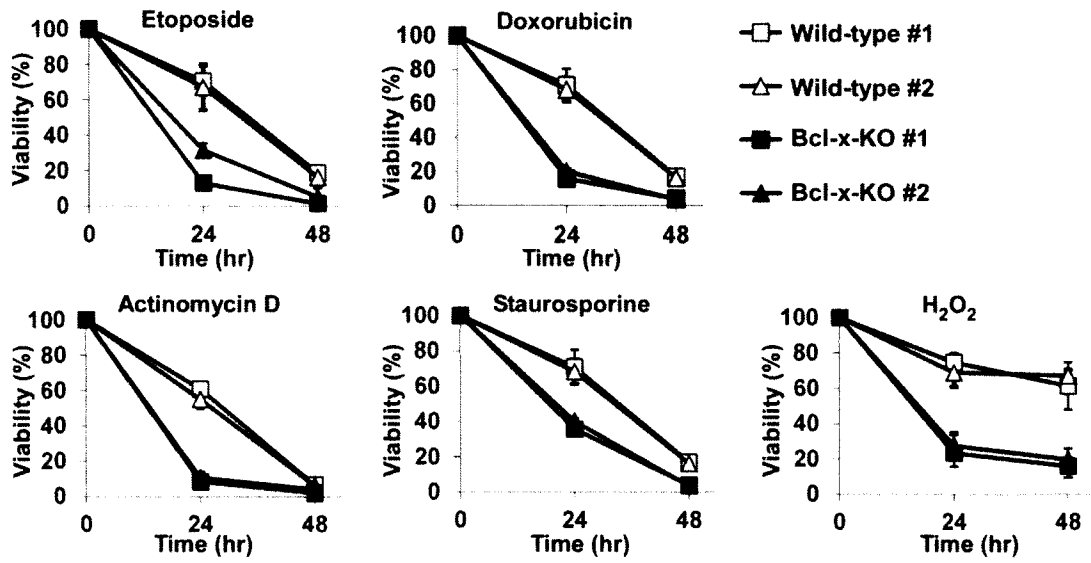
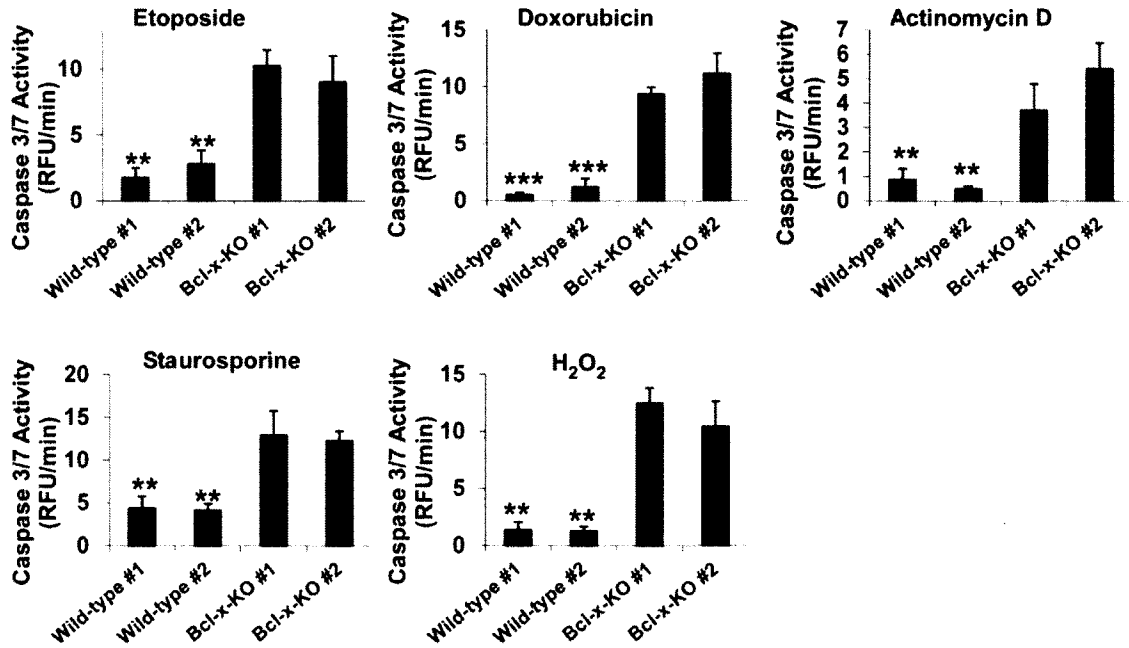
A**B**

Figure 2.3. Endogenous Bcl-x_L modulates cellular response to different apoptotic stimuli. (A) Apoptosis was induced by the indicated apoptosis agents: etoposide (5.0 μM); doxorubicin (1.0 μM); actinomycin D (0.2 μg/ml); staurosporine (5.0 nM); or hydrogen peroxide (0.4 mM). Bcl-x-KO MEFs were more sensitive to these reagents. Data represent mean ± standard deviation of three independent experiments performed in triplicate. **(B)** Caspase 3/7 activity was measured 12 hours following treatment with etoposide, doxorubicin, or staurosporine or 9 hours after actinomycin D and H₂O₂ treatment using fluorometric assay. Values are normalized to the values obtained in the untreated control cells. Data are shown as mean ± S.D. of three independent triplicate experiments. ***P*<0.01; ****P*<0.001.

To ensure that enhanced apoptosis observed in Bcl-x-KO MEFs was due to deficiency in Bcl-x_L protein expression only, Bcl-x_L cDNA was re-expressed in Bcl-x-KO MEFs (cell line 9) to obtain cells with different Bcl-x_L levels. Three cell lines were selected; cell line H (high) with Bcl-x_L expression level higher than the endogenous Bcl-x_L level, cell line M (medium) with Bcl-x_L expression level comparable to the endogenous level, and cell line L (low) with expression level lower than the endogenous Bcl-x_L level (Figure 2.4A). When cells were treated with different death stimuli described previously in Figure 2.3A, expression of Bcl-x_L in Bcl-x-KO MEFs was able to restore the Bcl-x-KO MEFs' resistance to apoptosis (Figure 2.4B). Importantly, Bcl-x_L protected cells against apoptotic stimuli in a Bcl-x_L dose-dependent manner, further substantiating that increased sensitivity of Bcl-x-KO MEFs to death stimuli is caused by the lack of endogenous Bcl-x_L expression (Figure 2.4B). The caspase 3/7 activity of different cell lines following treatment with the apoptotic agents was measured, and the correlation between caspase 3/7 activities with levels of cell death was observed, providing more evidence of the involvement of endogenous Bcl-x_L in apoptotic signaling (Figure 2.4C).

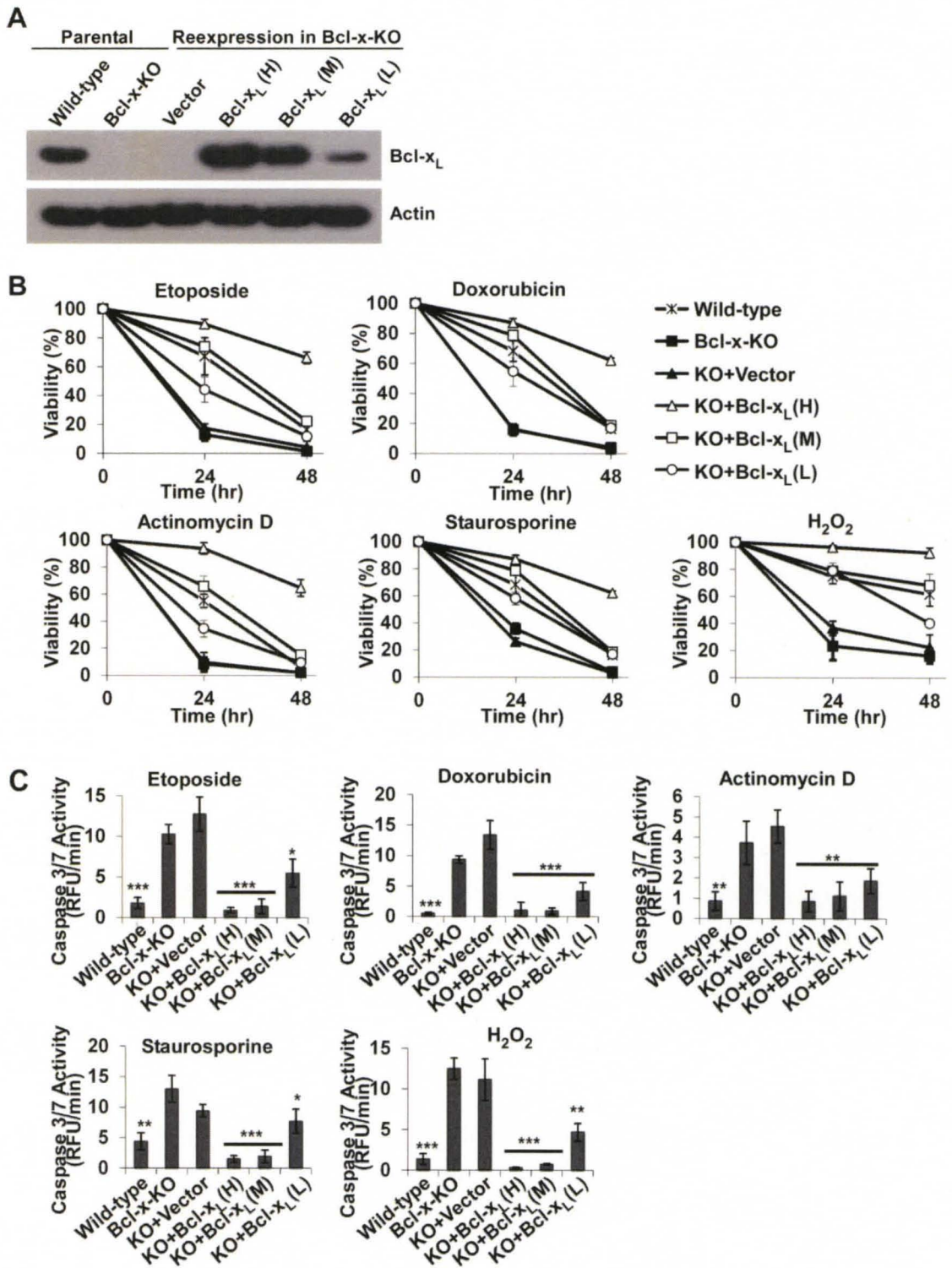


Figure 2.4. Reexpression of Bcl-x_L in Bcl-x-KO MEFs restores resistance to apoptotic stimuli in a Bcl-x_L dose-dependent manner. (A) Bcl-x_L was reexpressed in Bcl-x-KO MEFs. Western blot analysis was used to determine Bcl-x_L expression levels. **(B)** Viability of the indicated MEFs was measured in the presence of the indicated apoptotic stimuli. Data represent mean ± standard deviation of three triplicate independent experiments. **(C)** Caspase 3/7 activity was measured under the conditions described in Figure 2.3B. Values are normalized to the values of untreated control cells. Data show mean ± standard deviation of three independent experiments performed in triplicate. **P*<0.05; ***P*<0.01; ****P*<0.001.

2.3.3. Targeting Bcl-x_L mutants specifically to the cytosol, the ER, or the mitochondria

To investigate the anti-apoptotic functions of Bcl-x_L localized on different intracellular organelles, we constructed Bcl-x_L mutants that either lacked the membrane targeting sequence, or contained an ER-specific or a mitochondrial-specific membrane targeting sequences. The carboxyl-terminal transmembrane sequence of Bcl-x_L was deleted, and deleting this sequence specifically confines Bcl-x_L to the cytosol (Bcl-x_L-ΔC). The carboxyl-terminal transmembrane region of Bcl-x_L was replaced by the cytochrome b5 (cb5) membrane targeting sequence which directs Bcl-x_L specifically to the ER membrane, or the membrane targeting sequence of the *Listeria* protein ActA, which specifically targets Bcl-x_L to mitochondria (Figure 2.5A). The same targeting sequences have been used previously to target both anti- and pro-apoptotic Bcl-2 proteins to a specific organelle [105, 112, 113].

To confirm subcellular localization of Bcl-x_L mutant proteins, cDNAs of the respective Bcl-x_L mutants were subcloned into the plasmid containing the green fluorescent protein (EGFP-C1), and confocal microscopy was used to examine their subcellular localization. GFP-tagged Bcl-x_L mutants were transiently expressed in Bcl-x-KO MEFs. The mitochondrial protein Tom20 served as a mitochondrial maker and the ER protein calreticulin was selected as an ER marker. While the intracellular localization of GFP-tagged Bcl-x_L-ActA

superimposed with that of Tom20, the staining patterns for GFP-Bcl-x_L-ActA and calreticulin were clearly distinct (Figures 2.5B).

In contrast, GFP-tagged Bcl-x_L-cb5 was completely targeted at the ER with its fluorescence superimposed with that of calreticulin but not Tom20 fluorescence, indicating that Bcl-x_L-cb5 is completely localized at the ER (Figure 2.5B).

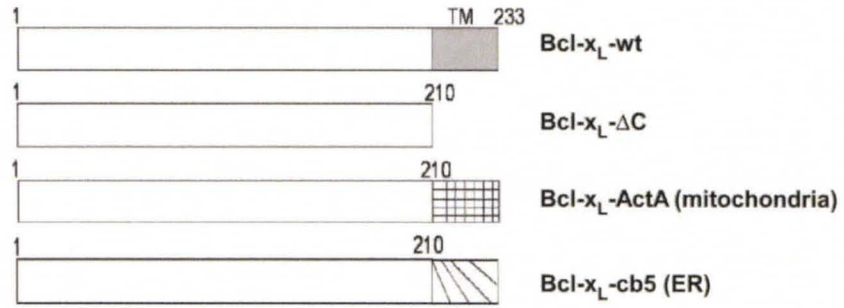
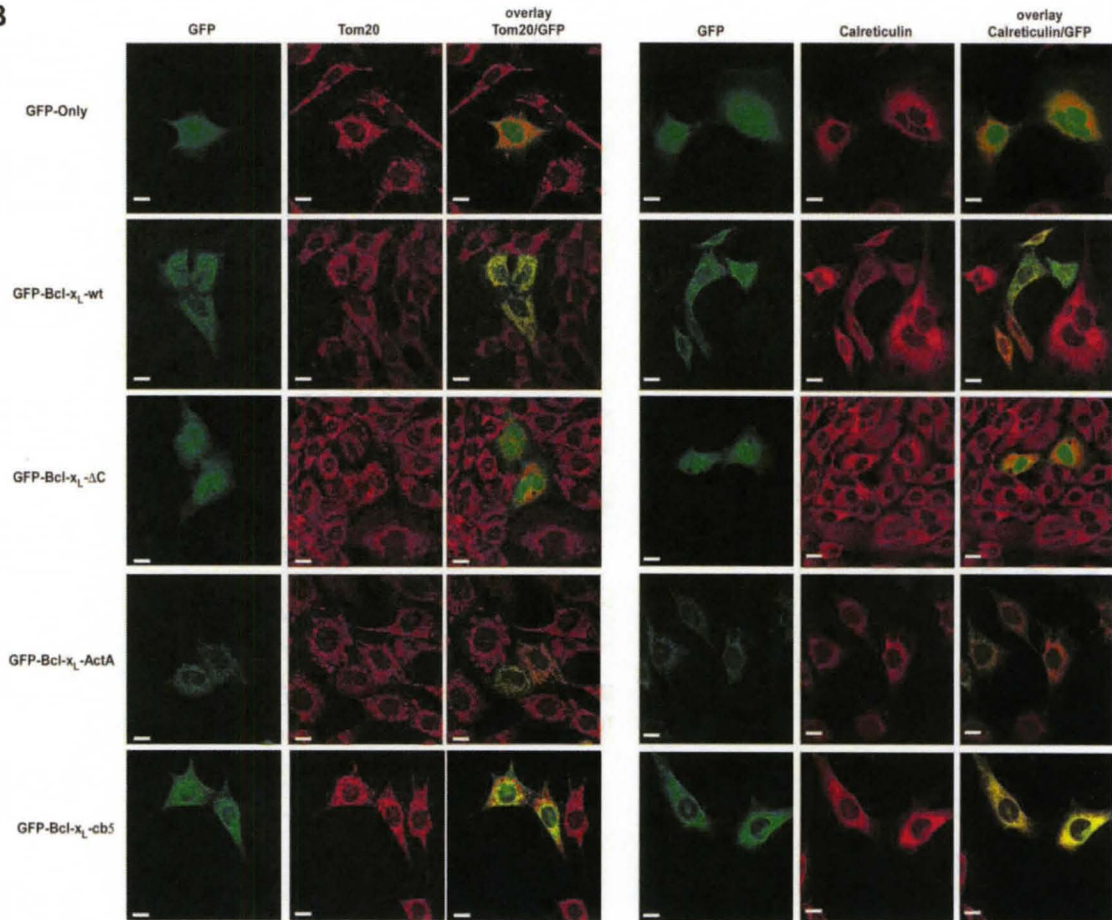
A**B**

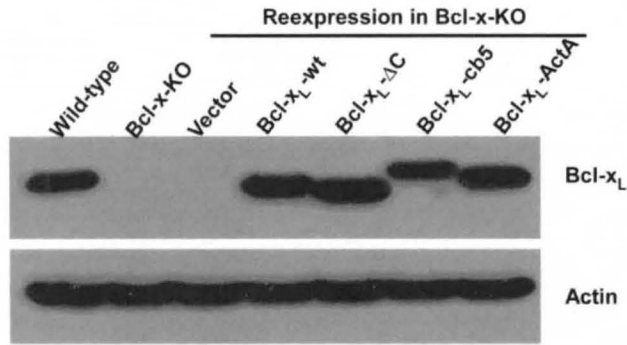
Figure 2.5. Generation of mitochondrially targeted and ER-targeted Bcl-x_L mutants. (A) Scheme of the Bcl-x_L mutants. The carboxyl-terminal transmembrane domain of Bcl-x_L was deleted (Δ C) and replaced with the mitochondria-targeting sequence of ActA or the ER-targeting sequence of cb5. (B) The indicated GFP and Bcl-x_L fusion proteins were transiently expressed in Bcl-x-KO MEFs. The mitochondrial protein Tom20 was detected as organelle marker, while the ER protein calreticulin was used as ER marker. The fluorescence was visualized by confocal microscopy. Scale bar, 10 μ m

2.3.4. Mitochondrially targeted Bcl-x_L prevents apoptosis more effectively than ER-targeted Bcl-x_L

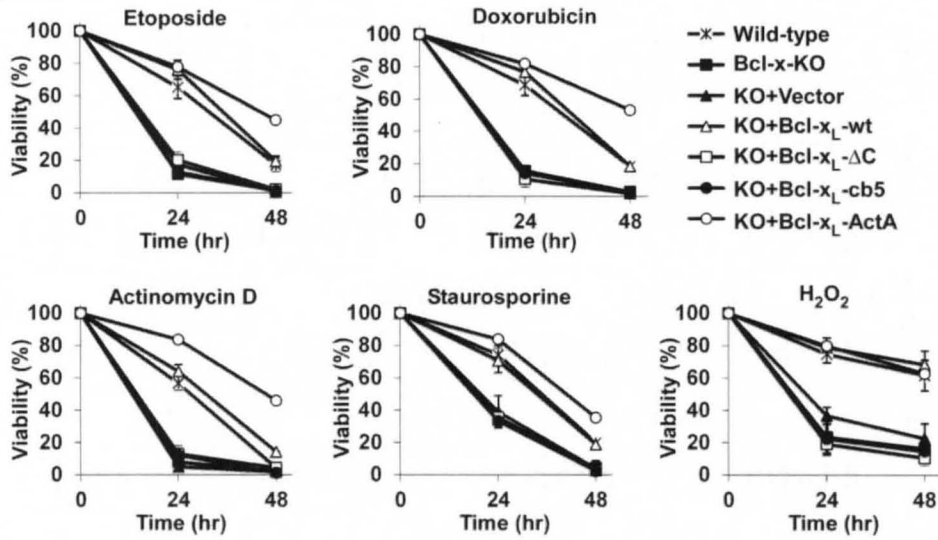
To investigate whether Bcl-x_L proteins targeted at specific organelles mediate different apoptotic signaling pathways, the mutant Bcl-x_L proteins were expressed in Bcl-x-KO MEFs (cell line 9) at levels comparable to that of endogenous Bcl-x_L (Figure 2.6A). Bcl-x-KO MEFs expressing different Bcl-x_L mutants were treated with various death reagents (etoposide, doxorubicin, actinomycin D, staurosporine, and H₂O₂), and cell viability determined. Expression of Bcl-x_L-ActA in Bcl-x-KO MEFs provided protection against all apoptotic reagents at the level comparable with that of wild-type Bcl-x_L (Figure 2.6B). In contrast, both Bcl-x_L lacking membrane-anchoring region (Bcl-x_L-ΔC) and ER-localized Bcl-x_L (Bcl-x_L-cb5) failed to protect cells against any of the death stimuli examined (Figure 2.6B). These data suggest that mitochondrial localization is an absolute requirement for Bcl-x_L to be protective in various apoptotic paradigms.

This was further confirmed by the experiments in which caspase 3/7 activity was measured in response to cell death stimuli. Caspase 3/7 activity of Bcl-x-KO MEFs expressing Bcl-x_L-cb5 or Bcl-x_L-ΔC was higher than that of cells expressing Bcl-x_L-ActA or wild-type Bcl-x_L (Figure 2.6C).

A



B



C

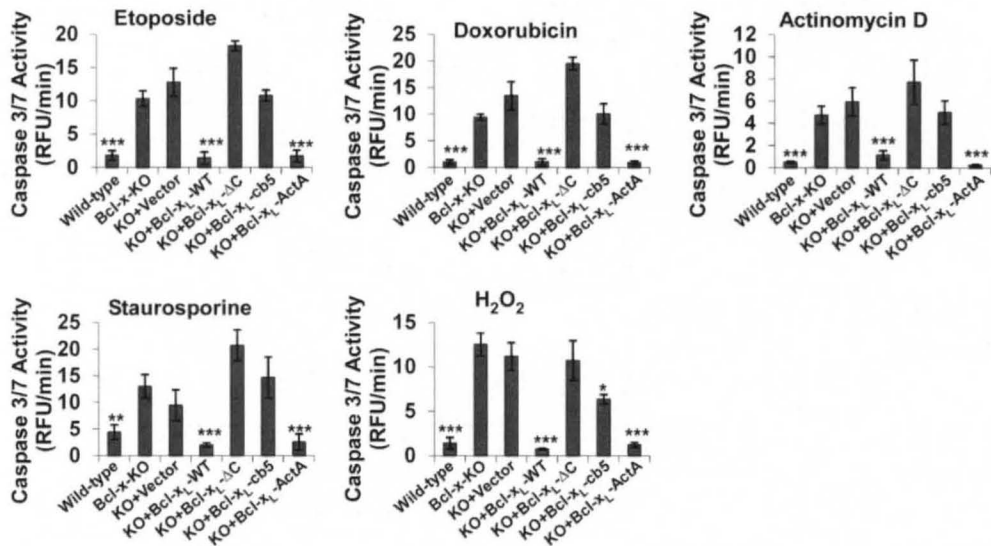


Figure 2.6. Mitochondrially targeted Bcl-x_L inhibits apoptosis more efficiently than Bcl-x_L targeted at the ER. (A) The indicated Bcl-x_L mutants were expressed in Bcl-x-KO MEFs at the levels similar to the endogenous Bcl-x_L level. Bcl-x_L expression was determined by Western blot analysis. **(B)** MEFs expressing different Bcl-x_L mutants were treated with either 5.0 μM etoposide, 1.0 μM doxorubicin, 0.2 μg/ml actinomycin D, 5.0 nM staurosporine or 0.4 mM H₂O₂, and cell viability was measured. The data depict mean ± standard deviation of three independent experiments. **(C)** Caspase 3/7 activity was measured as described in Figure 2.3B. Values are normalized to those of untreated cells. All data shown are the means ± standard deviation of experiments independently performed three times. **P*<0.05; ***P*<0.01; ****P*<0.001.

2.3.5. ER-targeted Bcl-x_L modulates ER Ca²⁺ homeostasis

Previously, Li et al. [107] demonstrated that overexpression of Bcl-x_L lowers the steady-state [Ca²⁺]_{ER} and affects intracellular Ca²⁺ ([Ca²⁺]_i) signaling by modulating channel activities of the ER Ca²⁺ release channel inositol trisphosphate (InsP₃) receptor [107, 114]. Here we investigated whether organelle-targeted Bcl-x_L proteins influenced InsP₃-dependent [Ca²⁺]_i signaling. To investigate whether organelle-targeted Bcl-x_L proteins influenced InsP₃-dependent [Ca²⁺]_i signaling, [Ca²⁺]_i was monitored in response to an increase in intracellular [InsP₃] evoked by flash photolysis of caged InsP₃ (Figure 2.7A). Maximal InsP₃ uncaging and/or receptor activation in these cells was produced by UV pulses of 250 ms duration. This level of InsP₃ evoked larger [Ca²⁺]_i transients in Bcl-x-KO MEFs compared with wild-type MEFs (Figures 2.7A and 2.7B). Reexpression of Bcl-x_L in Bcl-x-KO MEFs localized at the ER but not at mitochondria restored InsP₃-evoked Ca²⁺ signal to the level observed in wild-type MEFs (Figures 2.7A and Figure 2.7B). These data are consistent with previous studies showing that Bcl-x_L overexpression reduces ER Ca²⁺ store content and thus the magnitude of ER Ca²⁺ release in response to maximal InsP₃ stimulation [107].

As steady-state [Ca²⁺]_{ER} is determined by the balance between ER Ca²⁺ leakage and Ca²⁺ uptake by sarco/endoplasmic reticulum Ca²⁺-ATPase (SERCA), [Ca²⁺]_{ER} was further evaluated by monitoring [Ca²⁺]_i in response to inhibition of

ER Ca^{2+} uptake by the SERCA inhibitor cyclopiazonic acid (CPA) in the absence of external Ca^{2+} . A smaller Ca^{2+} response was evoked by cyclopiazonic acid in wild-type MEFs compared with Bcl-x-KO MEFs (Figure 2.7C). The ER Ca^{2+} release was quantified by calculating the integral of the $[\text{Ca}^{2+}]_i$ transient since the total released $[\text{Ca}^{2+}]$ more closely reflects the steady-state store content (Figure 2.7D). Again, the phenotype of wild-type MEFs was observed only in Bcl-x-KO MEFs expressing Bcl-x_L localized at the ER but not Bcl-x_L localized at the mitochondria. To confirm further the effects of organelle-targeted Bcl-x_L on ER Ca^{2+} store, direct measurements of $[\text{Ca}^{2+}]_{\text{ER}}$ were also carried out using the low affinity Ca^{2+} indicator Mag-fura-2. Since Mag-fura-2 compartmentalizes in the ER as well as in the cytoplasm, the plasma membrane was permeabilized to remove cytoplasmic indicator, and the cells were perfused with a Ca^{2+} free solution to allow passive depletion of ER Ca^{2+} store [115]. After equilibration, Ca^{2+} uptake into the store was induced by switching the perfusate to the solution containing 1.5 mM MgATP and 200 nM free $[\text{Ca}^{2+}]$. Once a steady-state had been reached, the solution was switched to one containing saturating $[\text{InsP}_3]$ (10 μM) without MgATP [116].

As depicted in Figure 2.7E, application of InsP_3 induced depletion of the ER Ca^{2+} store. This was a unidirectional measure of Ca^{2+} flux since the MgATP required for SERCA pump function was not present during InsP_3 addition. Consistent with the previous experiments, Bcl-x_L deficiency elevated steady-state Ca^{2+} in the ER that was rescued by Bcl-x_L expression on the ER (Figures 2.7E and 2.7F). In

addition, the magnitudes of Ca^{2+} release evoked by saturating $[\text{InsP}_3]$ mirrored the filling state of the ER [106] (Figure 2.7G), and are in agreement with the data from intact cells (Figure 2.7A). Taken together, these data show that expression of ER-targeted Bcl-x_L produces phenotypes that are entirely consistent with our current understanding of how this protein functions at the ER to regulated Ca^{2+} signaling.

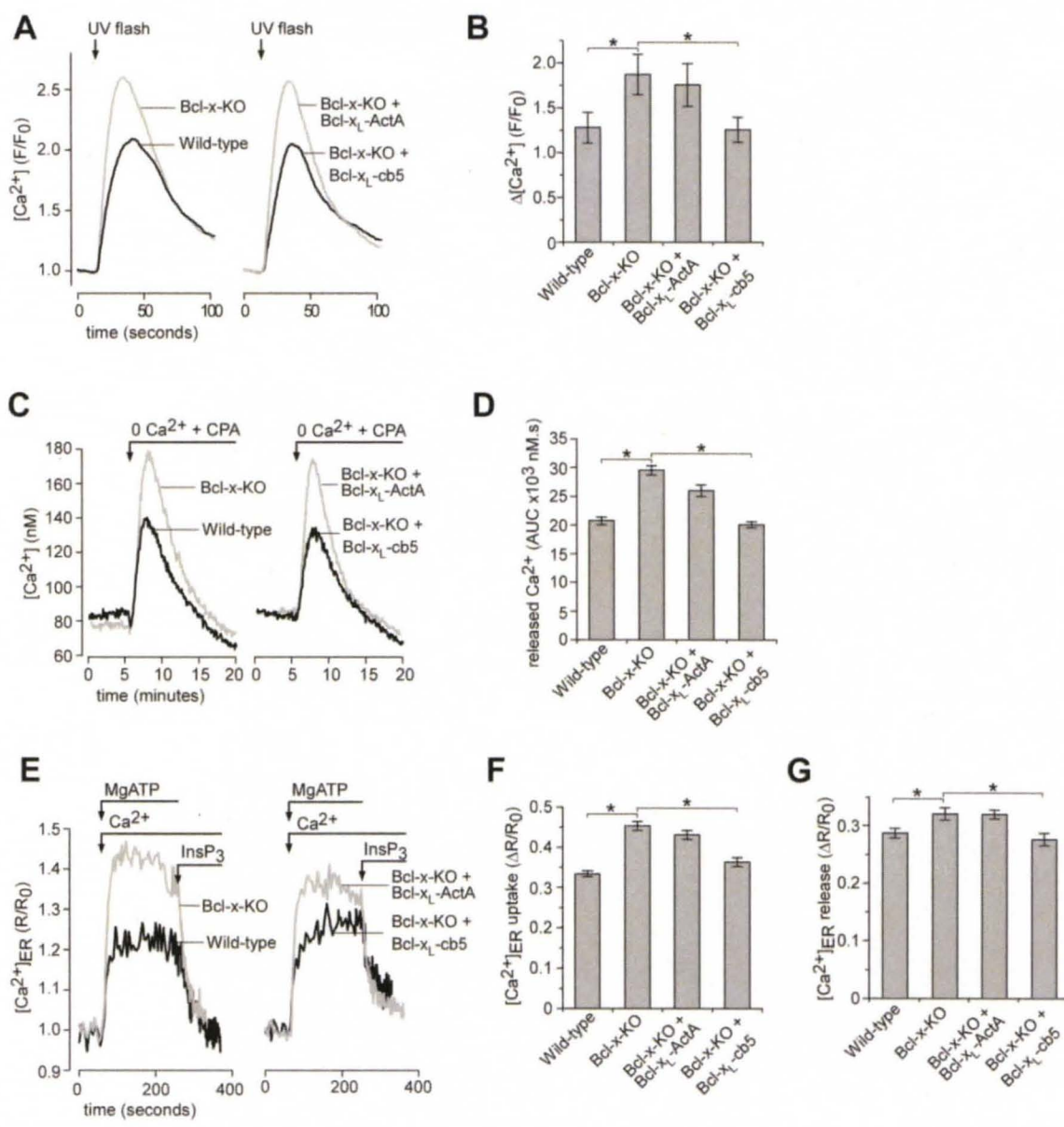
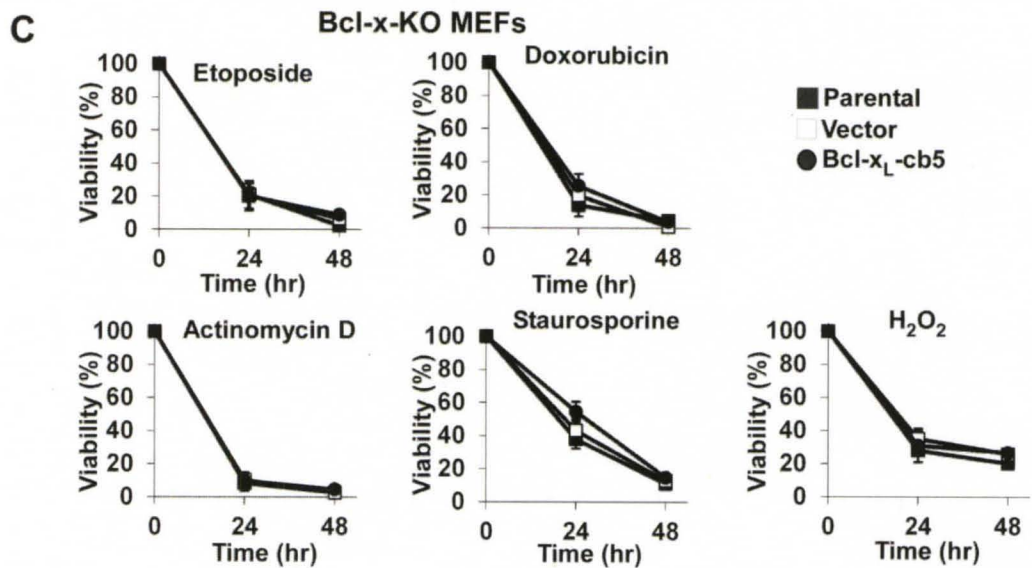
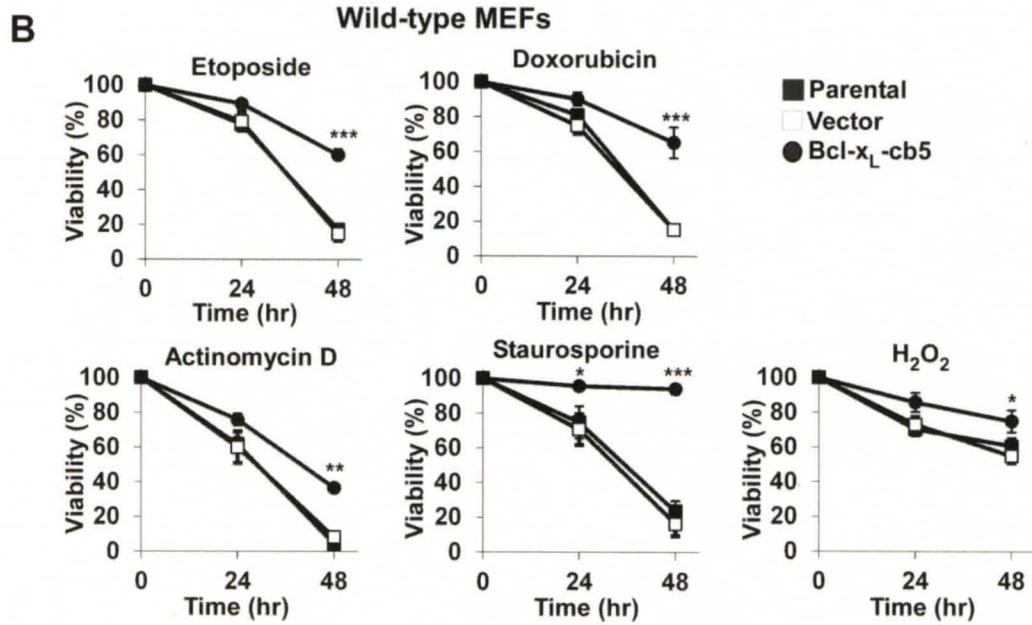
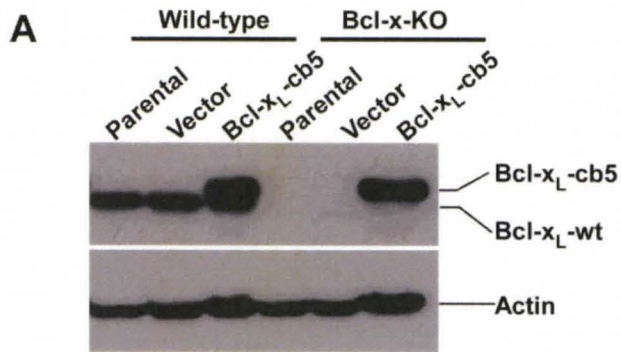


Figure 2.7. ER-localized Bcl-x_L but not mitochondrially targeted Bcl-x_L modulates ER Ca²⁺ homeostasis. (A) Representative [Ca²⁺]_i responses in fluo-2AM-loaded cells in response to flash photolysis of caged- InsP₃. (B) Summary bar graphs demonstrate the amplitude of [Ca²⁺]_i change after InsP₃ uncaging shown in A. Data represent the mean ± SEM amplitude of 31-66 cells pooled from at least three independent coverslip (*P<0.05; ANOVA). (C) The Ca²⁺ content of the ER was indirectly assessed by monitoring [Ca²⁺]_i measured by fura-2 in response to acute inhibition of ER Ca²⁺ uptake by cyclopiazonic acid (CPA; 10 μM). Representative traces of the indicated cell lines are shown. (D) Bar graphs summarizing the total released [Ca²⁺] assessed by measuring the area under the Ca²⁺ transient evoked by CPA, (Area Under Curve; AUC). Data represent the mean ± SEM of at least 50 cells pooled from at least three separate trials (*P<0.05; ANOVA). (E) Representative recordings of [Ca²⁺]_{ER} in permeabilized cells during store filling initiated by addition of 200 nM Ca²⁺ and 1.5 mM MgATP and store depletion by the application of 10 μM InsP₃. Each trace represents mean of 15-20 cells in a single image field. (F-G) Summary data (mean ± SEM) for 116-146 cells pooled from at least 3 independent trials. The steady-state uptake capacity of [Ca²⁺]_{ER} after store filling is shown in F and the amplitude of [Ca²⁺]_{ER} release in the presence of InsP₃ is shown in G; (*P<0.05; ANOVA).

2.3.6. Endogenous Bcl-x_L is essential for anti-apoptotic activities of ER localized Bcl-x_L.

Overexpressing ER-localized Bcl-x_L in the breast cancer line MCF-7 and Rat-1 fibroblasts has been shown to exhibit broader anti-apoptotic activities than Bcl-x_L targeted at mitochondria [113]. To explore the discrepancy between this finding and our observations that ER-localized Bcl-x_L failed to protect against apoptosis in Bcl-x-KO MEFs (Figure 2.6), Bcl-x_L-cb5 was stably expressed in wild-type and Bcl-x-KO MEFs at the similar levels, and uncloned populations of cells were obtained (Figure 2.8A). MEFs were then exposed to various death stimuli and cell viability was measured. While Bcl-x_L-cb5 did not possess any anti-apoptotic activities in Bcl-x-KO MEFs, expressing the same protein in wild-type MEFs markedly protected against cell death in all apoptotic paradigms examined, thus indicating that anti-apoptotic activities of Bcl-x_L targeted at ER depends on endogenous Bcl-x_L (Figure 2.8B and 2.8C). Examination of caspase 3/7 activity further confirmed the indispensable role of endogenous Bcl-x_L in the anti-apoptotic function of ER-targeted Bcl-x_L (Figure 2.8D and 2.8E).



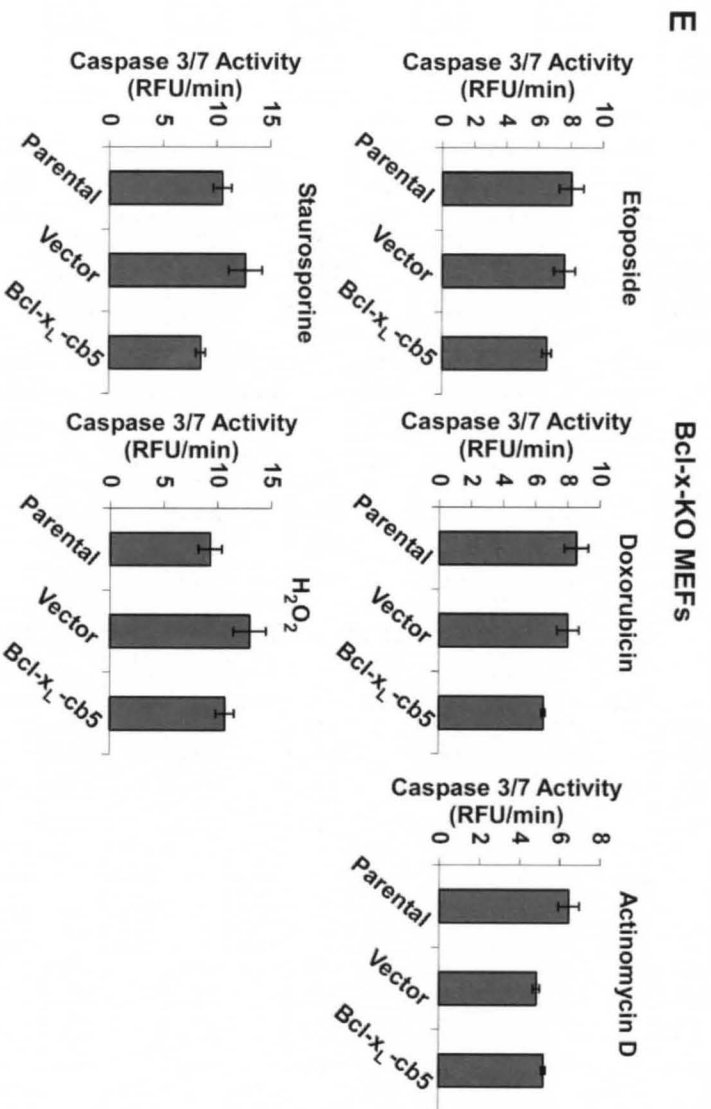
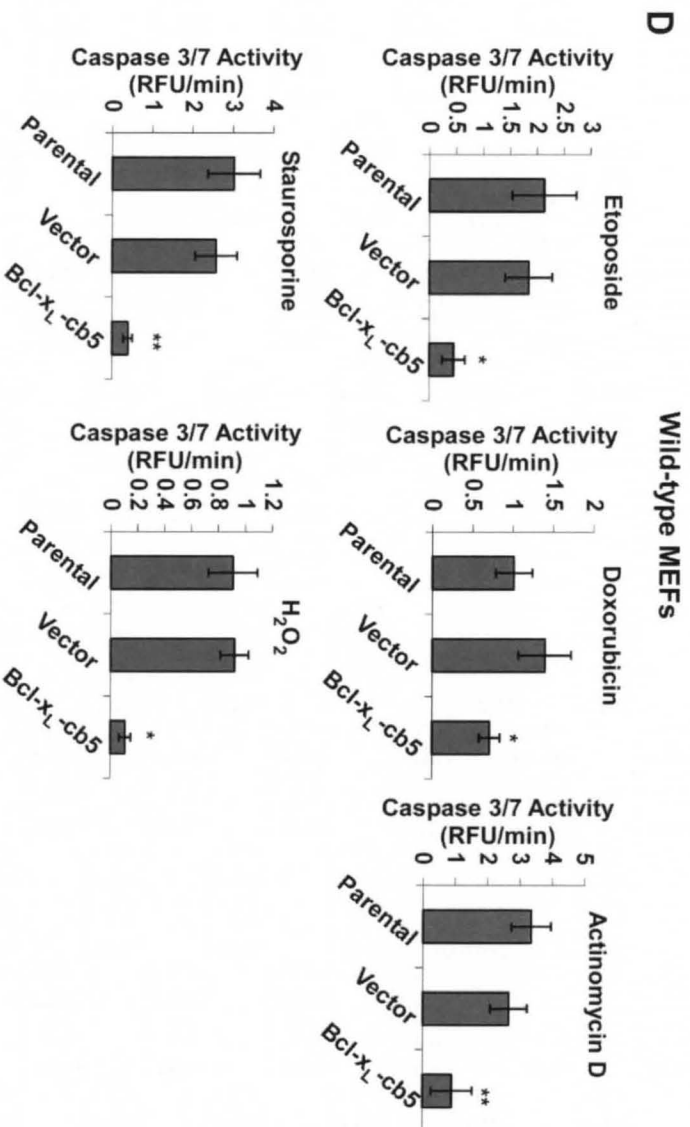


Figure 2.8. Anti-apoptotic activities of ER-targeted Bcl-x_L depend on endogenous Bcl-x_L. (A) Bcl-x_L was stably expressed in wild-type and Bcl-x-KO MEFs, and expression of Bcl-x_L in uncloned cell populations was determined by western blot analysis. Note that the molecular weights of Bcl-x_L-cb5 and endogenous Bcl-x_L are different. (B) Wild-type MEFs with or without Bcl-x_L-cb5 expressions were treated with the indicated death stimuli and cell viability was determined. The data depict mean ± standard deviation of three independent experiments. **P*<0.05; ***P*<0.01; ****P*<0.001. (C) The indicated Bcl-x-KO MEFs were treated with the apoptotic stimuli as shown in (B) and their effects on cell survival were examined. Mean ± standard deviation of three independent experiments are shown. (D) Upon treatment with etoposide, doxorubicin and staurosporine for 12 hours, actinomycin D for 7 hours and H₂O₂ for 9 hours, caspase 3/7 activity of various wild-type MEFs was determined using a fluorometric assay. Each experiment was performed in triplicate, and mean ± standard deviation of three independent experiments are shown. **P*<0.05; ***P*<0.01. (E) Different Bcl-x-KO MEFs were treated with the indicated apoptotic stimuli, and caspase 3/7 activity was measured. Data represent the mean ± standard deviation of three independent experiments.

2.4. Discussion

Anti-apoptotic Bcl-x_L is localized at both mitochondria and the ER [113]. At the mitochondria, Bcl-x_L functions to prevent OMM permeabilization during apoptotic stress, and also plays an important role in optimizing mitochondrial bioenergetic function through interactions with various membrane proteins [117-119]. Previous work demonstrate that Bcl-x_L functioned at the ER to modulate basal Ca²⁺ signaling and steady-state ER Ca²⁺ store content by interacting with the InsP₃ receptor [107, 114]. Collectively, these studies reveal that Bcl-x_L has diverse physiological roles that appear to depend on its intracellular localization. In this specific aim, we sought to understand better the relationship between intracellular localization of Bcl-x_L and apoptosis protection. Our approach was to generate a Bcl-x_L-deficient model in which Bcl-x_L targeted at different organelles was expressed and its effects on apoptotic sensitivity were examined. MEFs deficient in Bcl-x_L expression were established from *bcl-x* heterozygous mice. Although alternative splicing of Bcl-x generates Bcl-x_L and Bcl-x_S, Bcl-x_L is the major splicing product in MEFs (Figure 2.1).

Unlike reducing Bcl-2 expression in LNCaP cells [111], knocking out Bcl-x_L expression in MEFs failed to induce compensatory changes in other Bcl-2 family members (Figure 2.2 and Table 2.1). As expected, MEFs deficient in Bcl-x_L expression were more sensitive to various death stimuli compared with wild-type MEFs. Furthermore, reexpression of wild-type Bcl-x_L in Bcl-x-KO MEFs restored

cellular protection against apoptotic insults in a Bcl-x_L dose-dependent fashion (Figure 2.3). These data demonstrate the validity of this experimental model. Bcl-2 protein are localized at both the mitochondria and the ER [101].

To distinguish between the functions of Bcl-x_L localized at different organelles, we targeted Bcl-x_L to a particular organelle by replacing the carboxyl transmembrane region of Bcl-x_L with known organelle targeting sequences. As mitochondria and the ER have been proposed to interact dynamically with each other inside cells [120], it is challenging to exclusively target proteins to a given organelle. Unlike previous studies in which anti-apoptotic Bcl-2 proteins targeted at a particular organelle were overexpressed [112, 113], stable cell lines in the current study were carefully selected so that mitochondria- or ER-localized Bcl-x_L was expressed at levels comparable to that observed in wild-type MEFs (Figure 2.6). It was expected that lower expression levels would also help ensure more exclusive targeting. Thus, the distinct patterns in the intracellular residence of targeted Bcl-x_L proteins are sufficient to reveal the distinctive roles of Bcl-x_L localized on different organelles.

We observed that in the Bcl-x-KO background mitochondrially localized Bcl-x_L functioned as effectively as wild-type protein in inhibiting apoptosis. On the other hand, ER-targeted Bcl-x_L failed to exhibit any anti-apoptotic activity in Bcl-x-KO MEFs (Figure 2.6). Intriguingly though, Bcl-x_L expression at the ER in Bcl-x-KO

MEFs completely rescued abnormal Ca^{2+} signaling phenotypes (Figure 2.7). It is well documented that steady-state ER Ca^{2+} correlates closely with apoptotic sensitivity increased ER Ca^{2+} , increased apoptosis, and vice versa. Here, increased ER Ca^{2+} content sensitizes cells to apoptotic stimuli by providing a greater pool of releasable Ca^{2+} that enhances mitochondrial Ca^{2+} uptake and susceptibility to OMM permeabilization [102, 104]. Both overexpression of Bcl-2 and Bcl-x_L have been shown to lower ER store Ca^{2+} [107, 114, 121, 122]. We reasoned that the discrepancy could be accounted for if Bcl-x_L localized at other organelles was essential for it to be anti-apoptotic at the ER.

Consistent with this reasoning, expression of ER-targeted Bcl-x_L was fully effective in protecting against apoptosis in wild-type MEFs (Figure 2.8). Thus, our current study provides molecular evidence that the protective function of Bcl-x_L at the ER requires Bcl-x_L localization at other cellular compartments. We speculate that this compartment is mitochondria, but further studies are needed to assess exactly how mitochondrially targeted Bcl-x_L is required to sense physiological changes conferred by Bcl-x_L at the ER, and how these signals are translated into apoptotic protection. It is possible that mitochondrial Bcl-x_L is required to facilitate ER-to-mitochondrial Ca^{2+} transfer, and enhanced mitochondrial bioenergetics subsequently renders cells to better withstand apoptotic challenges. In summary, we have developed Bcl-x_L-deficient MEFs suitable for the study of Bcl-x_L-regulated apoptotic pathways. We demonstrate that localization at mitochondria is necessary for endogenous levels of Bcl-x_L to provide apoptotic protection.

Furthermore, we show that localization of Bcl-x_L at the ER is required for normal Ca²⁺ homeostasis, but that targeting Bcl-x_L at the ER only provides increased apoptotic protection if Bcl-x_L is also present at other organelles.

CHAPTER III

**ENDOGENOUS BCL-x_L MODULATES CELLULAR RESPONSE TO
OXIDATIVE STRESS-INDUCED APOPTOSIS**

3.1. Introduction

Apoptosis is regulated by the Bcl-2 family of proteins which can be either pro-apoptotic or anti-apoptotic [3, 44, 45]. In healthy cells, Bcl-x_L binds to BH3-only Bcl-2 proteins and/or multidomain Bax and Bak, inhibiting their pro-apoptotic activities. In dying cells, BH3-only Bcl-2 proteins are activated. Activated BH3-only Bcl-2 proteins then either interact with Bax and Bak or bind to anti-apoptotic Bcl-2 proteins releasing them from their complexes with Bax and Bak, thus activating Bax and Bak. Activated Bax and Bak assemble permeation channels on OMM, releasing apoptogenic factors including cytochrome c and Diablo/Smac from the IMS of the mitochondria into the cytosol where they promotes activation of caspase cascade and apoptosis [54, 75]. Dysregulation of apoptotic signaling pathways has been associated with the development of many diseases including cancer, infections and neurodegeneration [1, 3].

Generation of reactive oxygen species (ROS) has also been implicated in neurodegenerative diseases such as Alzheimer disease and Parkinson's disease

[13], and in cancer [14]. The oxidative stress inducer H_2O_2 causes both apoptosis and necrosis. Mild to moderate levels of H_2O_2 cause apoptosis while higher levels induce necrosis [93]. The mechanisms through which oxidative stress inducers such as H_2O_2 promote apoptosis are not completely understood. However, recent evidence indicates that Bcl-2 proteins are involved in regulating oxidative stress-induced apoptosis [123]. Overexpressing Bcl-2 has been shown to suppress oxidant-induced apoptosis probably by inhibiting lysosomal membrane rupture [124, 125]. Several BH3-only Bcl-2 proteins have also been found to be involved in H_2O_2 -induced apoptosis [126-128]. Nonetheless, how anti-apoptotic Bcl-2 proteins coordinate with pro-apoptotic Bcl-2 proteins to regulate apoptosis remains unclear.

Here, we systematically explored the role of Bcl-2 proteins in the regulation of H_2O_2 -induced apoptosis. I show that endogenous Bcl-x_L inhibits cell death induced by H_2O_2 . Furthermore, upon H_2O_2 exposure, Noxa up-regulation and subsequent Mcl-1 expression decrease are essential for apoptosis. Our findings provide evidence that both anti- and pro-apoptotic Bcl-2 proteins modulate apoptotic signaling triggered by oxidative stress.

3.2. Materials and Methods

3.2.1. Reagent and cell culture

H₂O₂ was purchased from Sigma. Propidium iodide (PI) was obtained from Molecular Probes. The Lipofectamine™ RNAiMAX and Lipofectamine™ 2000 reagents were obtained from Invitrogen. Mcl-1 and Bcl-x_L small interfering RNAs (siRNAs) were obtained from Santa Cruz Biotechnology, while caspase 3/7 assay kit was purchased from AnaSpec. Antibodies used for western blot analysis were anti-Bcl-x_{S/L} S-18 pAb (polyclonal antibody) and anti-Bcl-2 mAb (monoclonal antibody) from Santa Cruz Biotechnology, anti-β-actin mAb from Sigma, anti-Mcl-1 pAb from Epitomics, anti-Bcl-w pAb from Cell Signaling Technology, peroxidase-conjugated goat anti-(rabbit IgG) and peroxidase-conjugated goat anti-(mouse IgG) from Thermo Fisher Scientific.

MEFs studied here were deficient in Bcl-x_L (Bcl-x-KO), Mcl-1 (Mcl-1-KO), or Noxa (Noxa-KO). Bcl-x-KO MEFs expressing Bcl-x_L [Bcl-x_L(H), Bcl-x_L(M) and Bcl-x_L(L)] were also used. MEFs were cultured in DMEM (Mediatech; Manassas, VA) supplemented with 10% FBS (Gemini; West Sacramento, CA), 100 U/ml penicillin (Mediatech), and 100 µg/ml streptomycin (Mediatech) in an incubator with 95% humidity and 5% CO₂ at 37 °C.

3.2.2. Plasmid construction

The cDNAs of murine anti-apoptotic Bcl-2 protein Mcl-1, and a panel of ten pro-apoptotic BH3-only Bcl-2 proteins, including Bim, tBid, Puma, Bad, Bik, Noxa, Bnip3, Nix, Hrk, and Bmf were subcloned into the retroviral expression vector pBABE with the enhanced green fluorescent protein (EGFP) serving as a marker expressed from an internal ribosomal entry site (IRES) [pBABE-IRES-EGFP]. The pBABE-IRES-EGFP plasmid and plasmids containing cDNAs for the BH3-only Bcl-2 protein of interest were first digested with the appropriate restriction enzymes. DNA fragments of the vector (pBABE-IRES-EGFP) and the respective cDNAs of interest were purified after resolving by agarose gel electrophoresis and ligated using the Promega ligation reagent (Promega) at 16 °C overnight. The ligated product was then used for *Escherichia coli* (*E. coli*) transformation reaction with *NEB 5αF'*^α competent cells (New England Biolabs). Transformed *E. coli* was spread on LB plates containing carbenicillin antibiotics. These plates were also incubated overnight at 37 °C for colonies to grow. Then, single *E. coli* colonies were selected, and inoculated in 2 ml LB medium also supplemented with carbenicillin. Inoculum was then incubated at 37 °C for 6-8 hours.

Plasmid DNA of the inoculum was purified using miniprep kit (GenScript). It was then digested with EcoRI and BamHI restriction endonucleases (REs), and digested plasmid DNA was analyzed by agarose gel electrophoresis to examine the presence of DNA fragments with the size of the respective DNA of interest.

Sequence analysis was performed to determine the exact DNA composition of the respective pro-apoptotic BH3-only Bcl-2 proteins. Once the exact DNA composition was determined, the rest of the inoculum in the 2 ml LB media was transferred into a flask containing 400 ml LB media also supplemented with carbenicillin, and further incubated at 37 °C overnight. Plasmid DNA in the culture was purified using the cesium chloride (*CsCl*) ultra-centrifugation method. DNA sequence of the purified plasmids was again confirmed. The purified plasmids were then used for transfection and retroviral infection experiments.

3.2.3. Production of retroviral supernatants

The packaging cell line 293T was transfected with the plasmid carrying the respective gene of interest and the retroviral helper plasmids pMDG2.0 and pUVMC using the Lipofectamine 2000 reagent as a lipid transfection milieu. About 10⁶ cells were plated in 6 cm dish and allowed to grow to confluency. For cDNAs of each of ten BH3-only Bcl-2 proteins, 5 µg of plasmids DNA and 5 µg of retroviral packaging plasmids [pUVMC (2.5 µg) and pMDG2.0 (2.5 µg)] were diluted in 0.5 ml of Opti-MEM medium (Invitrogen). In a separate test tube, 20 µl of lipofectamine 2000 reagent was diluted in 0.5 ml of Opti-MEM medium. Both samples were incubated at room temperature for 5 minutes, mixed together and incubated for another 20 minutes. After 20 minute incubation, each sample was added to the T293 cells and incubated at 37 °C in a 5% CO₂ incubator for 4-6 hours. Media were replaced with 3 ml fresh media per dish. Cells were incubated

at 37 °C in a 5% CO₂ incubator for 48-72 hours prior to testing for transgene expression. Media containing retroviral supernatant was collected 48-72 hours post transfection. Ten µg/ml of polybrene (Sigma) was added to the retroviral supernatants to increase infection efficiency. The respective retroviral supernatants were used to infect various MEFs.

3.2.4. Cell viability

Cell viability was determined by PI exclusion method using flow cytometry analysis (FACScalibur, Beckon Dickinson; San Jose, CA). MEFs were plated in 48 well tissue culture plate at a density of approximately 10⁴ cells per well. MEFs were treated with different apoptotic stimuli or infected with retroviral supernatant containing the respective pro-apoptotic BH3-only Bcl-2 proteins. After the indicated time, MEFs were collected, 1.0 µg/ml of PI was added and cell viability was measured.

3.2.5. Caspase 3/7 activity

We used the Sensolyte[®] Homogeneous R110 Caspase 3/7 Assay Kit (AnaSpec) to measure caspase 3/7 activity. MEFs were plated at a density of approximately 2.5 x 10³ cells per well in a white-walled 96-well tissue culture plates and allowed to grow overnight. Caspase 3/7 activity was determined 9 hours following treatment with H₂O₂ according to the manufacturer's protocols. The slope of

fluorescence increase was calculated and normalized to that of untreated cells, and data were presented as the relative fluorescence unit versus time (RFU/min).

3.2.6. Western blot analysis

Cell pellets were collected and whole cell lysates generated by suspending cells in RIPA lysis buffer [150 mM sodium chloride, 1.0% (v/v) Triton X-100, 0.5% sodium deoxycholate, 0.1% sodium dodecyl sulphate, and 50 mM Tris, pH 8.0] containing protease inhibitors (Complete, Roche; Indianapolis, IN). Total protein concentration was determined using the BCA assay (Pierce; Rockford, IL). Equal amount (20 μ g) of protein per sample was loaded on a 4-12% Bis-Tris gel (Bio-Rad; Hercules, CA), transferred to PVDF (Millipore; Billerica, MA) and used to determine the expression of the respective proteins, with their appropriate primary and secondary antibodies indicated.

3.2.7. siRNA transfection

MEFs (Bcl-x-WT, Bcl-x-KO, Mcl-1-WT, and Mcl-1-KO) were plated in 6-well tissue culture plates at a cell density of 2×10^5 per well or in 48-well tissue culture plates with 1×10^4 cells in each well 24 hours before transfection. Mcl-1 siRNA and Bcl-x_L siRNA with a final concentration of 10 nM were transfected into MEFs with lipofectamine RNAiMax reagents (Invitrogen) following the manufacturer's protocol. Twenty four hours post transfection, MEFs were collected and the gene

silencing efficiency was examined by western blot analysis. Cell viability was measured using the PI exclusion method to determine if knock down of the two anti-apoptotic Bcl-2 proteins will cause spontaneous apoptosis.

3.2.8. Quantitative real-time polymerase chain reaction (qPCR)

Bcl-x wild-type, Noxa wild-type, and Noxa-KO MEFs were incubated with 0.4 mM H₂O₂ for 0, 7 and 15 hours in 10 cm tissue culture plates. Total RNA was isolated using the RNeasy kit (Qiagen) following the manufacturer's instructions. RNA concentration was determined using a NanoDrop 8000 Spectrophotometer (Thermo) and the quality of total RNA determined with a 2100 Bioanalyzer (Agilent). One microgram of total RNA was used for reverse transcription polymerase chain reaction (rt-PCR) to generate cDNA using a High Capacity Reverse Transcript Kit (ABI; Forest City, CA) according to the manufacturer's instructions. The rt-PCR product was used in a TaqMan gene expression assay (ABI, Forest City, CA). The TaqMan 20x probes for the ten BH3-only Bcl-2 proteins were used to detect expression levels of mRNA of the respective BH3-only Bcl-2 proteins with tubulin serving as endogenous control.

3.2.9. Statistical analysis

All experiments were performed in triplicates and results expressed as mean \pm standard deviation of at least three independent triplicate experiments. A two tail

student's t test was carried out and $P \leq 0.05$ was considered significant between samples and their respective controls.

3.3. Results

3.3.1. Endogenous Bcl-x_L inhibits H₂O₂-induced apoptosis

To determine whether endogenous Bcl-2 proteins might be involved in the regulation of oxidative stress-induced apoptosis, we exposed MEFs described before in Figure 2.1 H₂O₂. Both wild-type and Bcl-x-KO MEFs were incubated with 0.1–0.6 mM of H₂O₂ and cell viability was measured. Exposure to various concentrations of H₂O₂ resulted in more cell death in Bcl-x-KO MEFs compared with wild-type MEFs, and cytotoxicity of H₂O₂ was dose-dependent (Figure 3.1A). Among all concentrations examined, 0.4 mM H₂O₂ exposure generated the biggest difference in viability between wild-type and Bcl-x-KO MEFs. It has been reported that moderate H₂O₂ concentrations cause apoptotic cell death and higher levels of H₂O₂ induce necrosis [93].

Following 0.1–0.6 mM H₂O₂ exposure, caspase 3/7 activity was measured to explore the range of H₂O₂ concentrations that were inducing apoptosis in wild-type and Bcl-x-KO MEFs (Figure 3.1B). For both cell lines, MEFs treated with 0.4 mM H₂O₂ exhibited the highest levels of caspase 3/7 activity. Exposure to H₂O₂ concentrations higher than 0.4 mM induced more cell death, but lower caspase 3/7 activity, suggesting that 0.4 mM H₂O₂ provides the optimal level of apoptosis, and higher doses cause increasing MEF cell necrosis. Importantly, caspase 3/7 activity in Bcl-x-KO MEFs treated with 0.4 mM H₂O₂ was higher than

that in wild-type MEFs, indicating that endogenous Bcl-x_L is crucial for protection against H₂O₂-induced apoptosis.

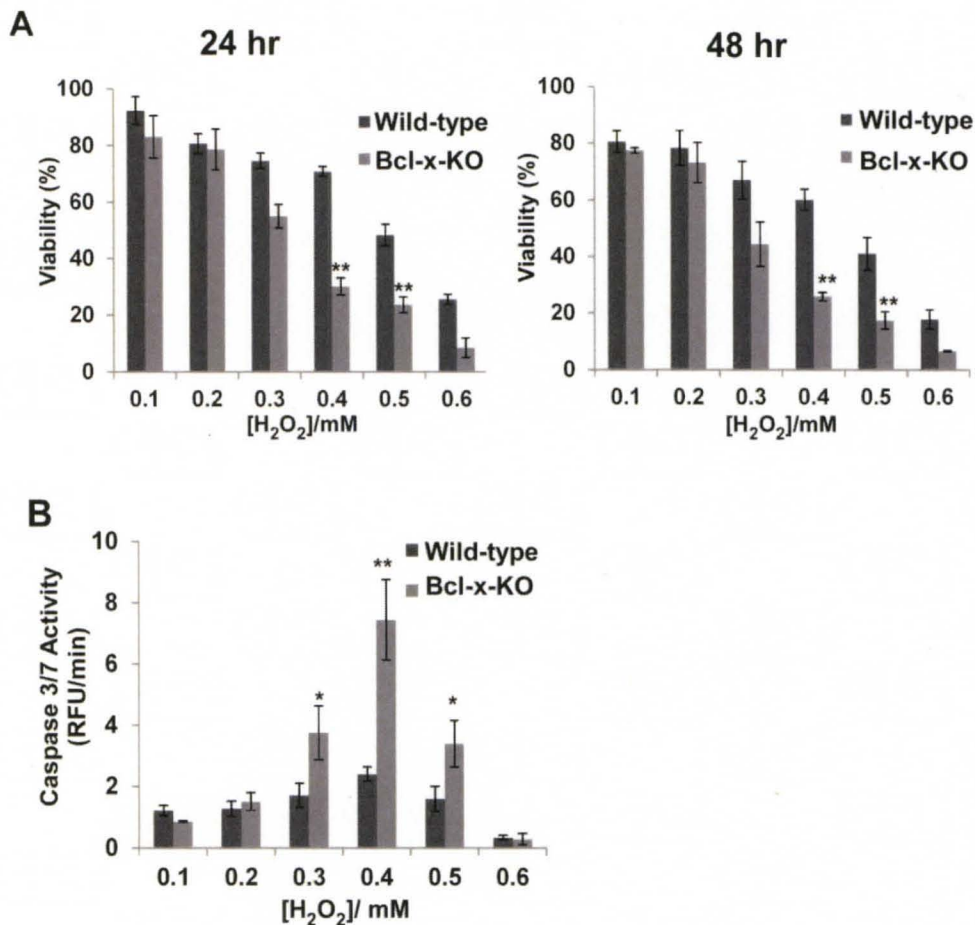


Figure 3.1. Endogenous Bcl-x_L inhibits H₂O₂-induced apoptosis (A) Wild-type and Bcl-x-KO MEFs were treated with 0.1–0.6 mM H₂O₂ for the indicated times and cell viability was measured. Results are mean± standard deviation for three independent experiments performed in triplicate. ***P*<0.01; Student's unpaired *t* test. (B) Fluorimetric assays were carried out to determine caspase 3/7 activity after 9 hour of treatment with 0.1–0.6 mM H₂O₂. Values are normalized to those of the untreated cells, and results are mean±S.D. for three independent experiments performed in triplicate. **P*<0.05; ***P*<0.01; Student's unpaired *t* test.

3.3.2. Endogenous Bcl-x_L differentially antagonizes the activity of different pro-apoptotic BH3-only Bcl-2 proteins

To determine the effects of pro-apoptotic BH3-only Bcl-2 proteins on cell viability of wild-type and Bcl-x-KO MEFs, the cDNA of a panel of ten pro-apoptotic BH3-only Bcl-2 proteins including Bad, Bnip3, Nix, Bim, Bik, tBid, Bmf, Hrk, Puma and Noxa were first subcloned into the retroviral expressing vector pBABE having an enhanced green fluorescent protein (EGFP) as a marker expressed from an Internal Ribosomal Entry Site (IRES) [pBABE/IRES/EGFP]. Each plasmid carrying the gene of interest was first transfected into T293 cells and retroviral supernatant collected. Wild-type and Bcl-x-KO MEFs were infected with retroviral supernatant expressing the individual BH3-only Bcl-2 proteins. As indicated by EGFP fluorescence intensity of cells, more than 95% of infected MEFs expressed the individual BH3-only Bcl-2 proteins. Quantitative real time polymerase chain reaction (qPCR) was performed to ensure that each BH3-only Bcl-2 protein was expressed at similar levels in both wild-type and Bcl-x-KO MEFs (Figure 3.2).

Cell viability was measured at 0, 24 and 48 hours using the PI exclusion method. The BH3-only Bcl-2 proteins were categorized into three groups based on their effects on cell viability of MEFs. The first group includes Bad, Bnip3, Nix, and Bik. As shown in Figure 3.3, when wild-type and Bcl-x-KO MEFs were infected with retroviral supernatant containing Bad, Bnip3, Nix, or Bik respectively, there was

no change in cell viability. Neither wild-type nor Bcl-x-KO MEFs underwent apoptosis upon infection, indicating that these proteins do not directly interact with endogenous Bcl-x_L. The second group includes tBid, Puma, Bim, Bmf and Hrk. When tBid, Puma, Bim, Bmf or Hrk were expressed in wild-type and Bcl-x-KO MEFs, there was no significant difference in cell viability. Both MEFs died at the same rate, showing that Bcl-x_L was not able to prevent cell death initiated by these BH3-only Bcl-2 proteins (Figure 3.3). Finally, Noxa expression induced significant cell death in Bcl-x-KO MEFs but not in wild-type MEFs, indicating that the endogenous Bcl-x_L is able to completely inhibit pro-apoptotic activities of Noxa (Figure 3.3).

These data suggest that endogenous levels of Bcl-x_L mediate cellular responses to pro-apoptotic BH3-only Bcl-2 protein expression by differentially antagonizing their activities. When these ten pro-apoptotic BH3-only Bcl-2 proteins were treated with the Bcl-x-KO MEFs reexpressing different Bcl-x_L levels described in Figure 2.4A above, we found out that reexpression of Bcl-x_L in the Bcl-x-KO MEFs also restored their ability to prevent apoptosis in a Bcl-x_L dose-dependent manner (Figure 3.4).

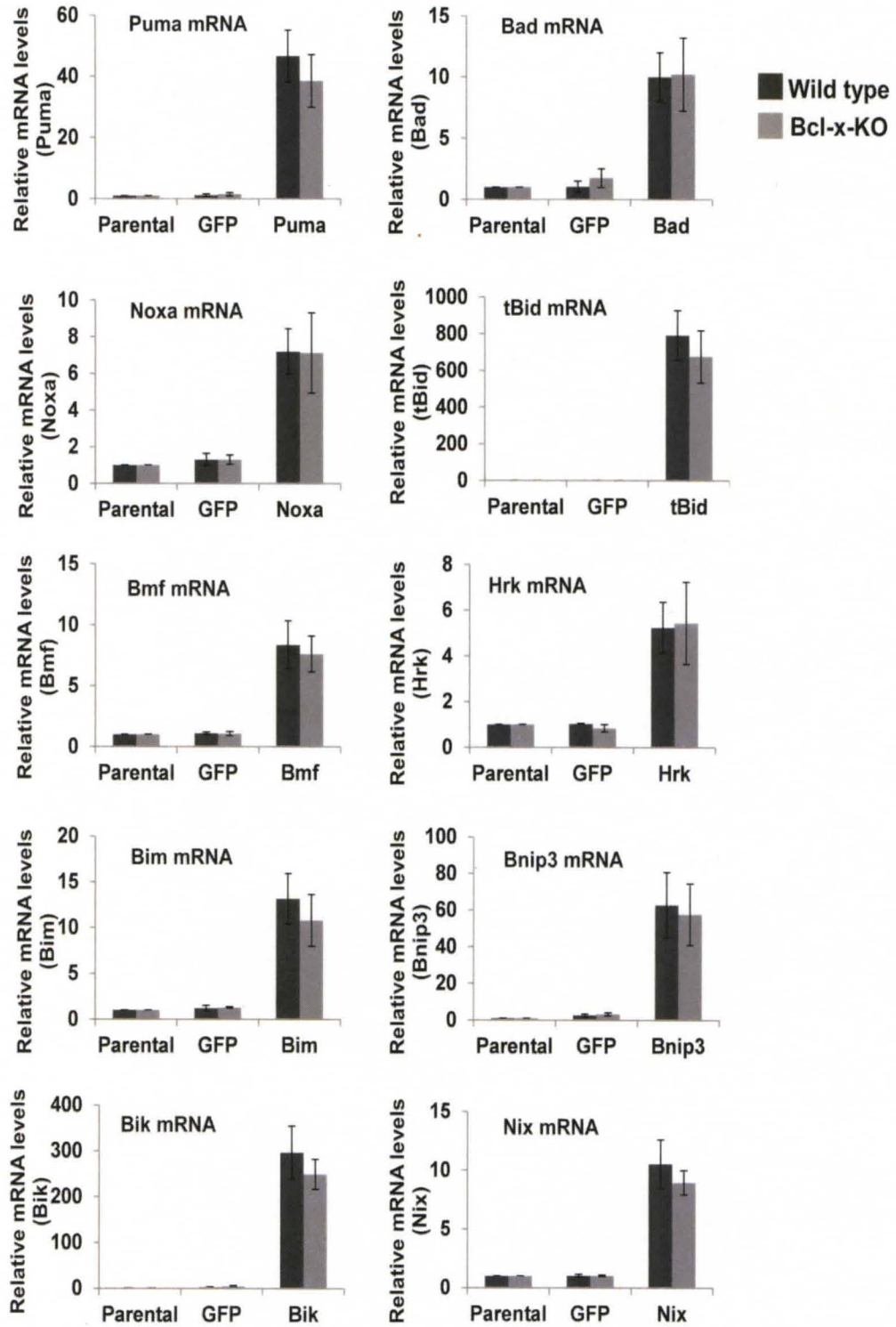


Figure 3.2. Expression levels of pro-apoptotic BH3-only Bcl-2 proteins in MEFs. Wild-type and Bcl-x-KO MEFs were infected with retroviral supernatants expressing the different pro-apoptotic BH3-only Bcl-2 proteins for 8 hours. Expression of the indicated BH3-only Bcl-2 proteins was determined by qPCR analysis. Note that the probes for human Bid were used to detect expression of tBid in MEFs and endogenous Bid expression levels in MEFs were almost undetectable. Data represents mean \pm standard deviation of three independent experiments performed in triplicates.

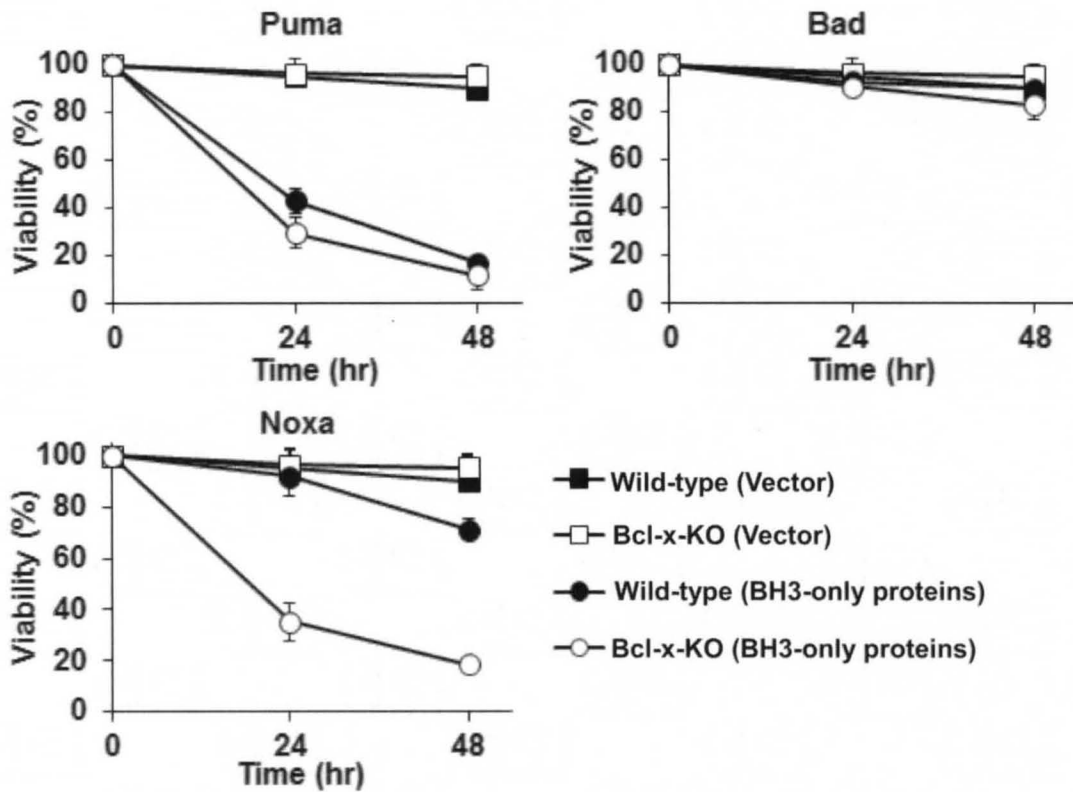


Figure 3.3. Endogenous Bcl-x_L most effectively inhibits Noxa-induced cell death. A panel of pro-apoptotic BH3-only Bcl-2 proteins was expressed in wild-type and Bcl-x-KO MEFs by retroviral infection, and cell viability was measured at the indicated time. The ten BH3-only Bcl-2 proteins were categorized into three groups based on the effectiveness of endogenous Bcl-x_L to antagonize their pro-apoptotic activities. Data representative one BH3-only Bcl-2 protein from each class are shown. Data represents mean \pm standard deviation of three independent experiments performed in triplicate.

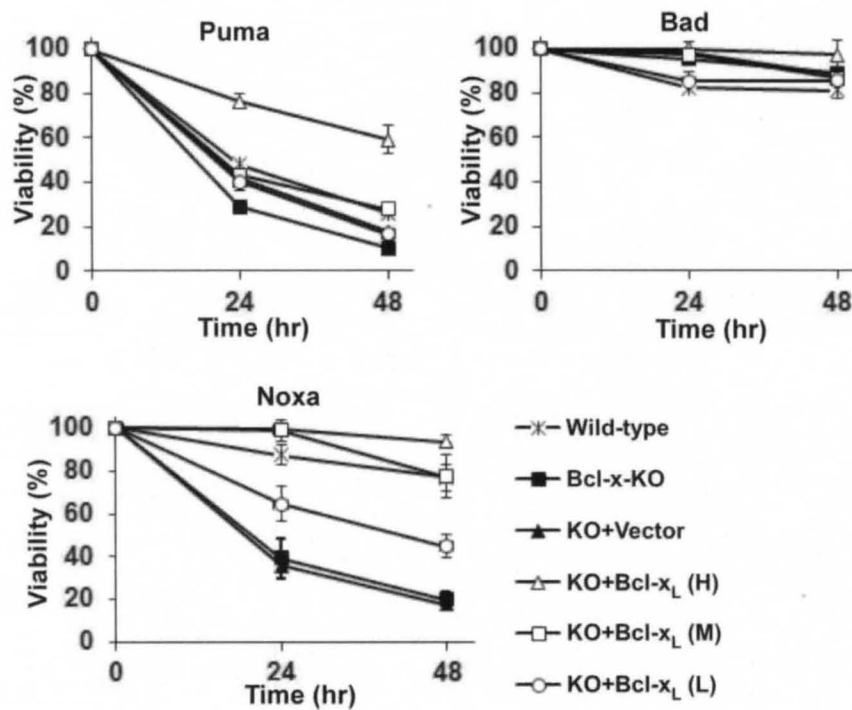


Figure 3.4. Reexpression of Bcl-x_L in Bcl-x-KO MEFs restores their ability to prevent BH3-only Bcl-2 proteins-induced apoptosis. Reexpression of Bcl-x_L in Bcl-x-KO MEFs restored resistance to apoptosis in a Bcl-x_L dose-dependent manner. The ten BH3-only Bcl-2 proteins were infected with the different cell lines described in Figure 2.4A and cell viability was measured at the indicated time. Data show mean ± standard deviation of three independent experiments performed in triplicate.

3.3.3. Endogenous Bcl-x_L prevents H₂O₂- and Noxa-induced apoptosis in a similar fashion

Next, we looked at the effect of endogenous Bcl-x_L on apoptosis induced by the oxidative stress inducers H₂O₂, and the pro-apoptotic BH3-only Bcl-2 proteins. Results demonstrate that endogenous Bcl-x_L most efficiently inhibits apoptosis induced by H₂O₂ (Figure 2.3A and Figure 3.1A), and the pro-apoptotic BH3-only Bcl-2 protein Noxa (Figure 3.3) in a similar manner. But, how the Bcl-2 proteins are involved in oxidative stress-induced apoptosis is largely unclear. Since endogenous Bcl-x_L was able to prevent Noxa- and H₂O₂-induced apoptosis in a similar fashion, I explored further the mechanism by which H₂O₂ induces apoptosis. Previous studies have shown that Noxa interacts with the anti-apoptotic Bcl-2 protein Mcl-1 and sequesters it for degradation. I therefore proposed that the oxidative stress inducer H₂O₂ activates Noxa expression, which in turn leads to Mcl-1 degradation and subsequent apoptosis. Therefore, I investigated the sequence of events involving the Bcl-2 proteins Bcl-x_L, Noxa and Mcl-1 during H₂O₂-induced apoptosis.

3.3.4. Noxa mediates H₂O₂-induced apoptosis

To investigate the role of the pro-apoptotic BH3-only Bcl-2 proteins on apoptosis induced by H₂O₂, I carried out microarray analysis to determine the global changes in mRNA expression levels of the different Bcl-2 proteins in wild type MEFs. Upon H₂O₂ exposure, the most notable increase in gene expression within

the BH3-only Bcl-2 protein family was Noxa, while the other BH3-only Bcl-2 proteins showed smaller changes in gene expression (Figure 3.5A). Noxa gene expression level was dramatically increased at the 7 hour time point, and the fold increase was smaller at the 15 hour time point, suggesting that the increase might be transient. The upregulation of Noxa mRNA was also validated using qPCR, indicating that Noxa expression is increased during oxidative stress inducer, H₂O₂-induced apoptosis (Figure 3.5B).

A

Gene Description	Fold changes	
	(7 hr)	(15 hr)
Phorbol-12-myristate-13-acetate-induced protein1 (Pmaip1, Noxa)	3.17	2.06
Bcl-2 binding component 3 (Puma)	1.42	1.28
Bcl-2-like 11 (Bim)	1.34	1.70
Bcl-2 /adenovirus E1B Interacting protein 3-like (Bnip3l, Nix)	1.10	1.24
Bcl-2-interacting killer (Bik)	1.10	1.02
Harakiri, Bcl-2 interactin protein (Hrk)	1.09	0.94
BH3 interacting domain death agonist (Bid)	0.96	0.87
Bcl-2 modifying factor (Bmf)	0.93	0.99
Bcl-2 associated agonist of cell death (Bad)	0.90	0.97
Bcl-2 /adenovirus E1B Interacting protein 3 (Bnip3)	0.82	0.77

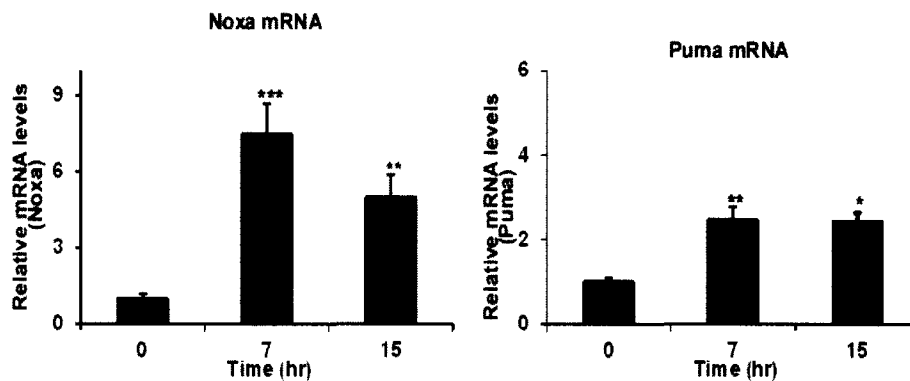
B

Figure 3.5. H₂O₂ induces Noxa expression. (A) Noxa mRNA displayed the greatest increase upon H₂O₂ treatment among BH3-only Bcl-2 proteins. Microarray analysis was used to determine changes of mRNA levels in wild-type MEFs after exposure to 0.4 mM H₂O₂ for 7 hours and 15 hours. The fold change in mRNA levels of different BH3-only Bcl-2 proteins was calculated using the values at 0 hour time point as a control. (B) Quantitative real-time polymerase chain reaction (qPCR) showed expression levels of Noxa and Puma mRNA after treating wild-type MEFs with 0.4 mM H₂O₂. Data represent the mean ± standard deviation of three independent experiments performed in triplicates. Asterisks indicate $P < 0.05$ (*), $P < 0.01$ (**), or $P < 0.001$ (***), Student's unpaired t test.

To further explore the importance of Noxa in H₂O₂-induced apoptosis, I investigated the effects of decreased Noxa expression on cell sensitivity to H₂O₂. MEFs deficient in Noxa expression (Noxa-KO) and their wild-type counterparts were provided by Professor Andreas Strasser (Walter and Eliza Hall Institute of Medical Research, Parkville, VIC Australia). Due to a lack of effective anti-murine Noxa antibodies, I failed to detect Noxa protein expression in any MEFs examined. However, the results from qPCR experiments confirmed that Noxa mRNA was expressed in wild-type but not in Noxa-KO MEF cells (Figure 3.6A). When treated with 0.1-0.6 mM H₂O₂, MEF cell death increased in a H₂O₂ dose-dependent manner and wild-type MEFs were more sensitive to H₂O₂ than Noxa-KO MEFs, providing evidence that H₂O₂-induced apoptosis is primarily mediated by Noxa in MEFs (Figure 3.6B). Furthermore, the biggest difference in cell viability between wild-type and Noxa-KO MEFs was observed for MEFs treated with 0.4 mM H₂O₂. Importantly, 0.4 mM H₂O₂ exposure induced highest caspase 3/7 activity among all concentrations tested (Figure 3.6C).

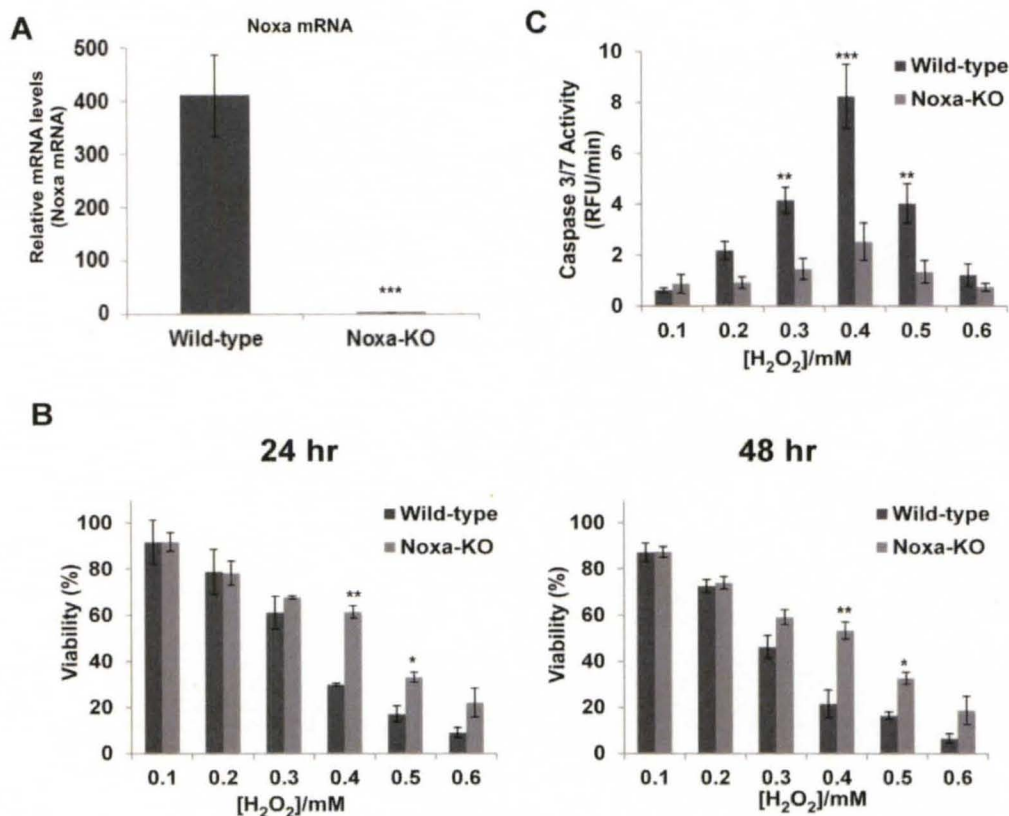


Figure 3.6. H₂O₂-induced apoptosis is mediated by Noxa. (A) Noxa mRNA levels in wild-type and Noxa-KO MEFs were determined by qPCR. (B) Noxa wild-type and Noxa-KO MEFs were treated with 0.1-0.6 mM H₂O₂ and cell viability measured at the indicated time. Data represent mean ± standard deviation of three separate triplicate experiments. (C) Caspase 3/7 activity was determined using the fluorometric assay after treatment of wild-type and Noxa-KO MEFs with 0.1-0.6 mM H₂O₂ for 9 hours. Values were normalized to those of untreated control cells. Asterisks indicate $P < 0.05$ (*), $P < 0.01$ (**), or $P < 0.001$ (***), Student's unpaired t test.

3.3.5. Reduction of Mcl-1 expression in response to H₂O₂ treatment is dependent on Noxa but not on Bcl-x_L.

As the pro-apoptotic BH3-only Bcl-2 protein Noxa has been shown to interact with the anti-apoptotic Bcl-2 protein Mcl-1 and cause Mcl-1 degradation [129], we explored whether H₂O₂-induced Noxa expression led to reduced Mcl-1 expression levels. Noxa wild-type and Noxa-KO MEFs were treated with H₂O₂, and Mcl-1 expression levels were determined by western blot analysis (Figure 3.7A and 3.7B). Upon H₂O₂ exposure, Mcl-1 protein was decreased in Noxa-expressing wild-type cells in a time-dependent manner. In contrast, Mcl-1 expression was not affected by H₂O₂ in Noxa-KO MEFs (Figure 3.7A and 3.7B). The lack of Mcl-1 downregulation in Noxa-KO MEFs provides more evidence that H₂O₂-induced Mcl-1 expression reduction is mediated by Noxa. Since pro-apoptotic activities of Noxa depend on endogenous Bcl-x_L expression (Figure 3.3), we examined the influence of endogenous Bcl-x_L in Mcl-1 expression decrease caused by H₂O₂ exposure. When treated with H₂O₂, Mcl-1 expression levels decreased to comparable degrees in both wild-type and Bcl-x-KO MEFs, indicating that Bcl-x_L does not influence the Mcl-1 down-regulation induced by H₂O₂ (Figure 3.7C and 3.7D).

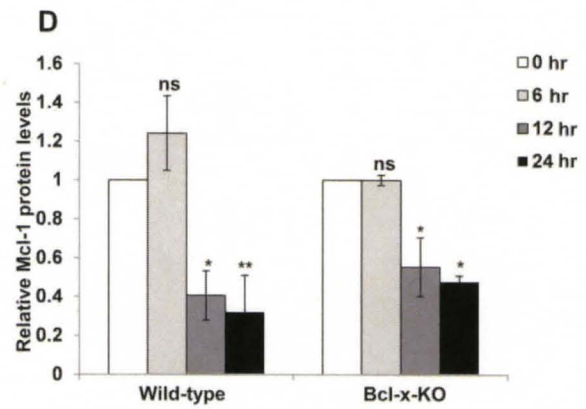
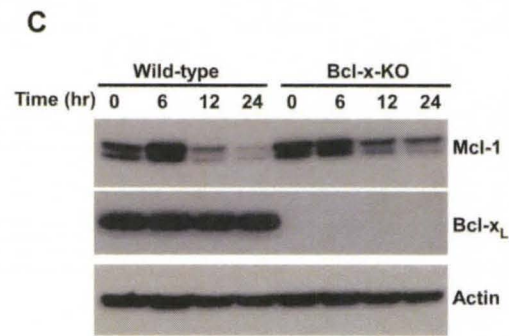
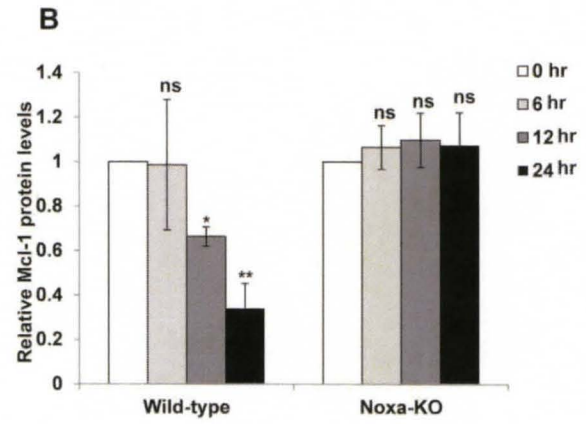
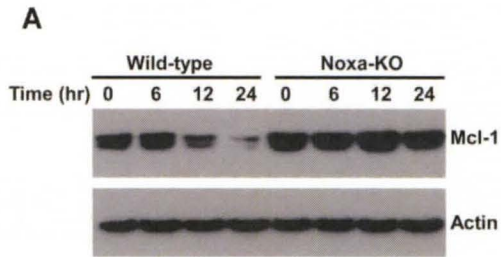


Figure 3.7. Mcl-1 expression reduction in response to H₂O₂ depends on Noxa but not Bcl-x_L. (A) Wild-type and Noxa-KO MEFs were exposed to 0.4 mM H₂O₂ for the indicated time and cell lysates were collected. Western blot analysis determined the Mcl-1 expression levels. Images represent one of three independent experiments. (B) Normalized summary of Mcl-1 levels in the indicated cell lines shown in (A). The values of Mcl-1 levels were normalized to those in the untreated cells. Data represent the mean ± standard deviation of three independent experiments. (C) Wild-type and Bcl-x-KO MEFs were treated with 0.4 mM H₂O₂ and cell lysates were obtained at the indicated time points. Mcl-1 expression levels were assessed by western blot analysis. The results of one of three independent experiments are shown. (D) The levels of Mcl-1 shown in (C) were normalized as described in (B). Data represent the mean ± standard deviation of three independent experiments. Asterisks indicate $P < 0.05$ (*) or $P < 0.01$ (**), and (ns) no significance, Student's unpaired t test.

3.3.6. Mcl-1 overexpression inhibits H₂O₂-induced apoptosis

To further explore the importance of Mcl-1 reduction in H₂O₂-induced apoptosis, Mcl-1 was overexpressed in wild-type and Bcl-x-KO MEFs by retroviral infection and western blot analysis used to determine Mcl-1 expression levels in MEFs (Figure 3.8A). MEFs with different Mcl-1 expression levels were exposed to 0.4 mM H₂O₂ and cell viability was determined. Overexpressed Mcl-1 prevented H₂O₂-induced apoptosis in both wild-type and Bcl-x-KO MEFs (Figure 3.8B). In addition, caspase 3/7 activity measurement confirmed that Mcl-1 overexpression inhibited apoptosis induced by H₂O₂ (Figure 3.8C), in support of the notion that Noxa-mediated decrease in Mcl-1 might be involved in H₂O₂ cytotoxicity.

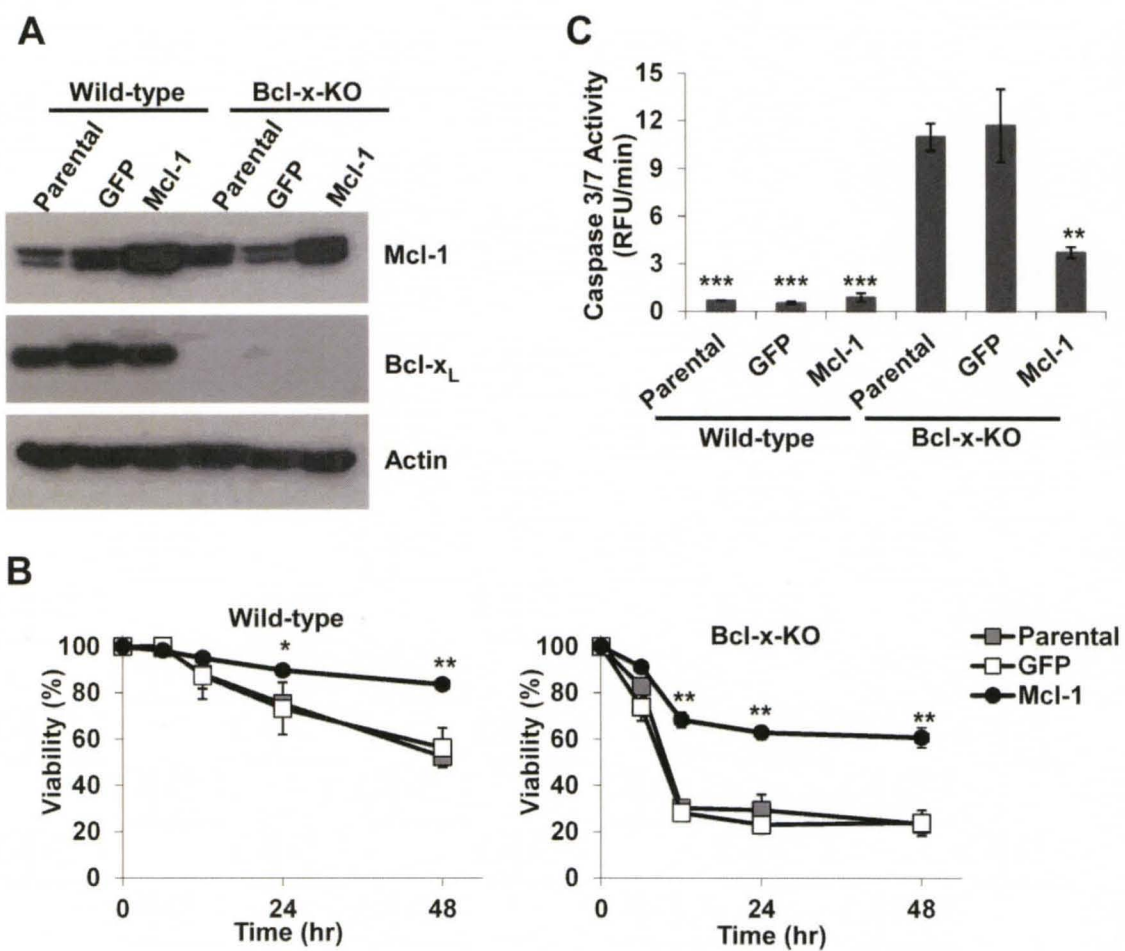


Figure 3.8. Mcl-1 overexpression inhibits H₂O₂-induced apoptosis. (A) Mcl-1 was stably overexpressed in both wild-type and Bcl-x-KO MEFs. Western blot analysis determined the expression levels of Mcl-1 in the indicated cell lines. **(B)** Wild-type and Bcl-x-KO MEFs with or without Mcl-1 overexpression were treated with 0.4 mM H₂O₂ for the indicated time period, and cell viability measured. Data represent the mean ± standard deviation of three independent experiments performed in triplicate. Asterisks indicate $P < 0.01$ (**) or $P < 0.001$ (***), Student's unpaired t test. **(C)** Caspase 3/7 activity was determined using the fluorometric assay for cell lines described in (A) following 9 hour treatment with 0.4 mM H₂O₂. Values were normalized to those of the untreated cells. Data are shown as the mean ± standard deviation of three independent experiments performed in triplicate. Asterisks indicate $P < 0.05$ (*) or $P < 0.01$ (**), Student's unpaired t test.

3.3.7. Reduction of both Bcl-x_L and Mcl-1 protein expression in MEFs induces spontaneous apoptosis (synthetic lethality).

We have shown that lacking endogenous Bcl-x_L expression sensitized cells to both H₂O₂ treatment (Figure 2.3A) and Noxa expression (Figure 3.3), and Noxa-dependent decrease in Mcl-1 expression is important for cell death induced by H₂O₂ (Figure 3.8B). Therefore, we reasoned that Bcl-x_L and Mcl-1 were two anti-apoptotic Bcl-2 proteins critical to prevent apoptosis in general and H₂O₂-induced apoptosis in particular. Thus, we investigated the influence of reducing Bcl-x_L and Mcl-1 expression simultaneously on cell survival. To this purpose, we first reduced Mcl-1 expression in Bcl-x-KO MEFs. Upon Mcl-1 siRNA transient expression, Mcl-1 expression decreased in both wild-type and Bcl-x-KO MEFs, whereas expression of other anti-apoptotic Bcl-2 proteins, including Bcl-x_L, Bcl-2 and Bcl-w, appeared unchanged (Figure 3.9A). The reduction of Mcl-1 expression in wild-type MEFs was more dramatic than that in Bcl-x-KO MEFs (Figure 3.9B). While knocking down Mcl-1 expression failed to affect spontaneous wild-type cell death, reduced Mcl-1 expression in Bcl-x-KO MEFs caused significantly more cell death (Figure 3.9C).

To further validate the role of Bcl-x_L and Mcl-1 in maintaining cell survival, a reciprocal experiment was performed to knock down Bcl-x_L expression in wild-type and Mcl-1-KO MEFs (Figure 3.9D). Twenty four hours following transfection, Bcl-x_L expression was reduced to comparable levels in wild-type and Mcl-1-KO MEFs by Bcl-x_L siRNA (Figure 3.9E). Much higher levels of spontaneous

apoptosis were observed in Mcl-1-KO MEFs with reduced Bcl-x_L expression, whereas decreased Bcl-x_L expression did not affect cell survival in wild-type MEFs (Figure 3.9F). Overall, these results indicate that Bcl-x_L and Mcl-1 are important in maintaining MEF cell survival and suppressing both of them leads to spontaneous apoptosis.

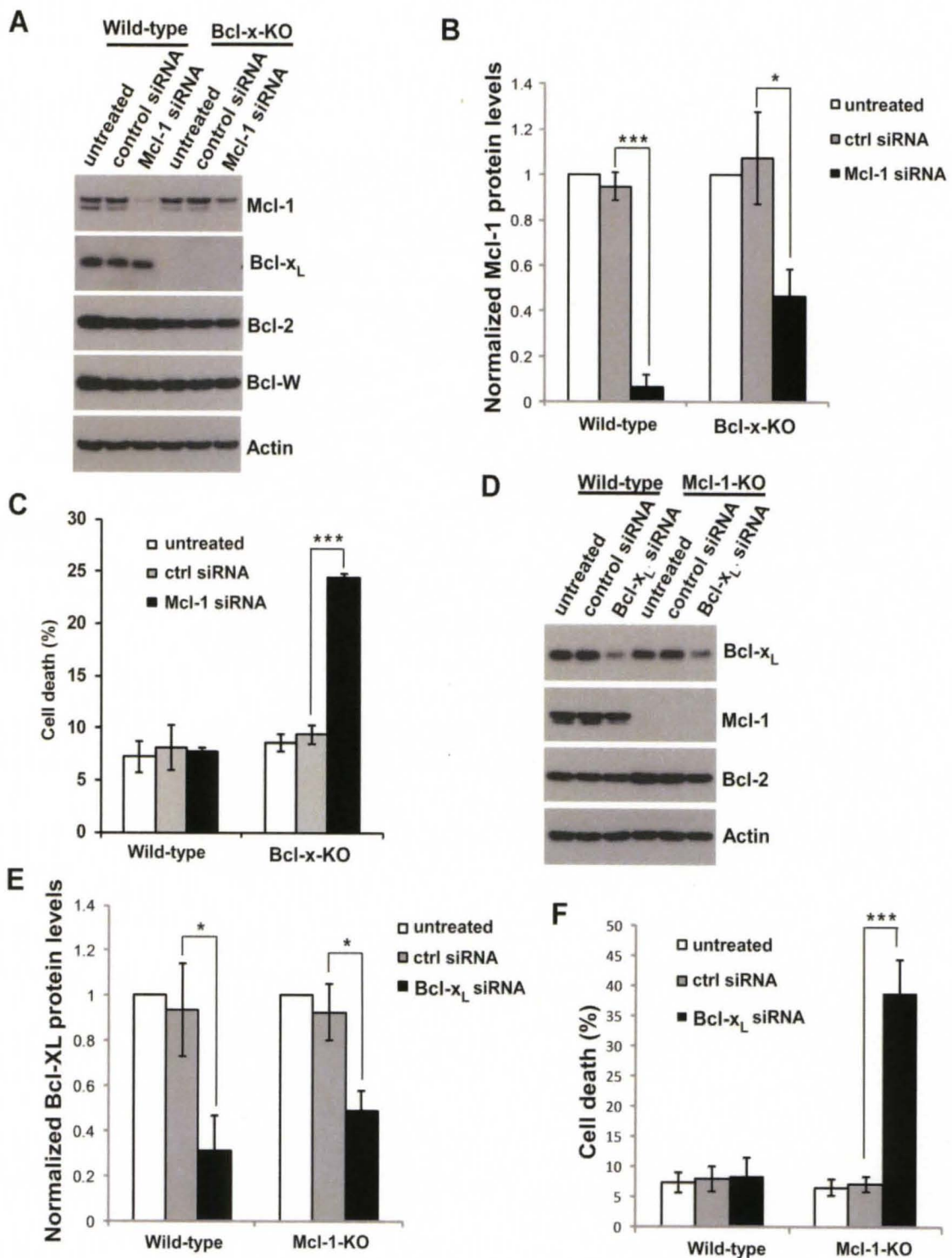


Figure 3.9. Reduction in Bcl-x_L and Mcl-1 expression simultaneously induces spontaneous apoptosis. (A) Expression of Mcl-1 and several anti-apoptotic Bcl-2 proteins in the indicated wild-type and Bcl-x-KO MEFs were determined by western blot 24 hours post siRNA transfection. **(B)** The summary of normalized Mcl-1 levels shown in (A). Mcl-1 levels were normalized to those in the untreated cells. Data represent the mean \pm standard deviation of three independent experiments. **(C)** Reduction of Mcl-1 expression in Bcl-x-KO MEFs induced spontaneous cell death 24 hours following siRNA transfection. Mean \pm standard deviation for three independent experiments are shown. **(D)** Bcl-x_L expression was reduced in both wild-type and Mcl-1-KO MEFs by siRNA 24 hours after transfection. **(E)** Normalized summary of Bcl-x_L levels in the indicated cell lines shown in (D). Data represent the mean \pm standard deviation of three different experiments. **(F)** Decreasing Bcl-x_L expression caused cell death in Mcl-1-KO MEFs 24 hours following transfection. Mean \pm standard deviation for three independent experiments are shown. Asterisks indicate $P < 0.05$ (*) or $P < 0.001$ (***), Student's unpaired t test.

3.4. Discussion

Oxidative stress-induced apoptosis is a well-described phenomenon, but the precise mechanisms through which oxidative stress is coupled with ultimate cell death are not completely clear. In this specific aim, I investigated the roles of both anti- apoptotic and pro-apoptotic Bcl-2 proteins in regulating cell death caused by oxidative stress in the form of H₂O₂. Upon H₂O₂ exposure, endogenous anti-apoptotic Bcl-x_L seemed to be essential for MEF cell survival. Systematic examination of the involvement of pro-apoptotic BH3-only Bcl-2 proteins in H₂O₂-induced apoptosis revealed that Noxa was the major mediator of H₂O₂ cytotoxicity in MEFs. Furthermore, H₂O₂-induced Noxa expression led to reduction in Mcl-1 expression, which in turn co-operated with decreased Bcl-x_L levels to trigger apoptotic signaling. Overall, our studies provide molecular evidence that Bcl-2 family of proteins function co-operatively to modulate cellular responses to oxidative stress.

Cellular responses to any apoptotic trigger, including oxidative stress, are modulated by complex Bcl-2 networks [46, 75]. In response to apoptotic stimuli, activity of BH3-only Bcl-2 proteins is up-regulated either by an increase in transcription or by post-translational modification, such as caspase-8-mediated proteolysis of Bid [130], phosphorylation of Bim [131], and dephosphorylation of Bad [132]. This present study focuses on investigating whether transcriptional induction of a particular BH3-only Bcl-2 protein mediates oxidative stress-

triggered cell death. The possible role of post-translational modification of BH3-only Bcl-2 proteins in oxidative stress-induced apoptosis is not addressed here. It is conceivable that post-translational modification of one or more BH3-only Bcl-2 proteins might also be involved in apoptosis induced by oxidative stress. Modest caspase 3/7 activity observed in H₂O₂-treated Noxa-KO MEFs suggests that BH3-only Bcl-2 proteins other than Noxa are also involved in oxidative stress-induced apoptosis, albeit a minor role in MEFs.

Several BH3-only Bcl-2 proteins have been proposed to be involved in cell death caused by H₂O₂. Murine retinal explants deficient in Bim expression are more resistant to H₂O₂ treatment compared with retinal explants expressing Bim [133]. In fibroblasts, Bik expression is crucial for H₂O₂-triggered cell death [127]. In agreement with our observations, Noxa is largely responsible for the cytotoxicity of H₂O₂ in T leukemia Jurkat cells [128]. Thus, the involvement of a particular BH3-only Bcl-2 protein in H₂O₂-induced apoptosis appears to depend on cell type, which could be attributed to cell type-specific transcriptional responses to cell death stimuli. While the proline- and acid-rich (PAR) subfamily of basic leucine-zipper (bZIP) transcriptional factor family is responsible for Bik expression increase in H₂O₂-exposed MEFs [127], the activating transcription factor 4 (ATF4) has been implicated in the induction of Noxa expression in Jurkat cells upon H₂O₂ exposure [128]. It is still unclear how oxidative stress-induced apoptosis signalling is transduced into the nucleus to induce the transcription of BH3-only Bcl-2 proteins. The cytotoxicity of oxidative stress is believed to be

mediated by reactive oxygen species (ROS) and reactive iron [134, 135]. Membrane rupture of lysosomes, the organelle with most abundant labile iron, results in translocation of redox-active iron to the nucleus, which might be responsible for generating oxidative damage to DNA and subsequent transcriptional responses [136]. In support of this model, the lysosomotropic iron chelator deferoxamine (DFO) prevents production of more reactive species of ROS, lysosomal rupture and subsequent cell death [134, 135, 137].

It has been proposed that BH3-only Bcl-2 proteins function to inhibit activities of anti-apoptotic Bcl-2 proteins and/or activate multidomain effector Bcl-2 proteins Bak and Bax [74]. The differential interactions between BH3-only Bcl-2 proteins and anti-apoptotic Bcl-2 proteins enable the complex Bcl-2 network to modulate apoptotic signalling. Through BH3 peptide and protein binding assays, the interactions between BH3-only Bcl-2 proteins and anti-apoptotic Bcl-2 proteins have been quantified [138, 139]. While some BH3-only Bcl-2 proteins, such as Bim and Puma, engage all anti-apoptotic Bcl-2 proteins, Noxa is believed to interact with Mcl-1 with highest affinity *in vitro*. Although Bim, Puma, Bmf, and Hrk have been shown to bind to Bcl-x_L, endogenous Bcl-x_L failed to provide any protection against the expression of each of these BH3-only Bcl-2 proteins (Figure 3.3). One possible scenario is that endogenous Bcl-x_L was overwhelmed by expression of these BH3-only Bcl-2 proteins. However, our current knowledge of the interactions between BH3-only Bcl-2 proteins and Bcl-x_L are largely based on studies of BH3 domain peptides and recombinant proteins. The results

obtained from these *in vitro* studies might not truthfully reflect the physiological interactions between endogenous Bcl-x_L and BH3-only Bcl-2 proteins inside cells. Remarkably, Noxa was the only BH3-only Bcl-2 protein whose pro-apoptotic activities were completely abolished by endogenous Bcl-x_L, even though cytotoxicity of Noxa on Bcl-x-KO MEFs was comparable to those of Bim, Puma, Bmf, tBid and Hrk (Figure 3.3).

The simple explanation for this observation is that endogenous Bcl-x_L directly binds to Noxa and completely sequesters all ectopically expressed Noxa. Indeed, a recent study indicates that Bcl-x_L may directly interact with Noxa in HeLa cells [140]. However, the observed interaction between Bcl-x_L and Noxa is weak, as only overexpressed Bcl-x_L but not endogenous Bcl-x_L has been found to bind Noxa following DNA damage. This seems not to be the case in our studies. If endogenous Bcl-x_L directly bound and sequestered Noxa in H₂O₂-treated MEFs, reduction of Mcl-1 expression would be more dramatic in Bcl-x-KO MEFs, since more unbound Noxa proteins would be available to engage Mcl-1 in the absence of Bcl-x_L. In fact, similar reduction of Mcl-1 expression was observed in wild-type and Bcl-x-KO MEFs (Figure 3.7), suggesting that Noxa does not directly engage endogenous Bcl-x_L in MEFs. Instead, our studies provide evidence that H₂O₂-induced Noxa expression causes Mcl-1 down-regulation, which is involved in H₂O₂ cytotoxicity.

Our data demonstrate that Bcl-x_L and Mcl-1 are two major anti-apoptotic Bcl-2 proteins protecting cells against basal pro-apoptotic activities in healthy cells. Apoptosis was initiated when Mcl-1 expression was reduced in Bcl-x-KO MEFs or Bcl-x_L expression was decreased in the MEFs lacking Mcl-1 expression (Figure 3.9), which is consistent with the previous studies in HeLa cells [140]. The nature of basal pro-apoptotic activities triggering apoptosis in the absence of Bcl-x_L and Mcl-1 is not completely understood. One intriguing possibility is that multidomain Bak is kept inactive by Bcl-x_L and Mcl-1 in healthy cells [129]. But in the presence of apoptotic stimuli, BH3-only Bcl-2 proteins are activated to displace both Bcl-x_L and Mcl-1 from Bak, such as Bad for Bcl-x_L and Noxa for Mcl-1. Bak is then freed and activated, and activated Bak subsequently forms permeation channels on mitochondria and promotes OMM permeabilization. However, other studies indicate that Bak is not kept in check by Bcl-x_L and or Mcl-1[141]. Instead, the mitochondrial protein voltage-dependent anion channel 2 (VDAC2) is found to sequester Bak and keep it inactive. Whether Bak activation is responsible for oxidative stress-induced cell death or not warrants further investigation. In summary, our studies define the important roles of several members of the Bcl-2 protein family in H₂O₂-induced apoptosis (Figure 3.10).

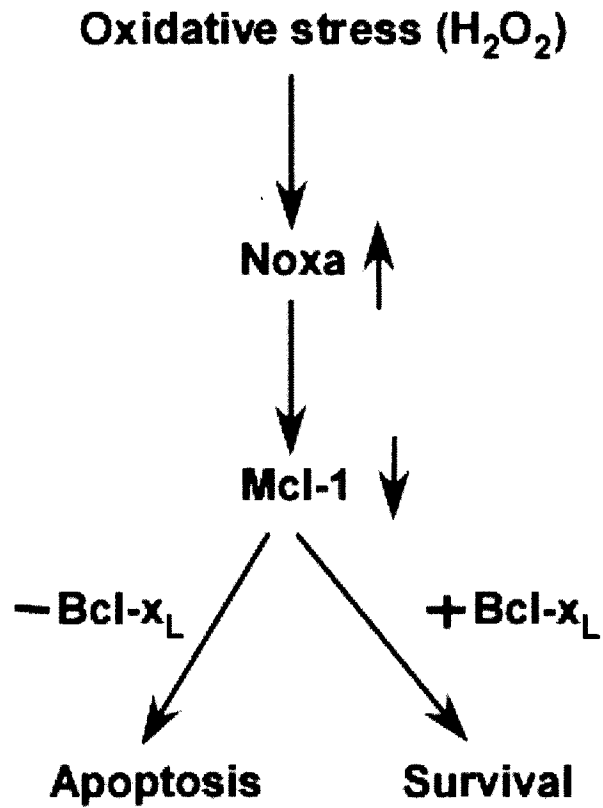


Figure 3.10. Bcl-2 proteins coordinately regulate H₂O₂-induced apoptosis.

Oxidative stress (H₂O₂) induces Noxa expression, leading to reduction of Mcl-1 expression. In the absence of Bcl-x_L, cells undergo apoptosis. Endogenous Bcl-x_L protects against cell death induced by H₂O₂.

CHAPTER IV

THE IMPORTANT ROLE OF LYSOSOMAL MEMBRANE PERMEABILIZATION DURING OXIDATIVE STRESS-INDUCED APOPTOSIS

4.1. Introduction

Apoptosis is regulated by the Bcl-2 family of proteins, which can either be pro-apoptotic or anti-apoptotic [3, 44, 45]. Pro-apoptotic Bcl-2 proteins promote or induce apoptosis by increasing OMMP, whereas anti-apoptotic Bcl-2 proteins inhibit OMMP and prevent or delay apoptosis [46, 74, 75]. Although mitochondria play a central role in apoptosis regulation, other organelles including the ER, the golgi apparatus, and the lysosomes are also involved in apoptosis regulation [53, 142, 143]. Lysosomes are major intracellular organelles responsible for degrading and recycling of cellular components. Lysosomes contain at least 50 hydrolytic enzymes including nucleases, proteases, phospholipases, lipases, phosphatases, sulfatases and glycosidases which, upon release, can degrade macromolecules in the cytosol [144].

The best characterized lysosomal enzymes belong to the cathepsin protease family. A wide variety of stressors including osmotic stress, growth factor deprivation, death receptor activation, proteasome inhibitors and oxidative stress

inducers have been shown to target lysosomes and cause lysosomal membrane permeabilization (LMP) through which lysosomal hydrolytic enzymes are released into the cytosol [145]. The degree of lysosomal damage determines the cell's fate. Massive lysosomal damage causes an excessive release of lysosomal contents into the cytosol resulting in indiscriminate degradation of cellular contents and cytoplasmic acidification, which in turn promotes cell death by necrosis. On the other hand, selective or partial lysosomal damage induces cell death by apoptosis [146-148]. For instance, in $\text{TNF}\alpha$ -treated cells, cathepsin B, D and L released into the cytosol trigger apoptosis by converting the inactive full length pro-apoptotic BH3-only Bcl-2 protein Bid into its truncated (activated) form (tBid) promoting subsequent OMMP and caspase activation [145, 149].

Oxidative stress inducers, including H_2O_2 , are capable of inducing cell death by both necrosis and apoptosis; mild oxidative stress causes apoptosis whereas severe oxidative stress triggers necrosis [93]. The extent of oxidative stress determines the degree of lysosomal membrane damage. In lysosomes, H_2O_2 interacts with iron to generate highly reactive hydroxyl radicals that initiate lipid peroxidation of lysosomal membranes and subsequent LMP. In support of this model, the iron chelating agent desferrioxamine (DFO) has been shown to abolish oxidative stress-triggered LMP and apoptosis [150]. However, the involvement of LMP in oxidative stress-induced apoptosis signaling and how LMP is modulated by the Bcl-2 protein network are unclear. Here, I investigated the temporal relation between LMP and OMMP during oxidative stress-induced

apoptosis. In mouse embryonic fibroblasts (MEFs), H₂O₂ was able to induce LMP prior to OMMP during apoptosis. Outer mitochondrial membrane permeabilization and subsequent apoptosis signaling, but not LMP, depended on Noxa expression. The iron chelating agent DFO prevented H₂O₂-induced OMMP and apoptosis by inhibiting LMP and subsequent increase in Noxa expression. Therefore, LMP-induced Noxa expression is critical for OMMP and subsequent activation of the apoptosis cascade during oxidative stress.

4.2. Materials and Methods

4.2.1. Reagents

DFO, etoposide, doxorubicin, actinomycin D, hydrogen peroxide (H₂O₂), acridine orange (AO), and ferric ammonium citrate were purchased from Sigma (St. Louis, MO). Staurosporine, cisplatin, and carboplatin were from Enzo (Farmingdale, NY). Propidium iodide (PI), MitoTracker Green, MitoTracker Red, and puromycin were from Invitrogen (Carlsbad, CA). Unless otherwise stated, all reagents were dissolved in DMSO. DMEM, penicillin/streptomycin (P/S), trypsin, and L-glutamine were obtained from Mediatech (Manassas, VA), and FBS was purchased from Gemini (Broderick, CA). The jetPRIME® transfection reagent was from Polyplus-transfection (NYC, NY). The SensoLyte® Homogeneous Rh110 caspase 3/7 assay kit was from AnaSpec (San Jose, CA). Antibodies (Abs) used for western blot were anti-β-actin mAb (Sigma), anti-Noxa pAb (Imgenex; San Diego, CA), anti-cytochrome c (BD Pharmingen), peroxidase-conjugated goat anti-rabbit IgG (Thermo; Waltham, MA) and peroxidase-conjugated goat anti-mouse IgG (Thermo).

4.2.2. Cell lines and cell culture

MEFs deficient in the expression of the anti-apoptotic Bcl-2 protein Bcl-x_L (Bcl-x-KO) and their wild-type counterparts were used. Noxa-KO MEFs and their wild-type counterparts were provided by Professor Andreas Strasser (Walter and Eliza Hall Institute of Medical Research, Parkville, VIC Australia). All MEFs were

grown and maintained in DMEM supplemented with 10% FBS and 100 units/ml of penicillin and 100 µg/ml of streptomycin.

The bulk populations of the human colon cancer cell lines (HCT116) stably expressing Noxa shRNA or the control luciferase shRNA were provided by Dr. Onno Kranenberg (University Medical Center Utrecht; Utrecht, Netherlands). The limited dilution method was used to obtain single clones, and Noxa expression was examined by western blot. The HCT116 cells were grown and maintained in DMEM supplemented with 5% FBS, 100 units/ml of penicillin, 100 µg/ml of streptomycin, 2 mM L-glutamine and 0.5 µg/ml of puromycin. Cells were all cultured in a 5% CO₂ humidified incubator at 37 °C.

4.2.3. Plasmid construction and retrovirus production

Murine Noxa cDNA was subcloned into the retroviral expression vector pBABE-IRES-EGFP with the marker protein enhanced green fluorescence protein (EGFP) expressed from an internal ribosomal entry site (IRES) as described previously [151]. For retrovirus production, the human embryonic kidney (HEK)-293T cells were transfected with the plasmid pBABE-mNoxa-IRES-EGFP or the empty vector and the helper plasmids pUVMC and pMDG2.0 using the jetPRIME® transfection reagent. Retroviral supernatant was collected 48-72 hours after transfection and supplemented with 10 µg/ml polybrene to increase

infection efficiency. Retrovirus expressing murine Noxa or GFP-only was used to infect MEFs and cell viability was determined at the indicated time.

4.2.4. Cell viability

The propidium iodide (PI) exclusion method was used to determine cell viability. Cells were plated in 48-well tissue culture plates at the density of 1×10^4 cells per well 24 hours before exposure to death stimuli. Cells were pre-incubated with or without 1 mM of the high-affinity iron chelator DFO for two hours. Cells were then washed twice with fresh medium before exposure to the respective death stimuli. At the indicated time, cells were collected in the presence of 1.0 $\mu\text{g/ml}$ of PI and the percentage of live cells was measured using a flow cytometry analysis (FACScalibur, Beckon Dickinson; San Jose, CA) as described previously [103]. Cell viability of treated cells was calculated as the percentage of the viability of the untreated cells.

4.2.5. Caspase 3/7 activity

Approximately 5×10^3 MEFs were cultured in white-walled 96-well tissue culture plates for 24 hours. MEFs were pre-incubated with or without 1 mM DFO for two hours, washed twice with fresh medium before an exposure to the respective death stimuli. MEFs were treated with H_2O_2 or actinomycin D for 7 hours, exposed with etoposide, staurosporine, or doxorubicin for 12 hours, or infected

with the retroviral supernatant expressing Noxa for 14 hours. Caspase 3/7 activity was determined using the Sensolyte[®] Homogeneous R110 Caspase 3/7 Assay Kit (AnaSpec) according to the manufacturer's protocol. Caspase 3/7 activity of treated or infected cells was normalized to that of untreated controls. The results were presented as relative fluorescence units per minute (RFUs/min).

4.2.6. Western blot analysis

Equal amounts of proteins (30 µg) were separated on a 4-12% Bis-Tris gel (Bio-Rad; Hercules, CA) and transferred onto PVDF membrane (Millipore; Billerica, MA). The membrane was incubated with the appropriate primary or secondary antibodies either overnight at 4°C or at room temperature for 3 hours in 1X phosphate-buffered saline (PBS) containing 5% (w/v) nonfat dry milk (Bio-Rad) and 0.2% (v/v) Tween 20. Protein levels were detected using the enhanced chemiluminescent detection system (Pierce, Rockford, IL).

4.2.7. Microarray analysis

MEFs were pre-incubated with or without 1 mM DFO for 2 hours, washed twice with fresh medium before a treatment with either 0.4 mM H₂O₂ for 6 hours or 0.3 mM iron ammonium citrate for 24 hours. Total RNA was acquired using the RNeasy kit (Qiagen; Germantown, MD) according to the manufacturer's instructions. RNA concentrations were determined with a NanoDrop 8000

Spectrophotometer (Thermo), and the quality of total RNA was evaluated by a 2100 Bioanalyzer (Agilent; Santa Clara, CA). Global mRNA level alterations were determined using the GeneChip Mouse Gene 1.0 ST Array for H₂O₂ experiments or GeneChip Mouse Genome 430 2.0 Array for ferric ammonium citrate experiments (Affymetrix; Santa Clara, CA).

4.2.8. Quantitative real time Polymerase Chain Reaction (qPCR)

Total RNA was extracted using the RNeasy kit (Qiagen) and its concentration was measured using a NanoDrop 8000 Spectrophotometer (Thermo). Equal amounts (1 µg) of total RNA were reverse transcribed. The TaqMan 20x probes for murine and human Noxa (Applied Biosystems; Carlsbad, California) were used to determine Noxa mRNA expression levels in MEFs and HCT116 cells respectively. In MEFs tubulin was used as the endogenous control, whereas actin served as the endogenous control in human HCT116 cells.

4.2.9. Lysosomal membrane stability

The lysosomotropic base acridine orange (AO) was used to determine lysosomal membrane stability during H₂O₂-induced apoptosis. Two complementary experiments were carried out to measure lysosomal membrane stability by assessing changes in either green fluorescence (AO relocation method) or red fluorescence (AO uptake method) upon an exposure to H₂O₂ [143]. In both

cases, wild-type and Noxa-KO MEFs were plated in 48-well tissue culture plates at a density of 2×10^4 per well and cultured for 24 hours. For AO relocation experiments, the increase in green fluorescence was evaluated to detect early or minor changes in lysosomal membrane stability. MEFs were pre-incubated with or without 1 mM DFO for 2 hours, washed twice with fresh medium, before an exposure to 5 $\mu\text{g/ml}$ of AO for 30 minutes. MEFs were then treated with 0.4 mM H_2O_2 for the indicated time, and changes in green fluorescence were determined by flow cytometry (FACScalibur, FL1 channel). AO uptake experiments measured changes in red fluorescence to detect severe or late lysosomal membrane damage. Here, MEFs were pre-treated with or without 1 mM DFO for 2 hours, rinsed twice with fresh medium, followed by an exposure to 0.4 mM H_2O_2 for one hour. MEFs were then returned to normal culture conditions by washing and replacing with fresh medium. At the indicated time, cells were treated with 5 $\mu\text{g/ml}$ of AO for 15 minutes, and flow cytometry analysis was used to measure changes in red fluorescence (FACScalibur, FL3 channel).

4.2.10. Mitochondrial membrane potential

The mitochondrion-selective probes MitoTracker Green and MitoTracker Red were used to determine changes in mitochondrial membrane potential. Wild-type and Noxa-KO MEFs were plated in 48-well tissue culture plates at a density of 2×10^4 and cultured for 24 hours. Following a treatment with 0.4 mM H_2O_2 for the indicated time, MEFs were then incubated with 200 nM MitoTracker Green or

200 nM MitoTracker Red for 1 hour. Green and red fluorescence of collected MEFs were analyzed using a flow cytometer (FACScalibur). Mitochondrial membrane potential was shown as the ratio of fluorescence intensity of mitochondrial potential-sensitive MitoTracker Red (FL3 channel) and mitochondrial potential-independent MitoTracker Green (FL1 channel).

4.2.11. Statistical analysis

All experiments were performed in triplicate at least three times. Results are presented as mean \pm standard deviation. Statistical analysis was performed using the two-way ANOVA and the student's two tail t-test. A *P* value < 0.05 was considered significant.

4.3. Results

4.3.1. Oxidative stress-induced LMP is independent of Noxa expression.

In the lysosomes, the oxidative stress inducer H_2O_2 interacts with iron in a redox reaction to produce highly reactive hydroxyl radicals, which in turn cause LMP and subsequent apoptosis [152-154]. Our previous studies have shown that the elevated expression of the pro-apoptotic BH3-only Bcl-2 protein Noxa mediates apoptosis triggered by H_2O_2 [151]. To explore further the important role of Noxa expression in H_2O_2 -induced apoptosis, we first examined whether Noxa expression influenced H_2O_2 -induced LMP using MEFs deficient in Noxa expression (Noxa-KO) and their wild-type counterparts. The lysosomotropic base acridine orange (AO) is a metachromatic fluorochrome exhibiting red fluorescence when it is highly concentrated in intact lysosomes, but emitting green fluorescence when its concentration is low as observed in lysosomes with disrupted membrane integrity [124]. Two complementary approaches (AO relocation and AO uptake) were used to examine lysosomal membrane stability following H_2O_2 exposure. In AO relocation experiments, wild-type and Noxa-KO MEFs were first incubated with 5 $\mu\text{g/ml}$ of AO before exposure to 0.4 mM H_2O_2 . Thirty minutes post H_2O_2 treatment, there was a significant increase in green fluorescence levels in wild-type and Noxa-KO MEFs, indicating minor damage to lysosomal membrane integrity (Figure 4.1A). Importantly, the green fluorescence intensity increase was similar in both cell lines, providing evidence that Noxa expression did not influence H_2O_2 -induced LMP despite its critical role in mediating apoptotic signaling pathways. Furthermore, pre-incubating cells with 1

mM of the highly potent iron chelator desferrioxamine (DFO) prevented LMP independent of Noxa expression (Figure 4.1A).

To assess further the effects of Noxa expression on late lysosomal membrane rupture, we carried out AO uptake experiments to estimate the percentage of “pale” cells (cells with damaged lysosomes). Following one hour-treatment with H_2O_2 , MEFs were cultured in normal growth medium, and the intensity of red fluorescence emitted from AO inside cells was determined. Twenty four hours later, the fraction of cells displaying “pale” cell phenotype markedly increased in both wild-type and Noxa-KO MEFs, indicating late lysosomal membrane rupture (Figure 4.1B). Furthermore, the increase in late lysosomal membrane rupture was abolished by pre-incubation with DFO. Consistent with the results of AO relocation experiments (Figure 4.1A), H_2O_2 was able to induce comparable late lysosomal membrane rupture in wild-type and Noxa-KO MEFs (Figure 4.1C). Overall, these results indicate that H_2O_2 induces LMP independent of Noxa expression, suggesting that Noxa mediates H_2O_2 -triggered apoptosis at a phase downstream of destruction of lysosomal membrane integrity.

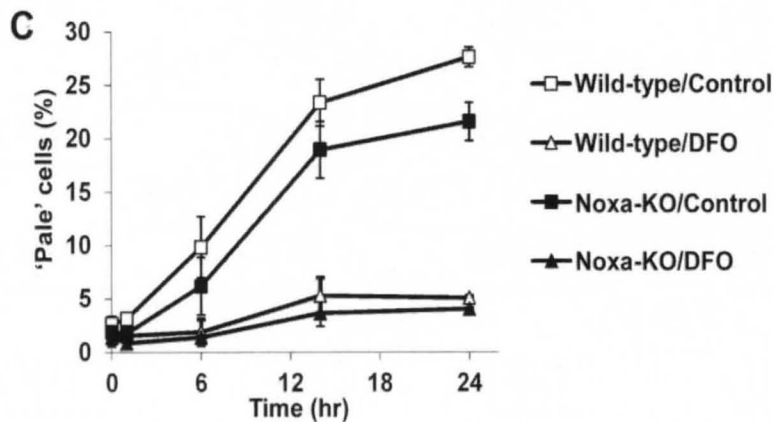
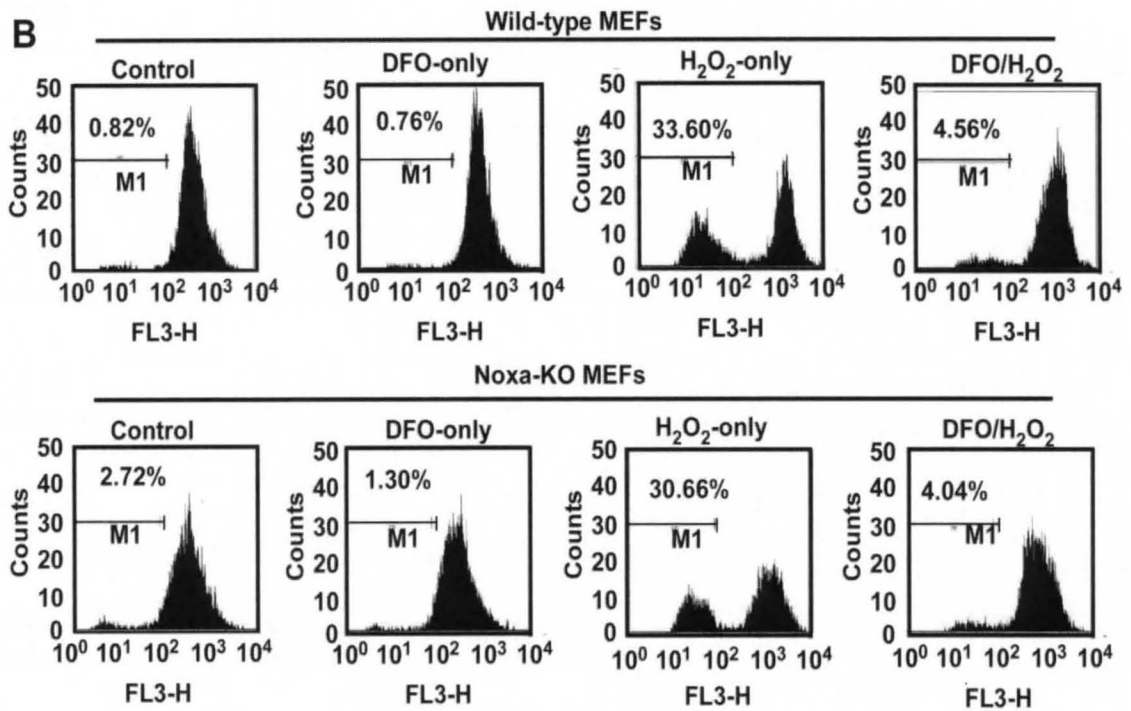
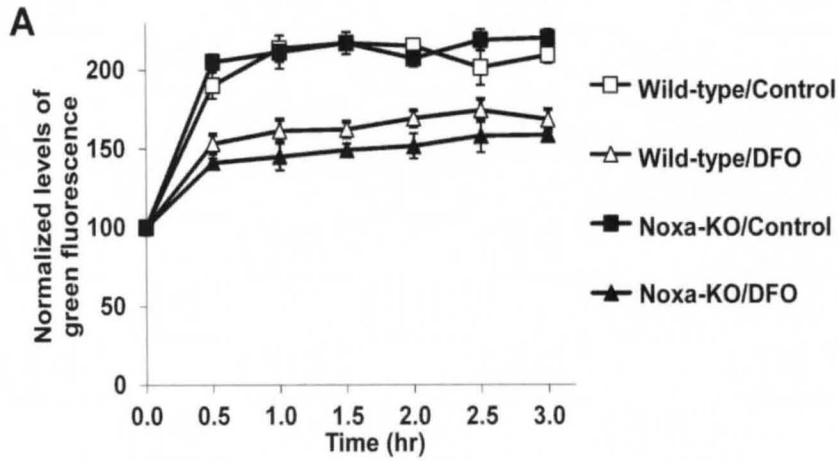


Figure 4.1. H₂O₂ induced Noxa-independent LMP. (A) Wild-type and Noxa-KO MEFs were pre-incubated with or without 1 mM DFO for 2 hours, followed by an exposure to 5 µg/ml acridine orange (AO) for 15 minutes. MEFs were then treated with 0.4 mM H₂O₂ for the indicated time. Green fluorescence emitted from AO inside cells was determined using flow cytometry analysis. Data represent mean ± standard deviation of three independent experiments performed in triplicates. **(B)** Following pre-incubation with or without 1 mM DFO for 2 hours, wild-type and Noxa-KO MEFs were exposed to 0.4 mM H₂O₂ for 1 hour. MEFs were then cultured in normal growth medium for 24 hours. MEFs deficient in intact lysosomes ('pale' cells) were analyzed by flow cytometry. Data represent one of three independent experiments. **(C)** The summary of the experimental results shown in (B). The data are shown as mean ± standard deviation of three independent experiments performed in triplicates.

4.3.2. Noxa-dependent outer mitochondrial membrane permeabilization (OMMP) occurs downstream of LMP during H₂O₂-induced apoptosis.

The OMMP and subsequent release of apoptogenic proteins such as cytochrome c from mitochondria to the cytosol are the molecular hallmarks of apoptosis [39]. To determine the temporal relation between MOMP and LMP during H₂O₂-induced apoptosis, we first examined the amounts of cytochrome c released into the cytosol as an indicator of OMMP. To this purpose, both wild-type and Noxa-KO MEFs were treated with H₂O₂, and the presence of cytochrome c in cytosolic fractions was determined by western blot (Figure 4.2A). The levels of cytochrome c in cytosolic fractions of Noxa-KO MEFs were largely unchanged upon 24-hour H₂O₂ exposure, indicating very little OMMP. However, the amounts of cytochrome c were notably higher in cytosolic fractions of wild-type cells after 14-hour H₂O₂ treatment, consistent with previously reported role of NOXA in mediating H₂O₂-induced apoptosis. As LMP was observed 30 minutes following H₂O₂ treatment in both wild-type and Noxa-KO MEF cells (Figure 4.1A), these results provide evidence that MOMP occurs following LMP during oxidative stress-induced apoptosis.

As a direct result of increased OMMP, mitochondrial membrane potential decreases in cells undergoing apoptosis, which has been commonly used as an indicator of OMMP [155]. To determine the temporal relation between OMMP and LMP during H₂O₂-induced apoptosis, we measured mitochondrial membrane

potential at different time following an exposure to H₂O₂ using the mitochondrial potential-sensitive probe MitoTracker Red and the mitochondrial potential-independent probe MitoTracker Green. An exposure to H₂O₂ led to a time-dependent decrease in mitochondrial membrane potential in both wild-type and Noxa-KO MEFs, but mitochondrial membrane potential dissipated much faster in wild-type MEFs compared with Noxa-KO MEFs (Figure 4.2B).

In contrast to the occurrence of LMP 30 minutes following H₂O₂ treatment (Figure 4.1B), no changes in mitochondrial membrane potential were detected in either MEF cell line within one hour of H₂O₂ exposure. Even after 6 hours of H₂O₂ exposure, mitochondrial membrane potential was reduced about 30% in wild-type MEFs, whereas mitochondria in Noxa-KO MEFs were still intact. Twenty-four hours of treatment with H₂O₂ almost completely disrupted mitochondrial membrane integrity in wild-type MEFs, but there was only about 25% reduction in mitochondrial membrane potential in Noxa-KO MEFs. Since Noxa-KO MEFs were more resistant to H₂O₂-induced OMMP, Noxa expression was important for OMMP induction, which is consistent with previous studies about the role of Noxa in H₂O₂-induced apoptosis [151]. Importantly, stabilizing lysosomal membranes by pre-incubation with DFO significantly inhibited H₂O₂-induced mitochondrial membrane potential reduction (Figure 4.2C). Thus, it is likely that mitochondrial membrane rupture occurs downstream of LMP in cells undergoing oxidative stress.

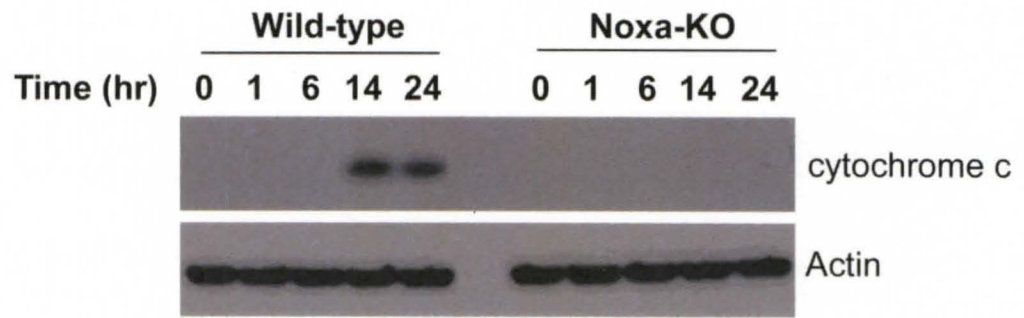
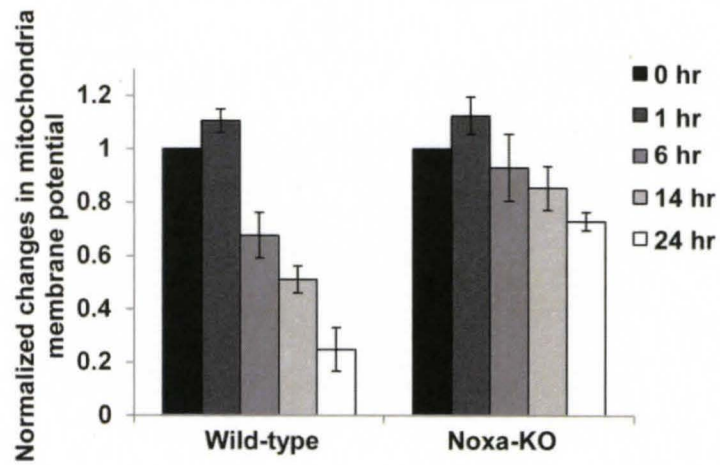
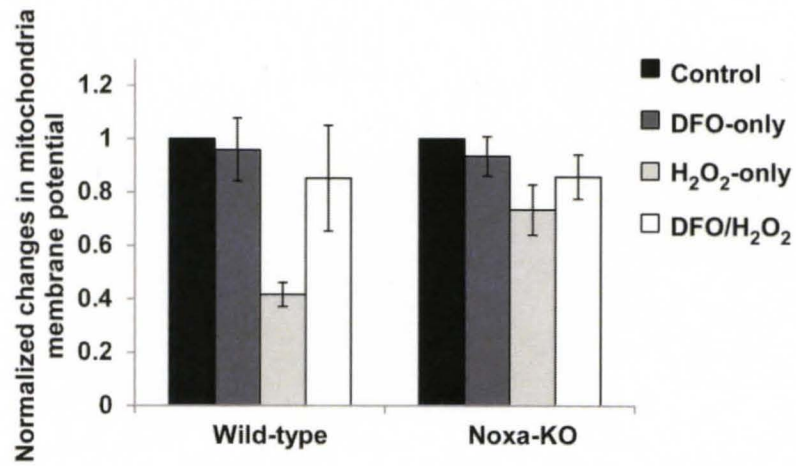
A**B****C**

Figure 4.2. Mitochondria membrane permeabilization is dependent on Noxa expression. (A) Wild-type and Noxa-KO MEF cells were treated with 0.4 mM H₂O₂. The amounts of cytochrome c in cytosolic fractions at the indicated time points were detected by western blot. (B) Following an exposure with 0.4 mM H₂O₂ for the indicated time, wild-type and Noxa-KO MEFs were incubated with 200 nM Mitotracker Red or 200 nM Mitotracker Green for 1 hour. Flow cytometer was used to measure red and green fluorescence intensity of MEFs. Mitochondrial membrane potential was calculated as the ratio of red to green fluorescence intensities and normalized. Experiments were performed in triplicates and mean ± standard deviation of three independent experiments is shown. (C) Wild-type and Noxa-KO MEFs were pre-incubated with or without 1 mM DFO for two hours before a treatment with 0.4 mM H₂O₂ for 24 hours. Changes in red and green fluorescence intensities were determined and mitochondrial membrane potential was calculated as shown in (A). Data are presented as mean ± standard deviation of three independent experiments performed in triplicate.

4.3.3. LMP is essential for Noxa-mediated apoptosis in H₂O₂-treated cells.

Since Noxa expression is critical for OMMP (Figure 4.2) but dispensable for LMP (Figure 4.1), we investigated the importance of LMP for Noxa-mediated apoptosis in H₂O₂-exposed cells. As expected, wild-type MEFs were more susceptible to H₂O₂ treatment compared with their Noxa-KO counterparts (Figure 4.3A). Upon H₂O₂ exposure, Noxa-mediated apoptosis was abolished in cells pretreated with DFO, providing evidence that the impact of LMP on cellular responses to H₂O₂ depends on Noxa expression (Figure 4.3A). In addition, caspase 3/7 activity was measured following an exposure to H₂O₂. While there was more caspase 3/7 activity in wild-type MEFs than Noxa-KO MEFs, pre-incubation with DFO significantly reduced caspase 3/7 activity in both cell lines (Figure 4.3B). The correlation between caspase 3/7 activity and the level of cell death indicates that LMP exerts its influence on H₂O₂-induced apoptosis through endogenous Noxa.

To further confirm the role of Noxa expression in H₂O₂-triggered LMP and subsequent apoptosis, Noxa expression in human colon cancer HCT116 cells was stably reduced by shRNA (Figure 4.3C). HCT116 cells with normal or reduced Noxa expression were exposed to H₂O₂ in the presence or absence of DFO pre-incubation. Consistent with the studies with MEFs (Figure 4.3A), the reduction of Noxa expression rendered HCT116 cells more resistant to H₂O₂ treatment, validating the critical role of Noxa in H₂O₂-triggered apoptosis.

Furthermore, DFO pre-incubation abolished H₂O₂ cytotoxicity in HCT116 cells with normal Noxa expression (Figure 4.3D), providing more evidence that the pro-apoptotic effects of Noxa on H₂O₂-induced apoptosis depends on LMP.

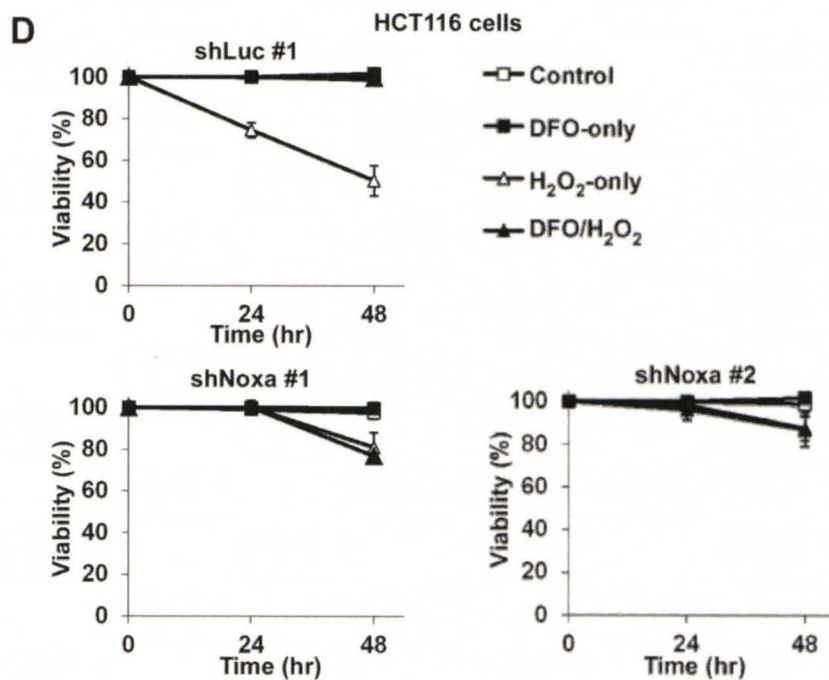
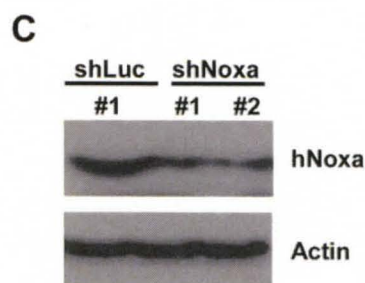
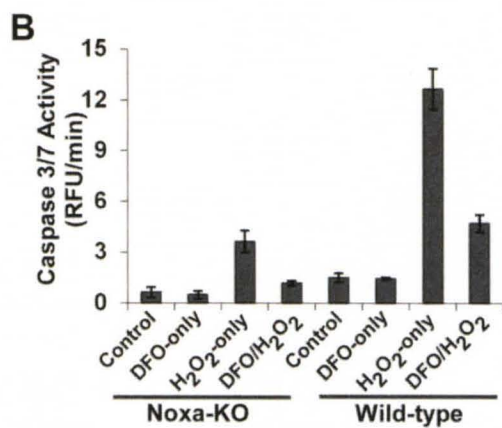
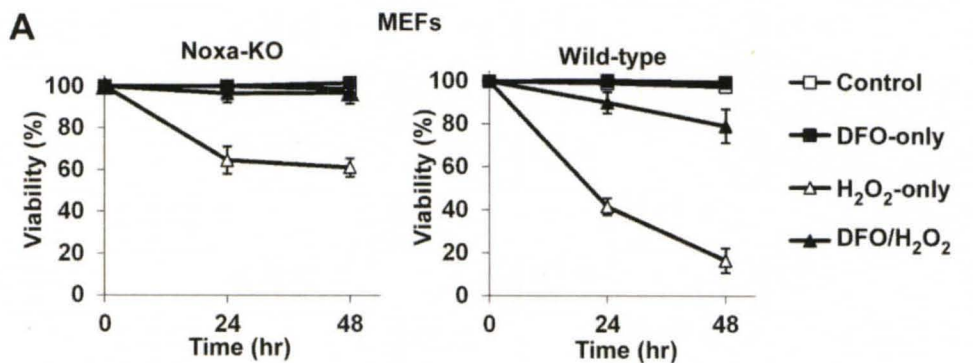


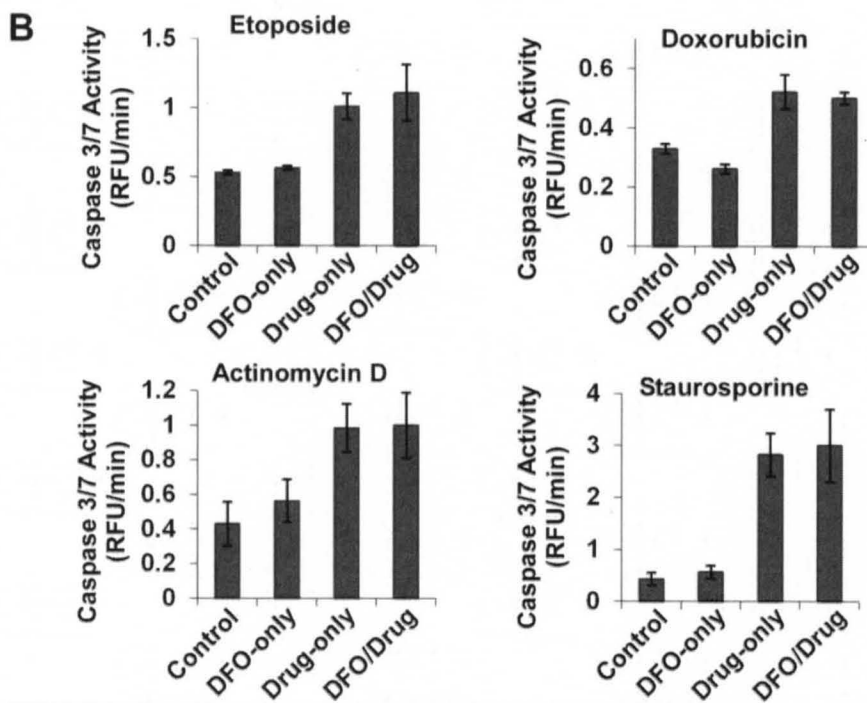
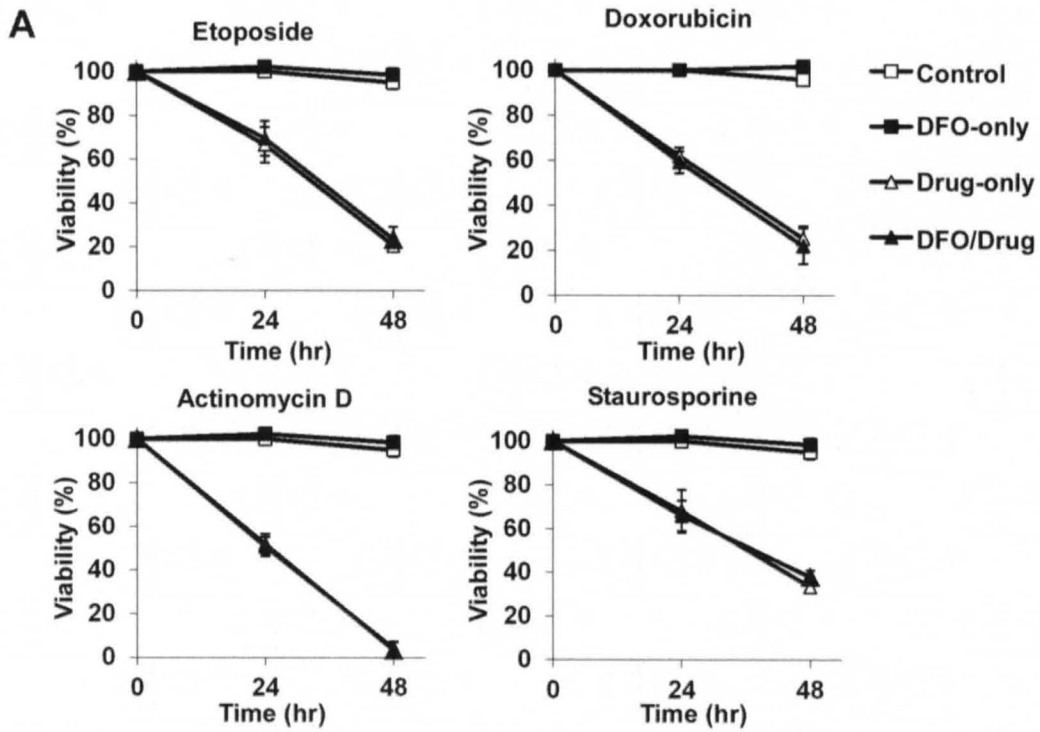
Figure 4.3. Stabilizing lysosomal membrane by DFO inhibits Noxa-dependent apoptosis induced by H₂O₂. (A) Wild-type and Noxa-KO MEFs were pre-incubated with or without 1 mM DFO for 2 hours. MEFs were then treated with 0.4 mM H₂O₂ for the indicated time, and cell viability was determined using a flow cytometry analysis. Data are presented as mean ± standard deviation of three different experiments that were carried out in triplicates. (B) Caspase 3/7 activity was measured after 2 hour-incubation with or without DFO followed by a treatment with 0.4 mM H₂O₂ for 6 hours. Data shown are mean ± standard deviation of three independent experiments performed in triplicates. (C) Noxa expression of was reduced in HCT116 cells by a small hairpin RNA (shRNA). The expression levels of Noxa were determined by western blot. (D) The HCT116 cells with normal (shLuc) or reduced (shNoxa) Noxa expression were incubated with or without DFO for 2 hours before an exposure with 0.4 mM H₂O₂ for the indicated time, and cell viability was measured. Mean ± standard deviation of three independent experiments is presented.

4.3.4. LMP is not involved in the regulation of some apoptosis paradigms

To examine whether the induction of LMP is also critical in other apoptosis paradigms, wild-type MEFs were treated with death stimuli that have diverse mechanisms of action, including the topoisomerase inhibitor etoposide, the DNA intercalating agent doxorubicin, the transcriptional inhibitor actinomycin D, and the protein kinase inhibitor staurosporine. MEFs were pretreated with DFO for 2 hours followed by a treatment with the respective death stimuli. Pre-incubation with DFO failed to prevent apoptosis induced by any of the four death stimuli examined (Figure 4.4A), indicating that LMP did not occur or was not involved in apoptosis signaling induced by any of these agents. These results demonstrate a specific role of LMP in regulating oxidative stress-induced apoptosis in MEFs. This was strengthened further by the observation that caspase 3/7 activity detected in MEFs treated with different death stimuli closely correlated with the cell viability measurements, and pre-incubation with DFO did not affect caspase 3/7 activity (Figure 4.4B).

To determine further the relevance of LMP in apoptotic signaling pathways initiated by chemotherapeutic drugs, human HCT116 cells with different Noxa expression levels were treated with cisplatin or carboplatin, two anti-cancer agents whose cytotoxicity has also been shown to depend on Noxa expression. HCT116 cells expressing normal levels of Noxa were more sensitive to both agents compared with their Noxa knockdown counterparts (Figure 4.4C).

Importantly, DFO failed to antagonize the pro-apoptotic activity of both drugs, indicating that LMP is irrelevant in apoptotic signaling triggered by cisplatin or related compounds (Figure 4C).



C

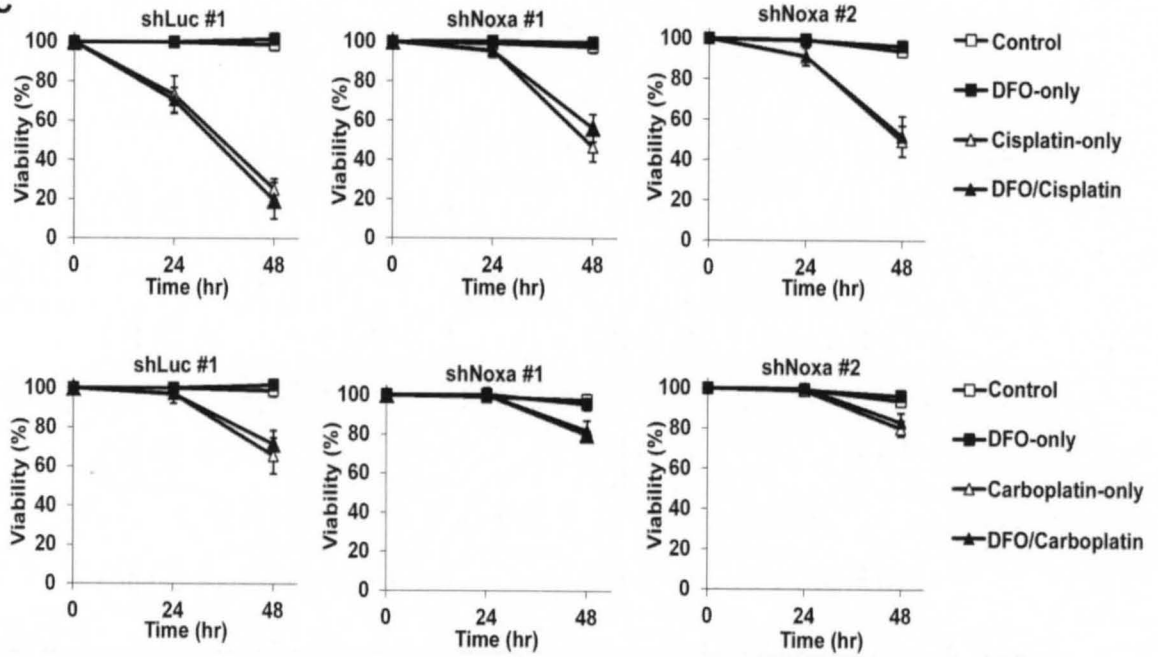


Figure 4.4. DFO fails to prevent apoptosis induced by other apoptotic stimuli. **(A)** Wild-type MEFs were incubated with or without 1 mM DFO for 2 hours, then treated with etoposide (5 μ M), doxorubicin (1 μ M), actinomycin D (0.2 μ g/ml), or staurosporine (5 nM) for the indicated time. Cell viability was determined using flow cytometry. Mean \pm standard deviation of three independent experiments that were performed in triplicates is presented. **(B)** Caspase 3/7 activity was measured following 12 hour-treatment with etoposide, doxorubicin, or staurosporine, or 9 hour-treatment with actinomycin D using a fluorometric assay. Data are presented as mean \pm standard deviation of three independent experiments performed in triplicate. **(C)** The human HCT116 cells (shLuc and shNoxa) were pre-incubated with or without 1 mM DFO for 2 hours before a treatment with cisplatin (50 μ M) or carboplatin (200 μ M). Cell viability was then measured using the PI exclusion method. Data are shown as mean \pm standard deviation of three independent experiments carried out three times.

4.3.5. LMP is not involved in apoptosis induced by ectopic Noxa expression.

As our studies have shown that stabilizing lysosomal membrane by DFO prevents Noxa-dependent apoptotic signaling triggered by H₂O₂ (Figure 4.3), it is possible that DFO directly antagonizes pro-apoptotic activities of Noxa. To explore this possibility, we examined whether DFO could affect the pro-apoptotic activities of ectopically expressed Noxa. As Noxa expression displays much higher killing activities in MEFs deficient in Bcl-x_L expression (Bcl-x-KO) compared with wild-type MEFs [151], both Bcl-x-KO and wild-type MEFs were pre-incubated with or without DFO before infection with retrovirus expressing Noxa. Unlike its activity on H₂O₂-induced apoptosis, DFO failed to prevent apoptosis induced by ectopic Noxa expression in both wild-type and Bcl-x-KO MEFs (Figure 4.5A). Caspase 3/7 activity measurements further validated the inability of DFO to antagonize pro-apoptotic activities of ectopic Noxa expression, indicating that DFO inhibits H₂O₂-induced apoptosis at a step upstream of Noxa expression (Figure 4.5B)

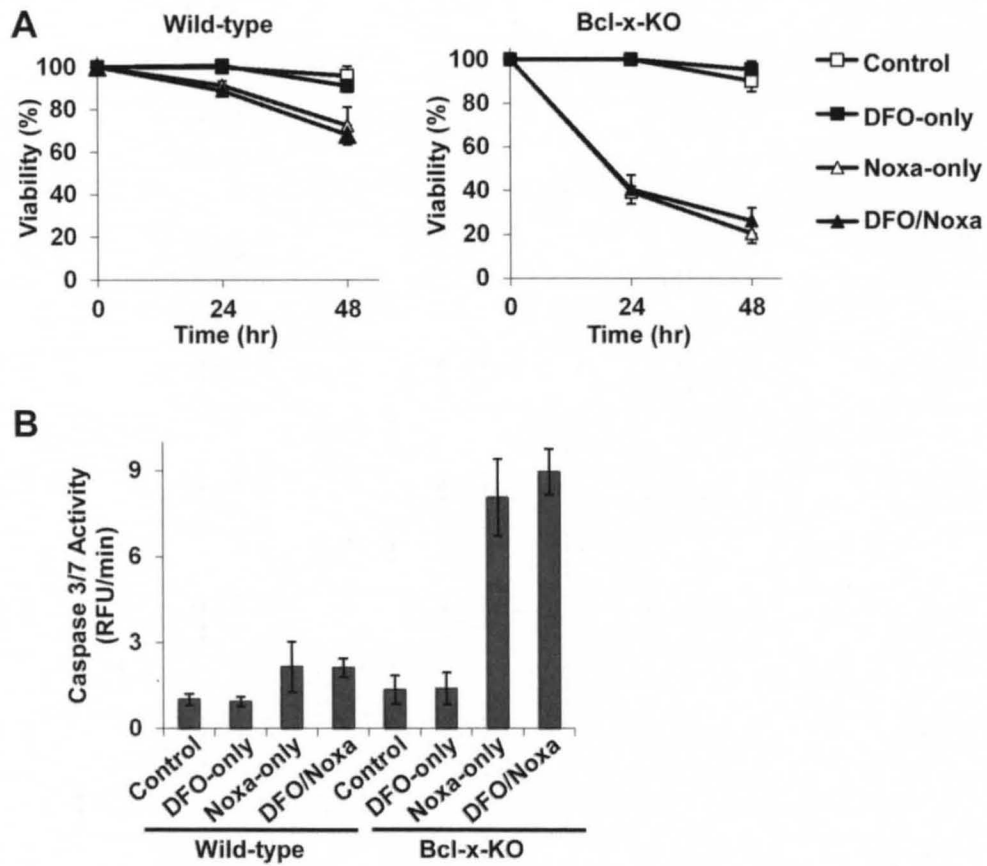


Figure 4.5. DFO does not prevent apoptosis induced by ectopic Noxa expression. (A) Noxa was retrovirally expressed in wild-type and Bcl-x-KO MEFs following a 2 hour-incubation with or without 1 mM DFO. Cell viability was measured at the indicated time using a flow cytometry analysis. Mean \pm standard deviation of three independent experiments that were conducted in triplicate is shown. (B) Caspases 3/7 activity was determined in wild-type and Bcl-x-KO MEFs using a fluorimetric assay upon pre-incubation with 1 mM DFO for 2 hours followed by retroviral infection for 14 hours. Mean \pm standard deviation of three independent experiments is shown.

4.3.6. H₂O₂-induced increase in Noxa expression is mediated by LMP.

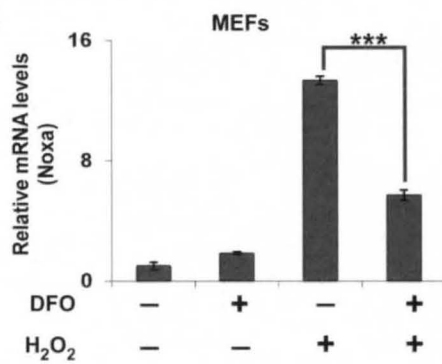
As the induction of Noxa expression is critical for H₂O₂-induced apoptosis, we systematically examined the effect of LMP on the expression of pro-apoptotic BH3-only Bcl-2 proteins in MEFs using microarray. While DFO itself did not significantly affect gene expression of BH3-only Bcl-2 proteins, stabilizing lysosomal membranes by DFO was able to abolish the effects of H₂O₂ on Noxa mRNA expression levels (Figure 4.6A). Quantitative real-time polymerase chain reaction (qPCR) experiments were also carried out to confirm that LMP mediates Noxa expression increase in oxidative stress-induced apoptosis (Figure 4.6B). Our studies have shown that Noxa expression mediates apoptosis-induced by H₂O₂ or cisplatin, but stabilizing lysosomal membrane by DFO was only able to prevent H₂O₂-induced but not cisplatin-triggered apoptosis (Figure 4.3).

To explore the distinct roles of LMP in different Noxa-dependent apoptosis paradigms, we examined the effect of DFO on Noxa expression induced by H₂O₂ and cisplatin respectively in HCT116 cells (Figure 4.6C). DFO abolished H₂O₂-caused Noxa mRNA induction, but failed to prevent cisplatin-induced increase in Noxa mRNA expression, correlating with the inability of DFO to inhibit apoptosis induced by cisplatin. The results of these experiments further validate the unique role of LMP-induced Noxa expression induction in apoptosis caused by oxidative stress.

A

Gene Description	Fold changes in mRNA expression (MEFs)			
	Control	DFO-only	H ₂ O ₂ -only	DFO/H ₂ O ₂
Phorbol-12-myristate-13-acetate-induced protein 1 (Pmaip1, Noxa)	1.00	1.02	16.96	6.55
Bcl2-interacting killer (Bik)	1.00	1.08	1.19	0.68
Bcl-2-like 11 (Bim)	1.00	1.18	2.20	1.25
BH3 interacting death agonist (Bid)	1.00	0.97	1.28	1.03
Bcl-2 modifying factor (Bmf)	1.00	1.14	1.16	0.99
Harakiri, Bcl2 interacting protein (Hrk)	1.00	1.19	1.14	1.12
Bcl-2 binding component 3 (Bbc3, Puma)	1.00	0.61	0.77	0.75
Bcl-2/adenovirus E1B interacting protein 3-like (Bnip3l, Nix)	1.00	0.99	1.02	0.95
Bcl-2 associated agonist of cell death (Bad)	1.00	0.83	1.03	1.04
Bcl-2/adenovirus E1B interacting protein 3 (Bnip3)	1.00	1.06	0.77	0.75

B



C

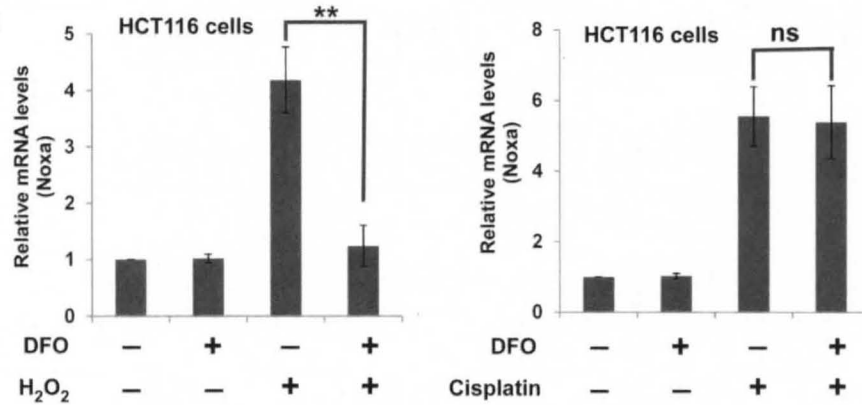


Figure 4.6. H₂O₂-induced increase in Noxa expression is specifically mediated by LMP. (A) Wild-type MEFs were pre-incubated with or without DFO for 2 hours, before treated with 0.4 mM H₂O₂ for 6 hours. Total RNA was extracted and microarray analysis was carried out to determine global changes in mRNA expression levels upon H₂O₂ treatment. **(B)** A qPCR analysis was performed using the total RNA generated in (A) to validate the results generated by microarray analysis. Data are presented as mean ± standard deviation of three independent experiments performed in triplicates. **(C)** DFO prevented Noxa expression increase induced by H₂O₂ but not cisplatin. After pre-incubation with or without DFO for 2 hours, HCT116 cells (shLuc) were treated with either 0.4 mM H₂O₂ for 6 hours or 50 μM cisplatin for 14 hours. Total RNA was collected and a qPCR analysis was performed to determine Noxa mRNA levels. Mean ± standard deviation of three independent experiments is presented. ***P*<0.01; ****P*<0.001; Student's unpaired t test. ns, no significance.

4.3.7. Iron overload specifically enhances Noxa expression

Lysosomal labile iron has been shown to translocate to the nucleus and cause oxidative damage to DNA during oxidative stress-induced apoptosis [134-136]. Therefore, it is possible that redox active iron released into the cytosol might be responsible for LMP-induced Noxa expression. To examine this possibility, the effects of exogenous iron on changes in global mRNA expression were determined by microarray experiments performed in wild-type MEFs treated with ferric ammonium citrate. Upon iron exposure, the most prominent increase in gene expression in the BH3-only Bcl-2 protein family was Noxa, which was similar to the expression profile of H₂O₂ exposure (Figure 4.7A). The degree of Noxa induction in iron-loaded cells was modest compared with that observed in cells exposed to H₂O₂ (Figure 4.6A), which could be attributed to the different array types used in these experiments. DFO was able to prevent iron-induced increase in Noxa expression but had little effect on the mRNA expression levels of other BH3-only Bcl-2 proteins. The qPCR analyses further confirmed that exogenous iron specifically induced Noxa mRNA expression level (Figure 4.7B).

A

Gene Description	Fold changes in mRNA expression (MEFs)			
	Control	DFO-only	Fe ³⁺ -only	DFO/Fe ³⁺
Phorbol-12-myristate-13-acetate-induced protein 1(Pmaip1, Noxa)	1.00	1.10	1.78	1.27
Bcl2-interacting killer(Bik)	1.00	0.83	1.01	0.99
Bcl-2-like 11 (Bim)	1.00	0.98	0.79	0.95
BH3 interacting death agonist (Bid)	1.00	0.99	0.93	0.98
Bcl-2 modifying factor (Bmf)	1.00	0.99	0.99	1.02
Harakiri, Bcl2 interacting protein (Hrk)	1.00	0.87	0.93	0.91
Bcl-2 binding component 3 (Bbc3, Puma)	1.00	1.09	1.13	0.94
Bcl-2/adenovirus E1B interacting protein 3-like (Bnip3l, Nix)	1.00	0.98	0.97	0.96
Bcl-2 associated agonist of cell death (Bad)	1.00	0.95	1.08	1.02
Bcl-2/adenovirus E1B interacting protein 3 (Bnip3)	1.00	1.09	0.93	1.04

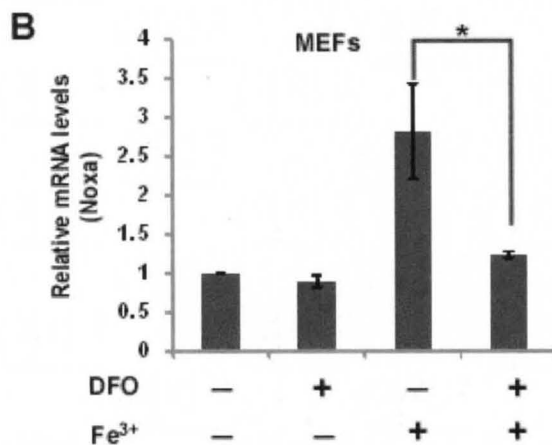


Figure 4.7. Exogenous iron specifically increases Noxa expression. (A)

Wild-type MEFs were pre-incubated with DFO before treatment with 0.3 mM iron ammonium citrate for 24 hours. Total RNA was extracted and used for microarray experiments to determine changes in mRNA expression levels. **(B)** Total RNA described in (A) was used for a qPCR analysis to determine Noxa mRNA expression levels. Mean \pm standard deviation of three independent triplicate experiments is presented.

* $P < 0.05$; Student's unpaired t test.

4.4. Discussion

Oxidative stress-triggered LMP is well documented, but the detailed mechanisms through which LMP is coupled with OMMP and eventual apoptosis are still unclear. Here we investigated the role of lysosomal membrane rupture in regulating apoptosis caused by the oxidative stress inducer H_2O_2 . Upon H_2O_2 exposure, the integrity of lysosomal membranes was disrupted independent of endogenous Noxa, despite its essential role in apoptosis signaling. Noxa-dependent OMMP appeared to occur downstream of LMP. Stabilizing lysosomal membranes specifically inhibited Noxa expression increase and Noxa-mediated apoptosis in H_2O_2 -treated cells. Overall, our studies provide molecular evidence that LMP modulates cellular responses to oxidative stress by regulating Noxa expression.

The mechanisms of apoptosis signaling induced by LMP have been under intensive study. It is generally believed that the rupture of lysosome membranes releases hydrolytic enzymes normally resided inside lysosomes into the cytosol, which may in turn trigger apoptotic signaling by hydrolyzing their substrates [149]. However, severe lysosomal membrane damage leads to a massive exodus of lysosomal enzymes into the cytosol, indiscriminately digesting cellular components, causing deleterious cytoplasmic acidification, and inducing necrosis instead of apoptosis. The concentration of H_2O_2 examined in our studies induced maximal apoptotic cell death but minimal necrosis in MEFs [151]. In this oxidative

stress paradigm, the induction of OMMP and subsequent apoptosis depended on Noxa expression (Figures 4.2 and 4.3). On the contrary, both early and late lysosomal membrane rupture occurred at same rates in wild-type and Noxa-KO MEFs (Figure 4.1), suggesting that hydrolytic activities of discharged lysosomal enzymes are unlikely to be responsible for initiating more prominent apoptotic cascades in Noxa-expressing cells. It is conceivable that partial lysosomal damage under the conditions in our studies only promotes limited release of lysosomal enzymes whose concentrations in the cytosol are not high enough to trigger apoptosis by themselves. Instead, the induction of Noxa expression by LMP is responsible for oxidative stress-induced apoptosis in MEFs. Thus, the strength of oxidative insults and the cell type could determine how apoptotic signaling is activated in response to oxidative insults.

Recent studies have demonstrated that both anti- and pro-apoptotic Bcl-2 proteins are involved in apoptotic signaling initiated by LMP. Overexpressing anti-apoptotic Bcl-2 in murine histiocytic lymphoma cells suppresses oxidant-induced apoptosis by stabilizing lysosomal membranes and the phosphorylation of Bcl-2 is required for this activity [124, 125]. In multiple apoptosis paradigms, Bax has been shown to translocate to lysosomes to mediate LMP, probably by oligomerizing and forming permeation channels on lysosomal membranes [156, 157]. Upon $\text{TNF}\alpha$ treatment, tBid is generated by caspase 8 and induces Bid-dependent lysosomal membrane rupture, leading to discharge of the lysosomal protease cathepsin B into the cytosol and eventual apoptosis [158, 159]. Given

that Noxa expression is dispensable for LMP induction in response to oxidative stress, Noxa likely functions at the mitochondrial level to mediate apoptosis, which is supported by our evidence about temporal relation of OMMP and LMP in H₂O₂-treated cells (Figures 4.1 and 4.2).

Although originally identified as a primary p53-response protein, Noxa expression increases in response to diverse apoptotic stimuli, including some chemotherapeutic agents [160]. Our studies indicate that during H₂O₂-induced apoptosis LMP induced Noxa expression increases in both MEFs and HCT116 cells (Figure 4.6). This induction of Noxa is unlikely caused by p53 activation, since MEFs examined in our studies have been immortalized by SV40 T antigen, a known p53 deactivator [151]. In contrast, the increase in Noxa expression in cells exposed to cisplatin or cisplatin-related compounds could depend on p53 [158, 161]. Thus, the different effects of stabilizing lysosomal membranes by DFO on cisplatin- or H₂O₂-induced apoptosis could be attributed to the underlying mechanisms of Noxa induction in these two apoptosis paradigms.

Lysosomes contain abundant labile iron, and the rupture of lysosomal membrane leads to redox-active iron translocation to the nucleus during oxidative stress [134, 135]. I reasoned that lysosomal redox-active iron might be responsible for subsequent transcriptional responses to oxidative responses, particularly pro-apoptotic Bcl-2 proteins. Indeed, the transcription profile of BH3-only Bcl-2

proteins in cells loaded with exogenous iron recapitulated that of cells undergoing oxidative stress (Figure 4.7), suggesting that LMP-triggered apoptosis signaling is transduced into the nucleus to induce Noxa transcription via released lysosomal redox-active iron. In support of this model, lysosomal redox-active iron has been reported to generate oxidative damage to DNA [136] and Noxa is known to be a DNA damage-responsive protein [160]. In summary, our studies reveal a novel mechanism by which lysosomal membrane stability regulates H₂O₂-induced apoptosis. Future research will focus on investigating the signaling pathway, particularly the involvement of redox-active iron, in the induction of Noxa expression.

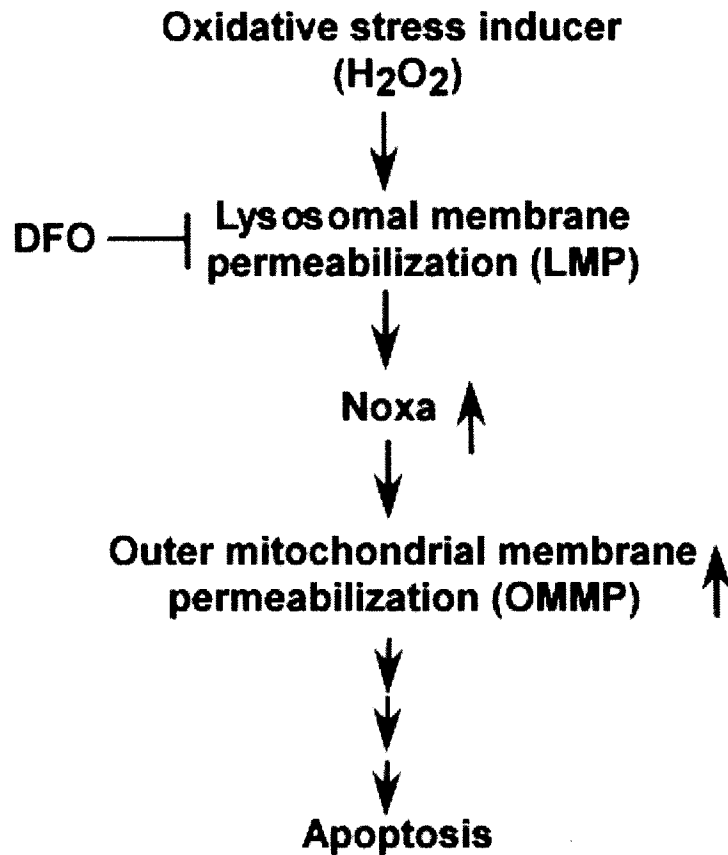


Figure 4.8. Oxidative stress-induced LMP promotes Noxa-dependent apoptosis. In lysosomes, the oxidative stress inducer H_2O_2 interacts with intralysosomal iron to generate highly reactive hydroxyl radicals and induce subsequent LMP, which can be inhibited by the iron chelating agent DFO. LMP leads to an increase in Noxa expression, which in turn induces OMMP and eventual activation of apoptosis signaling.

CHAPTER V

SUMMARY AND FUTURE PERSPECTIVES

5.1. Summary and conclusions

Previous studies have shown that overexpression of the anti-apoptotic Bcl-2 protein Bcl-x_L prevents apoptosis initiated by diverse apoptotic stimuli. The exact mechanism of how Bcl-x_L prevents apoptosis is still unclear and controversial. As Bcl-x_L likely functions to modulate OMM integrity, overexpression of Bcl-x_L could relocate Bcl-x_L to non-physiological locations inside cells, leading to unexpected biological consequences. Therefore, studying the activities of Bcl-x_L at endogenous levels will fill critical gaps in our understanding of the molecular and biochemical mechanisms by which Bcl-x_L regulates apoptosis.

Endogenous Bcl-x_L has been demonstrated to localize in the mitochondria, the ER, and the cytosol. I investigated the molecular functions of Bcl-x_L exclusively localized in a particular subcellular compartment on regulation of apoptosis and Ca²⁺ homeostasis using MEFs. The carboxyl-terminal transmembrane domain of Bcl-x_L was deleted to confine Bcl-x_L specifically to the cytosol. The carboxyl-terminus of Bcl-x_L was replaced with either the mitochondria targeting sequence of the Listeria protein ActA or the ER targeting sequence of cytochrome b5 (cb5),

which targets Bcl-x_L to the mitochondria or the ER respectively. Targeting Bcl-x_L at the mitochondria but not at the ER prevented apoptosis induced by diverse death stimuli to the degree observed in wild-type MEFs. However, expression of ER-targeted Bcl-x_L but not mitochondrially targeted Bcl-x_L was required to modulate Ca²⁺ homeostasis. Of importance, ER-targeted Bcl-x_L was able to protect cells against death stimuli in the presence of endogenous Bcl-x_L. These data indicate that mitochondrial Bcl-x_L can regulate apoptosis independently of ER Bcl-x_L and that when localized exclusively at the ER, Bcl-x_L impinges on Ca²⁺ homeostasis but does not affect apoptosis unless Bcl-x_L is present in additional cellular compartments.

Next I investigated how endogenous Bcl-x_L regulates oxidative stress-induced apoptosis. Oxidative stress has been known to induce both necrosis and apoptosis dependent on the severity of the oxidative stress to cells. Mild to moderate oxidative stress causes apoptosis whereas severe oxidative stress triggers necrosis [93, 151]. The exact mechanism through which oxidative stress inducers, including H₂O₂, promote apoptosis is unclear but recent evidence suggests the involvement of the Bcl-2 proteins. Thus, I investigated how the complex Bcl-2 protein network might regulate oxidative stress-induced apoptosis. Using MEFs, I found out that endogenous Bcl-x_L prevented apoptosis initiated by H₂O₂. Furthermore, the pro-apoptotic BH3-only Bcl-2 protein Noxa was required for H₂O₂-induced apoptosis and was the only BH3-only Bcl-2 protein whose pro-apoptotic activity was completely antagonized by endogenous Bcl-x_L. Upon H₂O₂

treatment, Noxa mRNA displayed the greatest increase among BH3-only Bcl-2 proteins. Also, expression levels of the anti-apoptotic Bcl-2 protein Mcl-1, the primary binding target of Noxa, were greatly reduced in cells treated with H₂O₂ in a Noxa-dependent fashion, and Mcl-1 overexpression prevent H₂O₂-induced apoptosis. Overall, these studies reveal a signaling pathway in which H₂O₂ activates Noxa, leading to a decrease in Mcl-1 expression and subsequent cell death in the absence of Bcl-x_L expression. Therefore, both anti-apoptotic and pro-apoptotic Bcl-2 proteins cooperate to regulate oxidative stress-induced apoptosis.

Finally, I investigated the important role of lysosomal membrane permeabilization (LMP) during oxidative stress-induced apoptosis. Previous studies have implicated LMP in oxidative stress-induced apoptosis, but the exact role of LMP in oxidative stress-triggered apoptotic cascade or how it is regulated by the Bcl-2 protein network is not completely understood. Here, I determined the temporal relation between LMP and OMMP using MEFs deficient in Noxa and their wild-type counterparts. Although Noxa expression was important for H₂O₂-triggered OMMP and subsequent apoptosis, H₂O₂-induced LMP was independent of Noxa expression. However, Noxa-dependent OMMP induction occurred downstream of LMP. When the lysosomal membranes were stabilized by the iron chelating agent DFO, H₂O₂-induced increase in Noxa expression and subsequent apoptosis was prevented probably by inhibition of LMP. DFO prevented H₂O₂-induced increase in Noxa expression but failed to prevent cisplatin-caused Noxa

expression induction, indicating that LMP is unique for oxidative stress-triggered apoptosis. Thus these studies reveal a novel signaling pathway for H₂O₂-induced apoptosis, in which an increase in Noxa expression couples LMP with OMMP and ultimate apoptosis.

5.2. Future perspectives

Further research will focus on investigating the signaling pathway, particularly lysosomal redox-active iron, involved in the regulation of Noxa expression. Because DNA damage causes increase in p53 proteins which in turn activates Noxa expression, I will further explore the involvement of H₂O₂ in DNA damage, activation of p53 proteins, increase in Noxa expression and subsequent apoptosis. I will also further elucidate the involvement of the crosstalk between mitochondrial-localized and ER-localized Bcl-x_L in apoptosis regulation and Ca²⁺ homeostasis.

REFERENCES

1. Reed, J.C., Dysregulation of Apoptosis in Cancer. *Journal of Clinical Oncology*, 1999. **17**(9): p. 2941.
2. Vaux, D.L. and S.J. Korsmeyer, Cell Death in Development. *Cell*, 1999. **96**(2): p. 245-254.
3. Cory, S., D.C.S. Huang, and J.M. Adams, The Bcl-2 family: roles in cell survival and oncogenesis. *Oncogene*, 2003. **22**(53): p. 8590-8607.
4. Ziegler, U. and P. Groscurth, Morphological Features of Cell Death. *Physiology*, 2004. **19**(3): p. 124-128.
5. Fuchs, Y. and H. Steller, Programmed Cell Death in Animal Development and Disease. *Cell*, 2011. **147**(4): p. 742-758.
6. Huang, D.C.S. and A. Strasser, BH3-Only Proteins—Essential Initiators of Apoptotic Cell Death. *Cell*, 2000. **103**(6): p. 839-842.
7. Fadeel, B. and S. Orrenius, Apoptosis: a basic biological phenomenon with wide-ranging implications in human disease. *Journal of Internal Medicine*, 2005. **258**(6): p. 479-517.
8. Tibbetts, M.D., L. Zheng, and M.J. Lenardo, The death effector domain protein family: regulators of cellular homeostasis. *Nat Immunol*, 2003. **4**(5): p. 404-409.
9. Majno, G. and I. Joris, Apoptosis, oncosis, and necrosis. An overview of cell death. *Am J Pathol*, 1995. **146**(1): p. 3-15.
10. Trump, B.E., et al., The Pathways of Cell Death: Oncosis, Apoptosis, and Necrosis. *Toxicologic Pathology*, 1997. **25**(1): p. 82-88.
11. Van Cruchten, S. and W. Van den Broeck, Morphological and Biochemical Aspects of Apoptosis, Oncosis and Necrosis. *Anatomia, Histologia, Embryologia*, 2002. **31**(4): p. 214-223.
12. Boise, L.H., et al., bcl-x, a bcl-2-related gene that functions as a dominant regulator of apoptotic cell death. *Cell*, 1993. **74**(4): p. 597-608.

13. Jenner, P., Oxidative stress in Parkinson's disease. *Annals of Neurology*, 2003. **53**(S3): p. S26-S38.
14. Upham, B.L. and J.G. Wagner, Toxicant-Induced Oxidative Stress in Cancer. *Toxicological Sciences*, 2001. **64**(1): p. 1-3.
15. Petros, A.M., E.T. Olejniczak, and S.W. Fesik, Structural biology of the Bcl-2 family of proteins. *Biochimica et Biophysica Acta (BBA) - Molecular Cell Research*, 2004. **1644**(2-3): p. 83-94.
16. Ellis, R.E., J. Yuan, and H.R. Horvitz, Mechanisms and Functions of Cell Death. *Annual Review of Cell Biology*, 1991. **7**(1): p. 663-698.
17. Xu, D., et al., The CARD-carrying caspase Dronc is essential for most, but not all, developmental cell death in *Drosophila*. *Development*, 2005. **132**(9): p. 2125-2134.
18. Gelbard, H.A., R.-M. Boustany, and N.F. Schor, Apoptosis in development and disease of the nervous system: II. Apoptosis in childhood neurologic disease. *Pediatric Neurology*, 1997. **16**(2): p. 93-97.
19. Gilbert, S.F., Opening Darwin's black box: teaching evolution through developmental genetics. *Nat Rev Genet*, 2003. **4**(9): p. 735-741.
20. Renehan, A.G., C. Booth, and C.S. Potten, What is apoptosis, and why is it important? Education and debate. *BMJ*, 2001. **322**(7301): p. 1536-1538.
21. King, C., et al., Homeostatic Expansion of T Cells during Immune Insufficiency Generates Autoimmunity. *Cell*, 2004. **117**(2): p. 265-277.
22. Fu, D., J.A. Calvo, and L.D. Samson, Balancing repair and tolerance of DNA damage caused by alkylating agents. *Nat Rev Cancer*, 2012. **12**(2): p. 104-120.
23. Kheifets, L., et al., The Sensitivity of Children to Electromagnetic Fields. *Pediatrics*, 2005. **116**(2): p. e303-e313.
24. Khoronenkova, Svetlana V., et al., ATM-Dependent Downregulation of USP7/HAUSP by PPM1G Activates p53 Response to DNA Damage. *Molecular Cell*, 2012. **45**(6): p. 801-813.
25. Hirao, A., et al., DNA Damage-Induced Activation of p53 by the Checkpoint Kinase Chk2. *Science*, 2000. **287**(5459): p. 1824-1827.

26. Liu, Y. and M. Kulesz-Martin, p53 protein at the hub of cellular DNA damage response pathways through sequence-specific and non-sequence-specific DNA binding. *Carcinogenesis*, 2001. **22**(6): p. 851-860.
27. Fairweather, D., Autoimmune Disease: Mechanisms, in eLS2001, John Wiley & Sons, Ltd.
28. Coultas, L. and A. Strasser, The role of the Bcl-2 protein family in cancer. *Seminars in Cancer Biology*, 2003. **13**(2): p. 115-123.
29. Fulda, S. and K.M. Debatin, Extrinsic versus intrinsic apoptosis pathways in anticancer chemotherapy. *Oncogene*, 2006. **25**(34): p. 4798-4811.
30. Henry-Mowatt, J., et al., Role of mitochondrial membrane permeabilization in apoptosis and cancer. *Oncogene*, 2004. **23**(16): p. 2850-2860.
31. Srinivasula, S.M., et al., Molecular Determinants of the Caspase-promoting Activity of Smac/DIABLO and Its Role in the Death Receptor Pathway. *Journal of Biological Chemistry*, 2000. **275**(46): p. 36152-36157.
32. Wajant, H., The Fas Signaling Pathway: More Than a Paradigm. *Science*, 2002. **296**(5573): p. 1635-1636.
33. Boldin, M.P., et al., A Novel Protein That Interacts with the Death Domain of Fas/APO1 Contains a Sequence Motif Related to the Death Domain. *Journal of Biological Chemistry*, 1995. **270**(14): p. 7795-7798.
34. Chinnaiyan, A.M., et al., FADD, a novel death domain-containing protein, interacts with the death domain of fas and initiates apoptosis. *Cell*, 1995. **81**(4): p. 505-512.
35. Wang, J., et al., Caspase-10 is an initiator caspase in death receptor signaling. *Proceedings of the National Academy of Sciences*, 2001. **98**(24): p. 13884-13888.
36. Bao, Q. and Y. Shi, Apoptosome: a platform for the activation of initiator caspases. *Cell Death Differ*, 2006. **14**(1): p. 56-65.
37. Ashkenazi, A., Targeting death and decoy receptors of the tumour-necrosis factor superfamily. *Nat Rev Cancer*, 2002. **2**(6): p. 420-430.
38. Boatright, K.M. and G.S. Salvesen, Mechanisms of caspase activation. *Current Opinion in Cell Biology*, 2003. **15**(6): p. 725-731.
39. Saraste, A. and K. Pulkki, Morphologic and biochemical hallmarks of apoptosis. *Cardiovascular Research*, 2000. **45**(3): p. 528-537.

40. Yigong, S., Caspase Activation: Revisiting the Induced Proximity Model. *Cell*, 2004. **117**(7): p. 855-858.
41. Lamkanfi, M., et al., Caspases in cell survival, proliferation and differentiation. *Cell Death Differ*, 2006. **14**(1): p. 44-55.
42. Knezevich, S., et al., Concurrent translocation of BCL2 and MYC with a single immunoglobulin locus in high-grade B-cell lymphomas. *Leukemia*, 2005. **19**(4): p. 659-663.
43. Cleary, M.L., S.D. Smith, and J. Sklar, Cloning and structural analysis of cDNAs for bcl-2 and a hybrid bcl-2/immunoglobulin transcript resulting from the t(14;18) translocation. *Cell*, 1986. **47**(1): p. 19-28.
44. Cory, S. and J.M. Adams, The Bcl2 family: regulators of the cellular life-or-death switch. *Nat Rev Cancer*, 2002. **2**(9): p. 647-656.
45. Hardwick, J.M. and R.J. Youle, SnapShot: BCL-2 Proteins. *Cell*, 2009. **138**(2): p. 404.e1-404.e2.
46. Youle, R.J. and A. Strasser, The BCL-2 protein family: opposing activities that mediate cell death. *Nat Rev Mol Cell Biol*, 2008. **9**(1): p. 47-59.
47. Tsujimoto, Y., Cell death regulation by the Bcl-2 protein family in the mitochondria. *Journal of Cellular Physiology*, 2003. **195**(2): p. 158-167.
48. Hsu, S.Y., et al., Bok is a pro-apoptotic Bcl-2 protein with restricted expression in reproductive tissues and heterodimerizes with selective anti-apoptotic Bcl-2 family members. *Proceedings of the National Academy of Sciences*, 1997. **94**(23): p. 12401-12406.
49. Suzuki, M., R.J. Youle, and N. Tjandra, Structure of Bax: Coregulation of Dimer Formation and Intracellular Localization. *Cell*, 2000. **103**(4): p. 645-654.
50. Antonsson, B., et al., Bax Is Present as a High Molecular Weight Oligomer/Complex in the Mitochondrial Membrane of Apoptotic Cells. *Journal of Biological Chemistry*, 2001. **276**(15): p. 11615-11623.
51. Hsu, Y.-T., K.G. Wolter, and R.J. Youle, Cytosol-to-membrane redistribution of Bax and Bcl-XL during apoptosis. *Proceedings of the National Academy of Sciences*, 1997. **94**(8): p. 3668-3672.
52. Mikhailov, V., et al., Association of Bax and Bak Homo-oligomers in Mitochondria. *Journal of Biological Chemistry*, 2003. **278**(7): p. 5367-5376.

53. Wang, X., et al., Bcl-2 proteins regulate ER membrane permeability to luminal proteins during ER stress-induced apoptosis. *Cell Death Differ*, 2011. **18**(1): p. 38-47.
54. Wei, M.C., et al., Proapoptotic BAX and BAK: A Requisite Gateway to Mitochondrial Dysfunction and Death. *Science*, 2001. **292**(5517): p. 727-730.
55. Yu, J., et al., PUMA Induces the Rapid Apoptosis of Colorectal Cancer Cells. *Molecular Cell*, 2001. **7**(3): p. 673-682.
56. Han, J.-w., et al., Expression of bbc3, a pro-apoptotic BH3-only gene, is regulated by diverse cell death and survival signals. *Proceedings of the National Academy of Sciences*, 2001. **98**(20): p. 11318-11323.
57. Whitfield, J., et al., Dominant-Negative c-Jun Promotes Neuronal Survival by Reducing BIM Expression and Inhibiting Mitochondrial Cytochrome c Release. *Neuron*, 2001. **29**(3): p. 629-643.
58. Shinjyo, T., et al., Downregulation of Bim, a Proapoptotic Relative of Bcl-2, Is a Pivotal Step in Cytokine-Initiated Survival Signaling in Murine Hematopoietic Progenitors. *Molecular and Cellular Biology*, 2001. **21**(3): p. 854-864.
59. Puthalakath, H., et al., ER Stress Triggers Apoptosis by Activating BH3-Only Protein Bim. *Cell*, 2007. **129**(7): p. 1337-1349.
60. Lei, K. and R.J. Davis, JNK phosphorylation of Bim-related members of the Bcl2 family induces Bax-dependent apoptosis. *Proceedings of the National Academy of Sciences*, 2003. **100**(5): p. 2432-2437.
61. Ley, R., et al., Activation of the ERK1/2 Signaling Pathway Promotes Phosphorylation and Proteasome-dependent Degradation of the BH3-only Protein, Bim. *Journal of Biological Chemistry*, 2003. **278**(21): p. 18811-18816.
62. Imaizumi, K., et al., Molecular Cloning of a Novel Polypeptide, DP5, Induced during Programmed Neuronal Death. *Journal of Biological Chemistry*, 1997. **272**(30): p. 18842-18848.
63. Sanz, C., et al., Specific and rapid induction of the proapoptotic protein Hrk after growth factor withdrawal in hematopoietic progenitor cells. *Blood*, 2000. **95**(9): p. 2742-2747.

64. Harris, C.A. and E.M. Johnson, BH3-only Bcl-2 Family Members Are Coordinately Regulated by the JNK Pathway and Require Bax to Induce Apoptosis in Neurons. *Journal of Biological Chemistry*, 2001. **276**(41): p. 37754-37760.
65. Bozyczko-Coyne, D., et al., CEP-1347/KT-7515, an inhibitor of SAPK/JNK pathway activation, promotes survival and blocks multiple events associated with A β -induced cortical neuron apoptosis. *Journal of Neurochemistry*, 2001. **77**(3): p. 849-863.
66. Datta, S.R., et al., Akt Phosphorylation of BAD Couples Survival Signals to the Cell-Intrinsic Death Machinery. *Cell*, 1997. **91**(2): p. 231-241.
67. Harada, H., et al., Phosphorylation and Inactivation of BAD by Mitochondria-Anchored Protein Kinase A. *Molecular Cell*, 1999. **3**(4): p. 413-422.
68. Wang, H.-G., U.R. Rapp, and J.C. Reed, Bcl-2 Targets the Protein Kinase Raf-1 to Mitochondria. *Cell*, 1996. **87**(4): p. 629-638.
69. Datta, S.R., et al., 14-3-3 Proteins and Survival Kinases Cooperate to Inactivate BAD by BH3 Domain Phosphorylation. *Molecular Cell*, 2000. **6**(1): p. 41-51.
70. Verma, S., L.-j. Zhao, and G. Chinnadurai, Phosphorylation of the Proapoptotic Protein BIK. *Journal of Biological Chemistry*, 2001. **276**(7): p. 4671-4676.
71. Roucou, X., et al., Bax oligomerization in mitochondrial membranes requires tBid (caspase-8-cleaved Bid) and a mitochondrial protein. *Biochem J*, 2002. **368**(Pt 3): p. 915-21.
72. Puthalakath, H., et al., The Proapoptotic Activity of the Bcl-2 Family Member Bim Is Regulated by Interaction with the Dynein Motor Complex. *Molecular Cell*, 1999. **3**(3): p. 287-296.
73. Breckenridge, D.G., et al., Regulation of apoptosis by endoplasmic reticulum pathways. *Oncogene*, 2003. **22**(53): p. 8608-8618.
74. Chipuk, J.E. and D.R. Green, How do BCL-2 proteins induce mitochondrial outer membrane permeabilization? *Trends in Cell Biology*, 2008. **18**(4): p. 157-164.
75. Danial, N.N. and S.J. Korsmeyer, Cell Death: Critical Control Points. *Cell*, 2004. **116**(2): p. 205-219.

76. van Delft, M.F. and D.C.S. Huang, How the Bcl-2 family of proteins interact to regulate apoptosis. *Cell Res*, 2006. **16**(2): p. 203-213.
77. Ranger, A.M., B.A. Malynn, and S.J. Korsmeyer, Mouse models of cell death. *Nat Genet*, 2001. **28**(2): p. 113-118.
78. Veis, D.J., et al., Bcl-2-deficient mice demonstrate fulminant lymphoid apoptosis, polycystic kidneys, and hypopigmented hair. *Cell*, 1993. **75**(2): p. 229-240.
79. Kamada, S., et al., bcl-2 Deficiency in Mice Leads to Pleiotropic Abnormalities: Accelerated Lymphoid Cell Death in Thymus and Spleen, Polycystic Kidney, Hair Hypopigmentation, and Distorted Small Intestine. *Cancer Research*, 1995. **55**(2): p. 354-359.
80. Motoyama, N., et al., Massive cell death of immature hematopoietic cells and neurons in Bcl-x-deficient mice. *Science*, 1995. **267**(5203): p. 1506-10.
81. Motoyama, N., et al., bcl-x Prevents Apoptotic Cell Death of Both Primitive and Definitive Erythrocytes at the End of Maturation. *The Journal of Experimental Medicine*, 1999. **189**(11): p. 1691-1698.
82. Wagner, K.U., et al., Conditional deletion of the Bcl-x gene from erythroid cells results in hemolytic anemia and profound splenomegaly. *Development*, 2000. **127**(22): p. 4949-4958.
83. Opferman, J.T., et al., Development and maintenance of B and T lymphocytes requires antiapoptotic MCL-1. *Nature*, 2003. **426**(6967): p. 671-676.
84. Print, C.G., et al., Apoptosis regulator Bcl-w is essential for spermatogenesis but appears otherwise redundant. *Proceedings of the National Academy of Sciences*, 1998. **95**(21): p. 12424-12431.
85. Hamasaki, A., et al., Accelerated Neutrophil Apoptosis in Mice Lacking A1-a, a Subtype of the bcl-2-related A1 Gene. *The Journal of Experimental Medicine*, 1998. **188**(11): p. 1985-1992.
86. Gonzalez-Garcia, M., et al., bcl-XL is the major bcl-x mRNA form expressed during murine development and its product localizes to mitochondria. *Development*, 1994. **120**(10): p. 3033-3042.
87. Kelekar, A. and C.B. Thompson, Bcl-2-family proteins: the role of the BH3 domain in apoptosis. *Trends in Cell Biology*, 1998. **8**(8): p. 324-330.

88. Minn, A.J., L.H. Boise, and C.B. Thompson, Bcl-x Antagonizes the Protective Effects of Bcl-x. *Journal of Biological Chemistry*, 1996. **271**(11): p. 6306-6312.
89. Lindenboim, L., et al., Bak but not Bax is essential for Bcl-xS-induced apoptosis. *Cell Death Differ*, 2005. **12**(7): p. 713-723.
90. Lindsten, T., et al., The Combined Functions of Proapoptotic Bcl-2 Family Members Bak and Bax Are Essential for Normal Development of Multiple Tissues. *Molecular Cell*, 2000. **6**(6): p. 1389-1399.
91. Moreau, C., et al., Minimal BH3 Peptides Promote Cell Death by Antagonizing Anti-apoptotic Proteins. *Journal of Biological Chemistry*, 2003. **278**(21): p. 19426-19435.
92. Certo, M., et al., Mitochondria primed by death signals determine cellular addiction to antiapoptotic BCL-2 family members. *Cancer Cell*, 2006. **9**(5): p. 351-365.
93. Hampton, M.B. and S. Orrenius, Dual regulation of caspase activity by hydrogen peroxide: implications for apoptosis. *FEBS Letters*, 1997. **414**(3): p. 552-556.
94. Vaux, D.L., S. Cory, and J.M. Adams, Bcl-2 gene promotes haemopoietic cell survival and cooperates with c-myc to immortalize pre-B cells. *Nature*, 1988. **335**(6189): p. 440-442.
95. Muchmore, S.W., et al., X-ray and NMR structure of human Bcl-xL, an inhibitor of programmed cell death. *Nature*, 1996. **381**(6580): p. 335-341.
96. Gross, A., J.M. McDonnell, and S.J. Korsmeyer, BCL-2 family members and the mitochondria in apoptosis. *Genes Dev*, 1999. **13**(15): p. 1899-1911.
97. Schwartz, P.S. and D.M. Hockenbery, Bcl-2-related survival proteins. *Cell Death Differ*, 2006. **13**(8): p. 1250-1255.
98. Jiang, X. and X. Wang, CYTOCHROME C-MEDIATED APOPTOSIS. *Annual Review of Biochemistry*, 2004. **73**(1): p. 87-106.
99. Newmeyer, D.D. and S. Ferguson-Miller, Mitochondria: Releasing Power for Life and Unleashing the Machineries of Death. *Cell*, 2003. **112**(4): p. 481-490.

100. Kuwana, T. and D.D. Newmeyer, Bcl-2-family proteins and the role of mitochondria in apoptosis. *Current Opinion in Cell Biology*, 2003. **15**(6): p. 691-699.
101. Germain, M. and G.C. Shore, Cellular Distribution of Bcl-2 Family Proteins. *Sci. STKE*, 2003. **2003**(173): p. pe10.
102. Pinton, P. and R. Rizzuto, Bcl-2 and Ca²⁺ homeostasis in the endoplasmic reticulum. *Cell Death Differ*, 2006. **13**(8): p. 1409-1418.
103. Wang, X., et al., ER stress modulates cellular metabolism. *Biochemical Journal*, 2011. **435**(1): p. 285-296.
104. Rong, Y. and C.W. Distelhorst, Bcl-2 Protein Family Members: Versatile Regulators of Calcium Signaling in Cell Survival and Apoptosis. *Annual Review of Physiology*, 2008. **70**(1): p. 73-91.
105. Zong, W.-X., et al., Bax and Bak can localize to the endoplasmic reticulum to initiate apoptosis. *The Journal of Cell Biology*, 2003. **162**(1): p. 59-69.
106. Eckenrode, E.F., et al., Apoptosis protection by Mcl-1 and Bcl-2 modulation of inositol 1,4,5-trisphosphate receptor-dependent Ca²⁺ signaling. *J Biol Chem*, 2010. **285**(18): p. 13678-84.
107. Li, C., et al., Apoptosis regulation by Bcl-xL modulation of mammalian inositol 1,4,5-trisphosphate receptor channel isoform gating. *Proceedings of the National Academy of Sciences*, 2007. **104**(30): p. 12565-12570.
108. Rong, Y.P., et al., Targeting Bcl-2-IP3 receptor interaction to reverse Bcl-2's inhibition of apoptotic calcium signals. *Mol Cell*, 2008. **31**(2): p. 255-65.
109. White, C., et al., The endoplasmic reticulum gateway to apoptosis by Bcl-X(L) modulation of the InsP3R. *Nat Cell Biol*, 2005. **7**(10): p. 1021-8.
110. Rong, Y.P., et al., The BH4 domain of Bcl-2 inhibits ER calcium release and apoptosis by binding the regulatory and coupling domain of the IP3 receptor. *Proc Natl Acad Sci U S A*, 2009. **106**(34): p. 14397-402.
111. RUBENSTEIN, M., C.M.P. HOLLOWELL, and P. GUINAN, Effects of BCL-2 Suppression by Antisense Oligonucleotides on Additional Regulators of Apoptosis Compensatory Change in Non-targeted Protein Expression. *In Vivo*, 2011. **25**(5): p. 725-732.
112. Zhu, W., et al., Bcl-2 mutants with restricted subcellular location reveal spatially distinct pathways for apoptosis in different cell types. *EMBO J*, 1996. **15**(16): p. 4130-41.

113. Fiebig, A., et al., Bcl-XL is qualitatively different from and ten times more effective than Bcl-2 when expressed in a breast cancer cell line. *BMC Cancer*, 2006. **6**(1): p. 213.
114. White, C., et al., The endoplasmic reticulum gateway to apoptosis by Bcl-XL modulation of the InsP3R. *Nat Cell Biol*, 2005. **7**(10): p. 1021-1028.
115. Eckenrode, E.F., et al., Apoptosis Protection by Mcl-1 and Bcl-2 Modulation of Inositol 1,4,5-Trisphosphate Receptor-dependent Ca²⁺ Signaling. *Journal of Biological Chemistry*, 2010. **285**(18): p. 13678-13684.
116. Foskett, J.K., et al., Inositol Trisphosphate Receptor Ca²⁺ Release Channels. *Physiological Reviews*, 2007. **87**(2): p. 593-658.
117. Alavian, K.N., et al., Bcl-xL regulates metabolic efficiency of neurons through interaction with the mitochondrial F1FO ATP synthase. *Nat Cell Biol*, 2011. **13**(10): p. 1224-1233.
118. Chen, Y.-b., et al., Bcl-xL regulates mitochondrial energetics by stabilizing the inner membrane potential. *The Journal of Cell Biology*, 2011. **195**(2): p. 263-276.
119. Vander Heiden, M.G., et al., Bcl-x L Promotes the Open Configuration of the Voltage-dependent Anion Channel and Metabolite Passage through the Outer Mitochondrial Membrane. *Journal of Biological Chemistry*, 2001. **276**(22): p. 19414-19419.
120. Sano, R., et al., GM1-Ganglioside Accumulation at the Mitochondria-Associated ER Membranes Links ER Stress to Ca²⁺-Dependent Mitochondrial Apoptosis. *Molecular Cell*, 2009. **36**(3): p. 500-511.
121. Pinton, P., et al., The Ca²⁺ concentration of the endoplasmic reticulum is a key determinant of ceramide-induced apoptosis: significance for the molecular mechanism of Bcl-2 action. *EMBO J*, 2001. **20**(11): p. 2690-2701.
122. Foyouzi-Youssefi, R., et al., Bcl-2 decreases the free Ca²⁺ concentration within the endoplasmic reticulum. *Proceedings of the National Academy of Sciences*, 2000. **97**(11): p. 5723-5728.
123. Susnow, N., et al., Bcl-2 family proteins as regulators of oxidative stress. *Seminars in Cancer Biology*, 2009. **19**(1): p. 42-49.

124. Zhao, M., J.W. Eaton, and U.T. Brunk, Protection against oxidant-mediated lysosomal rupture: a new anti-apoptotic activity of Bcl-2? FEBS Letters, 2000. **485**(2-3): p. 104-108.
125. Zhao, M., J.W. Eaton, and U.T. Brunk, Bcl-2 phosphorylation is required for inhibition of oxidative stress-induced lysosomal leak and ensuing apoptosis. FEBS Letters, 2001. **509**(3): p. 405-412.
126. Liu, Z., et al., PUMA Overexpression Induces Reactive Oxygen Species Generation and Proteasome-Mediated Stathmin Degradation in Colorectal Cancer Cells. Cancer Research, 2005. **65**(5): p. 1647-1654.
127. Ritchie, A., O. Gutierrez, and J.L. Fernandez-Luna, PAR bZIP-bik is a novel transcriptional pathway that mediates oxidative stress-induced apoptosis in fibroblasts. Cell Death Differ, 2009. **16**(6): p. 838-846.
128. Aikawa, T., et al., Noxa is necessary for hydrogen peroxide-induced caspase-dependent cell death. FEBS Letters, 2010. **584**(4): p. 681-688.
129. Willis, S.N., et al., Proapoptotic Bak is sequestered by Mcl-1 and Bcl-xL, but not Bcl-2, until displaced by BH3-only proteins. Genes & Development, 2005. **19**(11): p. 1294-1305.
130. Li, H., et al., Cleavage of BID by Caspase 8 Mediates the Mitochondrial Damage in the Fas Pathway of Apoptosis. Cell, 1998. **94**(4): p. 491-501.
131. Ley, R., et al., Regulatory phosphorylation of Bim: sorting out the ERK from the JNK. Cell Death Differ, 2005. **12**(8): p. 1008-1014.
132. Zha, J., et al., Serine Phosphorylation of Death Agonist BAD in Response to Survival Factor Results in Binding to 14-3-3 Not BCL-XL. Cell, 1996. **87**(4): p. 619-628.
133. Doonan, F., et al., Bim Expression Indicates the Pathway to Retinal Cell Death in Development and Degeneration. The Journal of Neuroscience, 2007. **27**(40): p. 10887-10894.
134. Kurz, T., et al., Lysosomal Redox-Active Iron Is Important for Oxidative Stress-Induced DNA Damage. Annals of the New York Academy of Sciences, 2004. **1019**(1): p. 285-288.
135. Persson, H.L., et al., Prevention of oxidant-induced cell death by lysosomotropic iron chelators. Free Radical Biology and Medicine, 2003. **34**(10): p. 1295-1305.

136. Kurz, T., et al., Relocalized redox-active lysosomal iron is an important mediator of oxidative-stress-induced DNA damage. *Biochem. J.*, 2004. **378**(3): p. 1039-1045.
137. Castino, R., et al., Chelation of Lysosomal Iron Protects Dopaminergic SH-SY5Y Neuroblastoma Cells from Hydrogen Peroxide Toxicity by Precluding Autophagy and Akt Dephosphorylation. *Toxicological Sciences*, 2011. **123**(2): p. 523-541.
138. Chen, L., et al., Differential Targeting of Prosurvival Bcl-2 Proteins by Their BH3-Only Ligands Allows Complementary Apoptotic Function. *Molecular Cell*, 2005. **17**(3): p. 393-403.
139. Kuwana, T., et al., BH3 Domains of BH3-Only Proteins Differentially Regulate Bax-Mediated Mitochondrial Membrane Permeabilization Both Directly and Indirectly. *Molecular Cell*, 2005. **17**(4): p. 525-535.
140. Lopez, H., et al., Perturbation of the Bcl-2 Network and an Induced Noxa/Bcl-xL Interaction Trigger Mitochondrial Dysfunction after DNA Damage. *Journal of Biological Chemistry*, 2010. **285**(20): p. 15016-15026.
141. Kim, H., et al., Hierarchical regulation of mitochondrion-dependent apoptosis by BCL-2 subfamilies. *Nat Cell Biol*, 2006. **8**(12): p. 1348-1358.
142. Bredesen, D.E., R.V. Rao, and P. Mehlen, Cell death in the nervous system. *Nature*, 2006. **443**(7113): p. 796-802.
143. Zhao, M., J.W. Eaton, and U.T. Brunk, Protection against oxidant-mediated lysosomal rupture: a new anti-apoptotic activity of Bcl-2? *FEBS Letters*, 2000. **485**(2-3): p. 104-108.
144. Luzio, J.P., P.R. Pryor, and N.A. Bright, Lysosomes: fusion and function. *Nat Rev Mol Cell Biol*, 2007. **8**(8): p. 622-632.
145. Boya, P. and G. Kroemer, Lysosomal membrane permeabilization in cell death. *Oncogene*, 2008. **27**(50): p. 6434-6451.
146. Brunk, U.T., et al., Photo-Oxidative Disruption of Lysosomal Membranes Causes Apoptosis of Cultured Human Fibroblasts. *Free Radical Biology and Medicine*, 1997. **23**(4): p. 616-626.
147. Antunes, F., E. Cadenas, and U.T. Brunk, Apoptosis induced by exposure to a low steady-state concentration of H₂O₂ is a consequence of lysosomal rupture. *Biochem. J.*, 2001. **356**(2): p. 549-555.

148. Johansson, A.-C., et al., Regulation of apoptosis-associated lysosomal membrane permeabilization. *Apoptosis*, 2010. **15**(5): p. 527-540.
149. Kirkegaard, T. and M. Jäättelä, Lysosomal involvement in cell death and cancer. *Biochimica et Biophysica Acta (BBA) - Molecular Cell Research*, 2009. **1793**(4): p. 746-754.
150. Persson, H.L., et al., Radiation-induced cell death: importance of lysosomal destabilization. *Biochem. J.*, 2005. **389**(3): p. 877-884.
151. Eno, C.O., et al., The Bcl-2 proteins Noxa and Bcl-xL co-ordinately regulate oxidative stress-induced apoptosis. *Biochemical Journal*, 2012. **444**(1): p. 69-78.
152. Boya, P., et al., Lysosomal Membrane Permeabilization Induces Cell Death in a Mitochondrion-dependent Fashion. *The Journal of Experimental Medicine*, 2003. **197**(10): p. 1323-1334.
153. Berndt, C., et al., Chelation of lysosomal iron protects against ionizing radiation. *Biochemical Journal*, 2010. **432**(2): p. 295-301.
154. Kurz, T., B. Gustafsson, and U.T. Brunk, Intralysosomal iron chelation protects against oxidative stress-induced cellular damage. *FEBS Journal*, 2006. **273**(13): p. 3106-3117.
155. Muñoz-Pinedo, C., et al., Different mitochondrial intermembrane space proteins are released during apoptosis in a manner that is coordinately initiated but can vary in duration. *Proceedings of the National Academy of Sciences*, 2006. **103**(31): p. 11573-11578.
156. Kågedal, K., et al., Lysosomal membrane permeabilization during apoptosis - involvement of Bax? *International Journal of Experimental Pathology*, 2005. **86**(5): p. 309-321.
157. Werneburg, N.W., et al., Tumor Necrosis Factor-related Apoptosis-inducing Ligand (TRAIL) Protein-induced Lysosomal Translocation of Proapoptotic Effectors Is Mediated by Phosphofurin Acidic Cluster Sorting Protein-2 (PACS-2). *Journal of Biological Chemistry*, 2012. **287**(29): p. 24427-24437.
158. Cuadrado, A., et al., A new p38 MAP kinase-regulated transcriptional coactivator that stimulates p53-dependent apoptosis. *EMBO J.*, 2007. **26**(8): p. 2115-2126.

159. Werneburg, N.W., et al., Tumor Necrosis Factor-related Apoptosis-inducing Ligand Activates a Lysosomal Pathway of Apoptosis That Is Regulated by Bcl-2 Proteins. *Journal of Biological Chemistry*, 2007. **282**(39): p. 28960-28970.
160. Ploner, C., R. Kofler, and A. Villunger, Noxa: at the tip of the balance between life and death. *Oncogene*, 2008. **27**(S1): p. S84-S92.
161. Kutuk, O., et al., Cisplatin overcomes Bcl-2-mediated resistance to apoptosis via preferential engagement of Bak: critical role of Noxa-mediated lipid peroxidation. *Carcinogenesis*, 2009. **30**(9): p. 1517-1527.

APPENDIX

List of Abbreviations

ANOVA	Analysis of variance
AO	Acridine Orange
APAF-1	Apoptotic protease activating factor 1
ATF4	Activating transcription factor 4
Bad	Bcl-2/Bcl-x _L -associated agonist of cell death
Bcl-2	B cell lymphoma/leukemia-2
BH	Bcl-2 Homology
Bid	BH3-interacting domain death agonist
Bik	Bcl-2-interacting killer
Bim	Bcl-2-interacting mediator of cell death
Bmf	Bcl-2-modifying factor
Bnip3	Bcl2/adenovirus E1B-interacting protein 3
Ca ²⁺	Calcium (II) ions
CPA	Cyclopiazonic acid
DFO	Desferrioxamine
DISC	Death-inducing signaling complex
DMSO	Dimethyl sulfoxide
DKO	Double knock out
DMEM	Dulbecco's Modified Eagle Medium
EGFP	Enhanced green fluorescent protein
<i>E. coli</i>	<i>Escherichia coli</i>

ER	Endoplasmic reticulum
FADD	Fas-associated death domain
FBS	Fetal bovine serum
H ₂ O ₂	Hydrogen peroxide
HBSS	Hanks balanced salt solution
Hrk	Activator of apoptosis harakiri
IAPs	Inhibitors of apoptosis proteins
ICM	Intracellular-like medium
IMS	Inter membrane space
InsP ₃ R	Inositol trisphosphate receptor
IP	Immuno-precipitation
IRES	Internal ribosomal entry site
KO	Knock out
LMP	Lysosomal membrane permeabilization
mAb	Monoclonal antibodies
Mcl-1	Myeloid cell leukemia sequence 1
MEFs	Mouse embryonic fibroblasts
mRNA	messenger Ribonucleic acid
Nix	Bcl2/adenovirus E1B-interacting protein like-3
OMMP	Outer mitochondrial membrane permeabilization
pAb	Polyclonal antibodies
PBS	Phosphate buffer saline
PCR	Polymerase chain reaction
PI	Propidium iodide
PKA	Protein kinase A
PP2A	Protein phosphatase 2A
P/S	Penicillin/Streptomycin

PS	Phosphatidylserine
Puma	p53 up-regulated modulator of apoptosis
qPCR	quantitative real time polymerase chain reaction
REs	Restriction endonucleases
RFUs	Relative fluorescent units
Rt-PCR	Reverse transcriptase polymerase chain reaction
ROS	Reactive oxygen species
SAPK/JNK	Stress-activated/c Jun N-terminal kinase
SERCA	Sarco/endoplasmic reticulum Ca ²⁺ -ATPase
siRNA	small interference- Ribonucleic acid
tBid	Truncated Bid
TM	Transmembrane
TNF	Tumor necrosis factor
TNFR	Tumor necrosis factor receptors
VDAC2	Voltage-dependent anion channel 2
WT	Wild type

CURRICULUM VITAE

COLINS OGWANDI ENO

PRESENT ADDRESS: Department of Pharmacology and Toxicology,
School of Medicine, University of Louisville,
505 S Hancock St. Rm 433A
Louisville, KY 40202

HOME ADDRESS: 6319 Fern Valley way #13
Louisville, KY 40219
(502)8513209
enos882@yahoo.com;
coeno001@louisville.edu

EDUCATION

- 08/2008-present:
- Ph.D., Department of Pharmacology and Toxicology, University of Louisville, Louisville, Kentucky
- 08/2008-05/2010:
- M.S., Department of Pharmacology and Toxicology, University of Louisville, Louisville, Kentucky
- 08/2005-05/2008:
- M.S., Department of Plant Sciences and Genetics, North Dakota States University, Fargo, North Dakota
- 10/2001-07/2004:
- B.Sc. Biochemistry, Department of Life Sciences, Faculty of Science, University of Buea, Cameroon, Central Africa

PROFESSIONAL EXPERIENCE

- 08/2008-present:
- Graduate research assistant, Department of Pharmacology and Toxicology, University of Louisville, Louisville, Kentucky (Advisor: Dr. Chi Li)

09/2005-05/2008:

- Graduate research assistant, Department of Plant Sciences, North Dakota States University, Fargo, North Dakota (Advisor: Dr. Marcelo J. Carena)

PROFESSIONAL MEMBERSHIPS

2010-present:

- American Society of Pharmacology and Experimental Therapeutics (ASPET).

2009-Present:

- Golden Key International Honor Society

MAJOR AWARDS AND SCHOLARSHIPS

2012:

- Recipient of NIH Annual Postdoctoral Fellowship/ National Graduate Student Research Conference
- University of Louisville Doctoral Dissertation Completion Award
- University of Louisville Sponsored Research Tuition Award
- University of Louisville Graduate Student Council (GSC) Travel Award
- University of Louisville School of Medicine (SOM) Research Committee Travel Award

2011:

- American Society of Pharmacology and Experimental Therapeutics (ASPET) Graduate Student Travel Award;
- University of Louisville Graduate Student Council (GSC) Travel Award
- University of Louisville School of Medicine (SOM) Research Committee Travel Award

2008-2010:

- University of Louisville Integrated Program in Biomedical Sciences (IPIBS) Doctoral Fellowship

2007:

- Charles and Linda Moses Presidential Graduate Fellowship, North Dakota State University, Fargo, North Dakota.

2005-2008:

- North Dakota State University Department of Plant Sciences Graduate Research Assistantship.

2002- 2004:

- Financial Aid for outstanding Performance from the Ministry of Higher Education, Cameroon.

PUBLICATIONS

Eno, C.O., Eckenrode, E.F., Olberding, K.E., Zhao, G., White, C., and Li, C. Distinct Roles of Mitochondria- and ER-localized Bcl-x_L in Apoptosis Resistance and Ca²⁺ Homeostasis. *Mol. Biol. Cell.* **2012**, **23**:13 **2605-2618**

Eno, C.O., Zhao, G., Olberding, K.E., and Li, C. The Bcl-2 Proteins Noxa and Bcl-x_L Coordinately Regulate Oxidative Stress-induced Apoptosis. *Biochemical Journal.* **2012**, **444**:69-78.

Wang, X., **Eno, C.O.**, Altman, B.J., Zhu, Y., Zhao, G., Olberding, K.E., Rathmell, J.C., and Li, C. ER stress modulates cellular metabolism. *Biochemical Journal.* **2011**, **435**:285-296.

MANUSCRIPTS IN PREPARATIONS

Zhao, G., Zhu, Y., **Eno, C.O.**, Liu, Y., DeLeeuw, L., Chaires, J.B., Trent, J.O., and Li, C. Induction of Tumor Cell Apoptosis by Direct Activation of the Pro-apoptotic Bcl-2 Protein Bax. (Under review at Cancer Research).

Eno, C.O., Zhao, G., and Li, C. Noxa couples lysosomal membrane permeabilization and apoptosis during oxidative stress. (Under review at Journal of Cell Biology).

Eno, C.O., Zhao, G., Olberding, K.E., and Li, C. The anti-apoptotic activity of the Bcl-2 protein Bcl-x_S in mouse embryonic fibroblasts. (To be submitted to PLoS One).

ABSTRACTS SUBMITTED TO REGIONAL AND NATIONAL MEETINGS

Eno, C.O., Eckenrode, E.F., Olberding, K.E., Zhao, G., White, C., and Li, C. Distinct Roles of Mitochondria- and ER-localized Bcl-XL in Apoptosis Resistance and Ca²⁺ Homeostasis. *Research!Louisville September 2012*.

Eno, C.O., Eckenrode, E.F., Olberding, K.E., Zhao, G., White, C., and Li, C. Distinct Roles of Mitochondria- and ER-localized Bcl-XL in Apoptosis Resistance and Ca²⁺ Homeostasis. *Experimental Biology San Diego CA April 21-25, 2012*.

Eno, C.O., Olberding, K.E., and Li, C. The C-terminal transmembrane domain and Loop region of Bcl-x_S are important for its anti-apoptotic activities. *Experimental Biology Washington DC April 9-13, 2011*.

Eno, C.O., Eckenrode, E.F., Olberding, K.E., Zhao, G., White, C., and Li, C. Distinct Roles of Mitochondria- and ER-localized Bcl-XL in Apoptosis Resistance and Ca²⁺ Homeostasis. *Brown Cancer Retreat November 2011*.

Eno, C.O., Zhao, G., Olberding, K.E., and Li, C. The Bcl-2 Proteins Noxa and Bcl-x_L Coordinately Regulate Oxidative Stress-induced Apoptosis. *Brown Cancer Retreat November 2011*.

Eno, C.O., Zhao, G., Olberding, K.E., and Li, C. The Bcl-2 Proteins Noxa and Bcl-x_L Coordinately Regulate Oxidative Stress-induced Apoptosis. *Research!Louisville October 2011*.

Eno, C.O., Olberding, K.E., and Li, C. Mechanism of regulation of apoptosis by the Bcl-2 proteins Bcl-x_L and Bcl-x_S. *Brown Cancer Retreat November 2010*.

Eno, C.O., Olberding, K.E., and Li, C. Mechanism of regulation of apoptosis by the Bcl-2 proteins Bcl-x_L and Bcl-x_S. *Research!Louisville October 2010*.

Eno, C.O., Olberding, K.E., and Li, C. Regulation of apoptosis by the anti-apoptotic Bcl-2 protein Bcl-x_L. *Ohio Valley Society of Toxicology November 2009*.

Eno, C.O., Olberding, K.E., and Li, C. Regulation of apoptosis by the anti-apoptotic Bcl-2 protein Bcl-x_L. *Brown Cancer Retreat November 2009*.

Eno, C.O., Olberding, K.E., and Li, C. Regulation of apoptosis by the anti-apoptotic Bcl-2 protein Bcl-x_L. *Research!Louisville October 2009*.

TECHNICAL SKILLS

CELL AND MOLECULAR BIOLOGY TECHNIQUES:

Polymerase chain reaction (PCR), reverse transcriptase PCR (rt-PCR), quantitative real time PCR (qPCR), molecular cloning, primer designing, isolation and quantification of genomic DNA, western blot analysis, flow cytometry analysis, Immuno-precipitation (IP), Immuno-fluorescence analysis, retroviral infection, microscopy, cell culture.

ANIMAL HANDLING TECHNIQUES

Subcutaneous tumor formation techniques (injection of mice), monitoring of mice for tumor growth, measure tumor size and calculate tumor growth rate, and intraperitoneal injection of drugs into mice.

COMPUTER SKILLS

Microsoft office (MS word, MS Excel, MS power point), Adobe Photoshop, Canvas, EndNote 9, Reference Manager.